

# Asymptotic Analysis of Localized Solutions to Some Linear and Nonlinear Biharmonic Eigenvalue Problems

M. C. KROPINSKI, A. E. LINDSAY, M. J. WARD

*Alan E. Lindsay; Department of Mathematics, University of Arizona, Tucson, Arizona, 85721, USA.*

*Michael J. Ward; Department of Mathematics, University of British Columbia, Vancouver, British Columbia, V6T 1Z2, Canada*

*Mary-Catherine A. Kropinski; Department of Mathematics, Simon Fraser University, Burnaby, British Columbia, Canada*

(Received October 6th, 2010)

In an arbitrary bounded 2-D domain, a singular perturbation approach is developed to analyze the asymptotic behavior of several biharmonic linear and nonlinear eigenvalue problems for which the solution exhibits a concentration behavior either due to a hole in the domain, or as a result of a nonlinearity that is non-negligible only in some localized region in the domain. The specific form for the biharmonic nonlinear eigenvalue problem is motivated by the study of the steady-state deflection of one of the two surfaces in a MEMS capacitor. The linear eigenvalue problem that is considered is to calculate the spectrum of the biharmonic operator in a domain with an interior hole of asymptotically small radius. One key novel feature in the analysis of our singularly perturbed biharmonic problems, which is absent in related second-order elliptic problems, is that a point constraint must be imposed on the leading order outer solution in order to asymptotically match inner and outer representations of the solution. Our asymptotic analysis also relies heavily on the use of logarithmic switchback terms, notorious in the study of Low Reynolds number fluid flow, and on detailed properties of the biharmonic Green's function and its associated regular part near the singularity. For a few simple domains, full numerical solutions to the biharmonic problems are computed to verify the asymptotic results obtained from the analysis.

Key words: biharmonic eigenvalue, biharmonic Green's function, point constraint, concentration phenomena, switchback terms

## 1 Introduction

We construct asymptotic solutions to some singularly perturbed linear and nonlinear biharmonic problems in two-dimensional domains  $\Omega$ . Each of the problems that we consider exhibits a localization behavior, whereby the solution concentrates at some special location  $x_0$  inside the domain. This concentration occurs either as a result of a nonlinear term that is non-negligible only in some narrow region near  $x_0$ , or else is due to a small hole in the domain that is centered at some  $x_0 \in \Omega$ . The asymptotic analysis of these biharmonic problems will reveal some novel features, including the necessity of imposing interior point constraints in the asymptotic construction of the solution. The imposition of such point constraints for the solution to second-order elliptic problems is, of course, not well-posed.

The specific form of our biharmonic nonlinear eigenvalue problems is motivated by mathematical models of a Micro-Electro-Mechanical System (MEMS) capacitor (cf. [26]). In this context, a simple capacitor consists of a rigid conducting ground plate located below a thin deformable elastic plate that is clamped along its boundary (see Fig. 1). The surface of the deformable plate is coated with a thin metallic conducting film so that it can deflect towards the rigid ground plate under an applied voltage  $V$ . For  $V < V^*$ , where  $V^*$  is called the *pull-in* voltage, the device reaches a stable equilibrium deflection, whereas for  $V > V^*$  no equilibrium deflections are possible.

For a MEMS capacitor occupying a region  $\Omega \subset \mathbb{R}^2$  with smooth boundary  $\partial\Omega$ , the narrow gap asymptotic analysis of [26] showed that the dimensionless steady-state deflection  $u(x)$  of the upper plate satisfies the biharmonic nonlinear

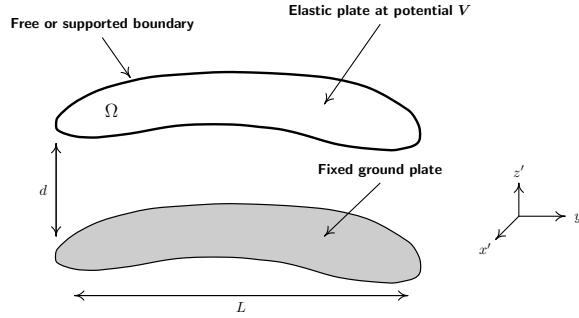


FIGURE 1. Schematic plot of the MEMS capacitor with a deformable elastic upper surface that deflects towards the fixed lower surface under an applied voltage.

eigenvalue problem

$$-\delta\Delta^2 u + \Delta u = \frac{\lambda}{(1+u)^2}, \quad x \in \Omega; \quad u = \partial_n u = 0, \quad x \in \partial\Omega. \quad (1.1)$$

In (1.1), the constant  $\delta > 0$  represents the relative effects of tension and rigidity on the deflecting plate, and  $\lambda \geq 0$  is the dimensionless ratio of electrostatic to elastic forces in the system, and is proportional to  $V^2$ , where  $V$  is the voltage applied to the upper plate. The boundary conditions in (1.1) assume that the upper plate is clamped along its rim. A solution to (1.1) can be interpreted physically as a balance between an elastic restoring force for the upper surface, and an electrostatic Coulomb force that attracts the upper surface to the lower rigid ground plate.

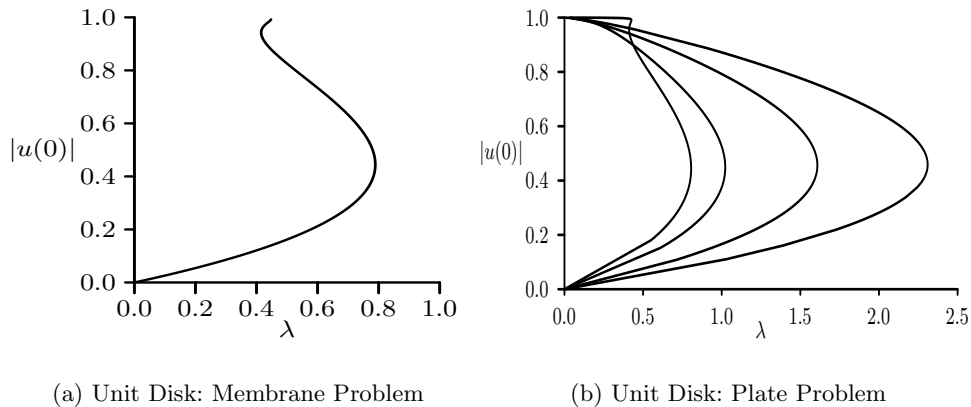


FIGURE 2. Numerically computed bifurcation diagrams of  $|u(0)|$  versus  $\lambda$  for (1.2) (left figure) and for (1.1) (right figure) in the unit disk. Left figure: the beginning of the infinite-fold point structure for (1.2) with  $\lambda \rightarrow 4/9$  as  $|u(0)| \rightarrow 1^-$ . Right figure: from left to right, the bifurcation curves for (1.1) correspond to  $\delta = 0.0001, 0.01, 0.05, 0.1$ . Notice that there is a maximal solution branch with  $\lambda \rightarrow 0$  as  $|u(0)| \rightarrow 1^-$ .

The special case  $\delta = 0$  in (1.1) corresponds to modeling the upper surface as a membrane instead of a plate. Omitting the requirement that  $\partial_n u = 0$  on  $\partial\Omega$ , (1.1) reduces to the basic MEMS membrane problem

$$\Delta u = \frac{\lambda}{(1+u)^2}, \quad x \in \Omega; \quad u = 0 \quad x \in \partial\Omega. \quad (1.2)$$

In the unit disk in  $\mathbb{R}^2$ , (1.2) was studied from various viewpoints in [16], [27], [13], and [11]. For the unit disk, one key feature of the bifurcation diagram of  $\|u\|_\infty$  versus  $\lambda$ , for the class of radially symmetric solutions of (1.2), is that there is an infinite number of fold points that cluster onto  $\lambda \rightarrow 4/9$  as  $\|u\|_\infty \rightarrow 1^-$ . More generally, in [14] it was proved that (1.2) has an infinite fold-point structure in a general 2-D domain that has two axes of symmetry,

although it is only conjectured that these fold points cluster onto some limiting value  $\lambda^*$  as  $\|u\|_\infty \rightarrow 1^-$ . For the unit disk in  $\mathbb{R}^2$ , a plot of the numerically computed bifurcation diagram showing the beginning of this infinite fold-point structure is given in Fig. 2(a). In contrast, for the biharmonic problem (1.1) in the unit disk in  $\mathbb{R}^2$ , it was shown in [22] that for any  $\delta > 0$  there is a maximal solution branch for which  $\lambda \rightarrow 0$  as  $\|u\|_\infty \rightarrow 1^-$ . In this sense, the effect of  $\delta > 0$  in (1.1) is to destroy the infinite fold-point structure associated with (1.2) in the unit disk in  $\mathbb{R}^2$ . A plot of the numerically computed bifurcation diagram of  $|u(0)|$  versus  $\lambda$  for (1.1), showing the maximal solution branch, is given in Fig. 2(b). In the unit disk, the singular perturbation analysis in [22] explicitly characterizes the limiting asymptotic behavior of the maximal solution branch  $\lambda(\varepsilon)$  and  $u(|x|; \varepsilon)$  in the limit  $\varepsilon = 1 - \|u\|_\infty \rightarrow 0^+$ .

In contrast to the wealth of results for (1.2), there are only a few rigorous results for the biharmonic problem (1.1). In the unit disk in  $\mathbb{R}^N$ , regularity properties of the solution along the primary bifurcation branch emanating from  $\lambda = 0$  and  $u = 0$  are analyzed in [7]. In [7], this analysis is extended to arbitrary 2-D domains. A survey of mathematical results for (1.2) and (1.1), with a comprehensive bibliography, is given in [9]. For an arbitrary 2-D domain, a formal asymptotic approach was used in [21] to calculate the pull-in voltage threshold corresponding to the saddle-node bifurcation point at the end of the primary bifurcation branch when either  $\delta \ll 1$  or  $\delta \gg 1$  in (1.1). Finally, for the unit disk, in [22] a formal asymptotic analysis of the limiting behavior of the maximal solution branch for (1.1) when  $\delta = \mathcal{O}(1)$  was given.

One main goal of this paper is explicitly characterize the limiting asymptotic behavior as  $\delta \rightarrow 0$  of the maximal solution branch to (1.1) in an *arbitrary 2-D domain*. Such a solution exhibits concentration in the sense that  $\lambda \rightarrow 0$  as  $\delta \rightarrow 0$ , but that the nonlinear term  $\lambda/(1+u)^2$  in (1.1) is non-negligible in  $\Omega$  only in the vicinity of some concentration point  $x_0 \in \Omega$  where  $u(x_0) + 1 \ll \mathcal{O}(1)$ . This concentration point  $x_0$ , which must be determined, is characterized by  $u(x_0) = -1 + \varepsilon$ , with  $\varepsilon \rightarrow 0^+$ , so that  $\|u\|_\infty = |u(x_0)| \rightarrow 1^-$ . Instead of treating the more complicated two independent small parameter problem  $\varepsilon \rightarrow 0$  and  $\delta \rightarrow 0$ , in §3 we use the method of matched asymptotic expansions to construct a solution branch  $\lambda(\delta)$  and  $u(x; \delta)$  to (1.1) as  $\delta \rightarrow 0^+$  for which  $u(x_0) = -1 + \delta$ . For  $\delta \rightarrow 0$ , our analysis determines the concentration point  $x_0$  and the explicit asymptotic formula for  $\lambda(\delta)$  as given in Principal Result 3.1. Our analysis of this problem requires a triple-deck asymptotic analysis, with two inner scales needed near the concentration point. It also relies heavily on the use of logarithmic switchback terms notorious in the singular perturbation analyses of low Reynolds number steady-state fluid flow (cf. [18], [19]).

In §4, we extend the asymptotic analysis of [22] for the maximal solution branch of the pure biharmonic nonlinear eigenvalue problem in the unit ball to the more general case of an arbitrary 2-D domain. By taking the limit  $\delta \rightarrow \infty$  in (1.1) and by suitably re-defining  $\lambda$ , the pure biharmonic nonlinear eigenvalue problem in an arbitrary 2-D domain  $\Omega$  is formulated as

$$\Delta^2 u = -\frac{\lambda}{(1+u)^2}, \quad x \in \Omega; \quad u = \partial_n u = 0, \quad x \in \partial\Omega. \quad (1.3)$$

In §4 the method of matched asymptotic expansions is used to explicitly characterize the limiting asymptotic behavior as  $\varepsilon \rightarrow 0^+$  of the maximal solution branch  $\lambda(\varepsilon)$ ,  $u(x, \varepsilon)$  of (1.3), for which  $u(x_0) = -1 + \varepsilon$ , where the concentration point  $x_0$  is to be found. Our analysis shows that, to leading order, the concentration point  $x_0$  must be a root of  $\nabla_x R(x; x_0)|_{x=x_0} = 0$  for which  $R(x_0; x_0) > 0$ , where  $R(x; x_0)$  is the regular part of the biharmonic Green's function  $G(x; x_0)$  defined for  $x_0 \in \Omega$  by

$$\Delta^2 G = \delta(x - x_0), \quad x \in \Omega; \quad G = \partial_n G = 0, \quad x \in \partial\Omega, \quad (1.4 a)$$

$$G(x; x_0) = \frac{1}{8\pi} |x - x_0|^2 \log |x - x_0| + R(x; x_0). \quad (1.4 b)$$

In Principal Result 4.1, we show that the limiting asymptotic behavior of  $\lambda(\varepsilon)$  for  $\varepsilon \rightarrow 0$  depends on  $R(x_0; x_0)$  and on the trace of the Hessian matrix of  $R(x; x_0)$  at  $x = x_0$ . In §4 we use a numerical boundary integral method, very similar to that developed in [12] for low Reynolds number flow problems, to numerically calculate these quantities for a square domain and for a class of dumbbell-shaped domains. The asymptotic result for the maximal solution branch of (1.3) for the square domain is then favorably compared with full numerical results computed from a finite-difference pseudo-arclength continuation scheme applied to (1.3). In addition, by computing  $R(x_0; x_0)$  numerically, we show for a one-parameter family of dumbbell-shaped domains that there can be multiple points  $x_0$  where concentration occurs when the domain is sufficiently non-convex.

We remark that there is a vast literature for the analysis of concentration behavior for second-order nonlinear elliptic problems with power law nonlinearities in domains in  $\mathbb{R}^N$  (see [28] and the references therein). However, due to the lack of a maximum principle and standard comparison principles for fourth order problems with clamped boundary conditions, there are only a few such studies for nonlinear biharmonic problems (cf. [15], [10], [29]). The analysis of (1.3) in §4 provides one of the first explicit examples of solution concentration behavior for a biharmonic nonlinear eigenvalue problem in an arbitrary 2-D domain. A related analysis is given in [29] for a nonlinear biharmonic problem in an arbitrary domain in  $\mathbb{R}^4$  with power law nonlinearity  $u^p$  with  $p \rightarrow +\infty$ . One very distinct feature of our analysis for (1.3) is that it is only the leading-order solution that is locally radially symmetric near the concentration point. Since the higher order terms, which generate non-radially symmetric corrections near the concentration point, differ from the leading-order term by only  $\mathcal{O}(-1/\log \varepsilon)$ , such terms must be explicitly accounted for in the asymptotic analysis of §4 in order to derive a two-term expansion for  $\lambda(\varepsilon)$  as  $\varepsilon \rightarrow 0$ .

In §5 we determine asymptotically the spectrum of the linear biharmonic eigenvalue problem in an arbitrary 2-D domain  $\Omega$  in which a small hole  $\Omega_\varepsilon$  of radius  $\mathcal{O}(\varepsilon) \ll 1$ , centered at  $x_0 \in \Omega$ , is removed from  $\Omega$ . This singularly perturbed spectral problem arises in the study of the vibration of a thin plate occupying a bounded region  $\Omega \setminus \Omega_\varepsilon \subset \mathbb{R}^2$ , where the linearized plate deflection  $w(x, t)$  satisfies  $\rho w_{tt} + D\Delta^2 w = 0$  for  $x \in \Omega \setminus \Omega_\varepsilon$ . Here  $\rho$  and  $D$  are the constant mass density per unit area and the constant flexural rigidity of the plate, respectively. By substituting  $w(x, t) = u(x)e^{i\omega t}$ , and imposing the clamped boundary conditions  $u = \partial_n u = 0$  for  $x \in \partial\Omega$  and for  $x \in \partial\Omega_\varepsilon$ , we obtain the biharmonic eigenvalue problem

$$\Delta^2 u - \lambda u = 0, \quad x \in \Omega \setminus \Omega_\varepsilon; \quad \int_{\Omega} u^2 dx = 1, \quad (1.5 a)$$

$$u = \partial_n u = 0, \quad x \in \partial\Omega; \quad u = \partial_n u = 0, \quad x \in \partial\Omega_\varepsilon, \quad (1.5 b)$$

where  $\lambda \equiv \rho\omega^2/D$ . The eigenvalue problem (1.5) admits a countably infinite spectrum  $\lambda_{m\varepsilon}$  for  $m = 0, 1, 2, \dots$  for which  $\lambda_{0\varepsilon} > 0$  and  $\lambda_{m\varepsilon} \rightarrow \infty$  as  $m \rightarrow \infty$ . The corresponding eigenfunctions  $u_{m\varepsilon}$  for  $m \geq 0$  are orthogonal in the sense that  $\int_{\Omega \setminus \Omega_\varepsilon} u_{m\varepsilon} u_{n\varepsilon} dx = 0$  for  $m \neq n$ .

By using the method of matched asymptotic expansions, in §5 we construct an asymptotic expansion characterizing the limiting behavior of any given eigenpair  $(\lambda_{m\varepsilon}, u_{m\varepsilon})$  of (1.5) in the limit of small hole radius  $\varepsilon \rightarrow 0$ . Although similar problems for the asymptotic behavior of the Laplacian eigenvalues in a perforated domain have been well-studied in [25], [32], [33], and [17] (see also the references therein), the only such study for the biharmonic eigenvalue problem (1.5) is given in [2] and [3].

One of the mathematical novelties of this problem, in contrast to the Laplacian eigenvalue problems of [25], [32] and [17], is that in the limit  $\varepsilon \rightarrow 0$  of small hole radius, then  $\lambda_{m\varepsilon} \sim \lambda_{m0}$  and  $u_{m\varepsilon} \sim u_{m0}$  for  $|x - x_0| \gg \mathcal{O}(\varepsilon)$ , where

$\lambda_{m0}$  and  $u_{m0}(x)$  satisfy the following limiting problem with a point constraint (cf. [2] and [3]):

$$\Delta^2 u_{m0} - \lambda_{m0} u_{m0} = 0, \quad x \in \Omega \setminus \{x_0\}; \quad \int_{\Omega} u_{m0}^2 dx = 1, \quad (1.6 a)$$

$$u_{m0} = \partial_n u_{m0} = 0, \quad x \in \partial\Omega; \quad u_{m0}(x_0) = 0. \quad (1.6 b)$$

Therefore, for  $\varepsilon \rightarrow 0$ , the boundary condition in (1.5 b) on  $\partial\Omega_\varepsilon$  is, effectively, replaced by the point constraint  $u_{m0}(x_0) = 0$ . Thus, the  $\varepsilon$ -dependent eigenfunction  $u_{m\varepsilon}$  does not tend to an eigenfunction of the biharmonic operator in the absence of the hole, but instead tends to an eigenfunction of the problem (1.6) with a point constraint. With (1.6) determining the leading-order behavior for  $\lambda_{m\varepsilon}$  and for  $u_{m\varepsilon}(x)$  for  $|x - x_0| \gg \mathcal{O}(\varepsilon)$ , in §5 we use the method of matched asymptotic expansions to determine an asymptotic expansion for  $\lambda_{m\varepsilon}$  as  $\varepsilon \rightarrow 0$  for two particular cases.

In §5.1 we consider the non-degenerate case where the condition  $\nabla u_{m0}(x_0) \neq 0$  holds. For this case, we show that the difference  $\lambda_{m\varepsilon} - \lambda_{m0}$  has an infinite order logarithmic expansion in powers of  $\nu = -1/\log \varepsilon$ , in which the shape of the hole determines the coefficients in the asymptotic expansion through a certain  $2 \times 2$  matrix  $\mathcal{M}$ . In addition, we show how to formulate a certain related problem that effectively sums this infinite order logarithmic expansion. Our asymptotic approach here is related to that used in [31] for the calculation of the drag and lift coefficients of a cylindrical body of asymmetric cross-section in a Low Reynolds number fluid flow. Our formal asymptotic results for this non-degenerate case  $\nabla u_{m0}(x_0) \neq 0$  are similar to those obtained using a different approach in [2]. In order to explicitly illustrate our results, we consider (1.5) for a unit disk that contains a hole of arbitrary shape centered at the origin of the disk. For this problem, the lowest eigenvalue  $\lambda_{00}$  of the limiting problem (1.6) with point constraint  $u_{00}(0) = 0$  has two independent eigenfunctions, which can be written in polar coordinate form as  $u_{00} = f(r) \cos \theta$  and  $u_{00} = f(r) \sin \theta$  for some  $f(r)$  with  $f(0) = 0$  (cf. [4]). By formulating and then numerically solving a simple problem that sums an infinite order logarithmic expansion for the eigenvalue, we show that the generic effect of a small hole of arbitrary shape centered at the origin is to split this limiting eigenvalue  $\lambda_{00}$  of multiplicity two into two distinct eigenvalue branches when  $0 < \varepsilon \ll 1$ .

In §5.2 we analyze (1.5) for the degenerate case where  $\nabla u_{m0}(x_0) = 0$ . For this case, a formal singular perturbation method is used to derive a three-term asymptotic expansion for  $\lambda_{m\varepsilon} - \lambda_{m0}$ . This is a new result not given in [2]. In particular, we obtain the leading-order estimate  $\lambda_{m\varepsilon} - \lambda_{m0} = \mathcal{O}([-\varepsilon \log \varepsilon]^2)$  as  $\varepsilon \rightarrow 0$ . When the small hole has a circular shape, the three-term asymptotic expansion is shown to depend only on the Hessian of the Green's function  $G(x; x_0)$  evaluated at  $x = x_0$ , where  $G$  satisfies  $\Delta^2 G - \lambda_{m0} G = \delta(x - x_0)$  in  $\Omega$  with  $G = \partial_n G = 0$  on  $\partial\Omega$ . Our asymptotic results are illustrated explicitly for the concentric annulus  $0 < \varepsilon < |x| < 1$ , and are compared very favorably with full numerical results.

As a way of motivating some of the novel features of the singular perturbation methodology used to study the problems in §3–5, in §2 we first consider three simple linear biharmonic boundary value problems (BVP's) in the concentric annulus  $0 < \varepsilon < |x| < 1$  in  $\mathbb{R}^2$  in the limit  $\varepsilon \rightarrow 0^+$ , and with the boundary conditions  $u = \partial_r u = 0$  on  $r \equiv |x| = \varepsilon$ . These simple model problems share several common features with the problems studied in §3–5. One key feature, is that in contrast to the study of singularly perturbed BVP's for second-order elliptic problems in perforated domains, the leading-order limiting problem as  $\varepsilon \rightarrow 0$  for our biharmonic BVP's is that the small hole is replaced by a point constraint for the limiting solution. The imposition of such a point constraint is impossible for solutions to Laplace's equation. However, since the biharmonic operator in 2-D has a free-space Green's function with a fundamental singularity  $|x - x_0|^2 \log |x - x_0|$ , which vanishes at  $x_0$ , such a point constraint is admissible for the biharmonic operator. In fact, biharmonic spline interpolation, which leads to only small oscillations in the

interpolant between adjacent interpolation points, explicitly exploits the idea that arbitrary point constraints can be imposed for the biharmonic operator in 2-D (cf. [34]). Finally, in §6 we conclude with a brief discussion of some related open problems.

## 2 Some Simple Singularly Perturbed Biharmonic Problems

In this section we consider three simple singularly perturbed biharmonic problems in the annulus  $0 < \varepsilon < |x| < 1$  in  $\mathbb{R}^2$  with  $\varepsilon \rightarrow 0^+$ . These model problems serve to illustrate the asymptotic methodology required to treat the linear and nonlinear biharmonic eigenvalue problems in §3 – §5 below. The first two model problems are formulated as

$$\Delta^2 u = 0, \quad x \in \Omega \setminus \Omega_\varepsilon, \quad (2.1 a)$$

$$u = f, \quad u_r = 0, \quad \text{on } r = 1; \quad u = u_r = 0, \quad r = \varepsilon. \quad (2.1 b)$$

Here  $\Omega$  is the unit disk centered at the origin and  $\Omega_\varepsilon \equiv \{x \mid |x| \leq \varepsilon\}$ . Two choices for  $f$  are considered: **Case I:**  $f = 1$ . **Case II:**  $f = \sin \theta$ . We obtain an exact solution for each of these two cases, and then reconstruct them with a singular perturbation analysis. The analysis will show some novel features of singularly perturbed biharmonic BVP's.

For **Case I** where  $f = 1$ , the radially symmetric solution to (2.1) is a linear combination of  $\{r^2, r^2 \log r, \log r, 1\}$ . The solution to  $\Delta^2 u = 0$ , which satisfies the conditions on  $r = 1$ , has the form

$$u = A(r^2 - 1) + Br^2 \log r - (2A + B) \log r + 1, \quad (2.2)$$

for any constants  $A$  and  $B$ . Upon imposing that  $u = u_r = 0$  on  $r = \varepsilon$ , we get two equations for  $A$  and  $B$

$$A = -\frac{B}{2} \left( 1 - \frac{2\varepsilon^2 \log \varepsilon}{1 - \varepsilon^2} \right), \quad A(1 + 2 \log \varepsilon - \varepsilon^2) + B(1 - \varepsilon^2) \log \varepsilon = 1. \quad (2.3)$$

Upon substituting the first equation for  $A$  into the second, we obtain that  $B$  satisfies

$$-\frac{B}{2} - \frac{B \log \varepsilon}{1 - \varepsilon^2} + \frac{B \varepsilon^2 \log \varepsilon}{1 - \varepsilon^2} + \frac{2\varepsilon^2 B (\log \varepsilon)^2}{(1 - \varepsilon^2)^2} + B \log \varepsilon = \frac{1}{1 - \varepsilon^2}, \quad (2.4)$$

which reduces to  $-B + 4\varepsilon^2 (\log \varepsilon)^2 B \sim 2 + \mathcal{O}(\varepsilon^2)$ . This determines  $B$ , and the first equation of (2.3) determines  $A$ . In this way, we get

$$B \sim -2 - 8\varepsilon^2 (\log \varepsilon)^2, \quad A \sim 1 + 4\varepsilon^2 (\log \varepsilon)^2. \quad (2.5)$$

From (2.5) and (2.2), we obtain that a two-term expansion in the outer region  $r \gg \mathcal{O}(\varepsilon)$  is

$$u \sim u_0(r) + \varepsilon^2 (\log \varepsilon)^2 u_1(r) + \mathcal{O}(\varepsilon^2 \log \varepsilon), \quad (2.6 a)$$

where  $u_0(r)$  and  $u_1(r)$  are defined by

$$u_0(r) = r^2 - 2r^2 \log r, \quad u_1 = 4(r^2 - 1) - 8r^2 \log r. \quad (2.6 b)$$

We emphasize that the leading-order outer solution  $u_0(r)$  satisfies the point constraint  $u_0(0) = 0$  and is not a  $C^2$  smooth function. Hence, in the limit of small hole radius, the  $\varepsilon$ -dependent solution does not tend to the unperturbed solution in the absence of the hole. This unperturbed solution would have  $B = 0$  and  $A = 0$  in (2.2), and consequently  $u \sim 1$  in the outer region. In fact, we note that  $u_0(r)$  can be written as  $u_0(r) = 1 - 16\pi G(r; 0)$ , where

$$G(r; 0) = \frac{1}{8\pi} \left( r^2 \log r - \frac{r^2}{2} + \frac{1}{2} \right), \quad (2.7)$$

is the biharmonic Green's function satisfying  $\Delta^2 G = \delta(x)$  with  $G = G_r = 0$  on  $r = 1$ .

Next, we show how to recover (2.6) from a matched asymptotic expansion analysis. In the outer region we expand the solution to (2.1) with  $f = 1$  as

$$u \sim w_0 + \sigma w_1 + \dots, \quad (2.8)$$

where  $\sigma \ll 1$  is an unknown gauge function, and where  $w_0$  satisfies the following problem with a point constraint:

$$\Delta^2 w_0 = 0, \quad 0 < r < 1; \quad w_0(1) = 1, \quad w_{0r}(1) = 0, \quad w_0(0) = 0. \quad (2.9)$$

Since  $G(0;0) = 1/(16\pi)$  from (2.7), the solution to (2.9) is  $w_0 = 1 - 16\pi G(r;0)$ , which yields

$$w_0 = r^2 - 2r^2 \log r. \quad (2.10)$$

The problem for  $w_1$  is

$$\Delta^2 w_1 = 0, \quad 0 < r < 1; \quad w_1(1) = w_{1r}(1) = 0, \quad (2.11)$$

which has the following solution in terms of unknown coefficients  $\alpha_1$  and  $\beta_1$ :

$$w_1 = \alpha_1 (r^2 - 1) + \beta_1 r^2 \log r - (2\alpha_1 + \beta_1) \log r. \quad (2.12)$$

The behavior of  $w_1$  as  $r \rightarrow 0$ , as found below by matching to the inner solution, will determine  $\alpha_1$  and  $\beta_1$ .

In the inner region we set  $r = \varepsilon\rho$  and obtain from (2.10) that terms of order  $\mathcal{O}(\varepsilon^2 \log \varepsilon)$  and  $\mathcal{O}(\varepsilon^2)$  will be generated in the inner region. Therefore, this suggests that in the inner region we must expand the solution as

$$v(\rho) = u(\varepsilon\rho) = (\varepsilon^2 \log \varepsilon) v_0(\rho) + \varepsilon^2 v_1(\rho) + \dots, \quad (2.13)$$

where  $v_0$  and  $v_1$  must satisfy  $v_j(1) = v_{j\rho}(1) = 0$  for  $j = 0, 1$ . Therefore, we obtain for  $j = 0, 1$  that

$$v_j = A_j (\rho^2 - 1) + B_j \rho^2 \log \rho - (2A_j + B_j) \log \rho. \quad (2.14)$$

We substitute (2.14) into (2.13) and write the resulting expression in terms of the outer variable  $r = \varepsilon\rho$ . A short calculation shows that the far-field behavior of (2.13) as  $\rho \rightarrow \infty$ , when written in the outer  $r$  variable, is

$$v \sim -(\log \varepsilon)^2 B_0 r^2 + (\log \varepsilon) [(A_0 - B_1)r^2 + B_0 r^2 \log r] + A_1 r^2 + B_1 r^2 \log r + (2A_0 + B_0) \varepsilon^2 (\log \varepsilon)^2 + \mathcal{O}(\varepsilon^2 \log \varepsilon). \quad (2.15)$$

In contrast, the two-term outer solution from (2.8), (2.10), and (2.12), is

$$u \sim r^2 - 2r^2 \log r + \sigma [\alpha_1 (r^2 - 1) + \beta_1 r^2 \log r - (2\alpha_1 + \beta_1) \log r] + \dots. \quad (2.16)$$

Upon comparing (2.16) with (2.15), we conclude that

$$B_0 = 0, \quad B_1 = A_0, \quad A_1 = 1, \quad B_1 = -2, \quad \sigma = \varepsilon^2 (\log \varepsilon)^2. \quad (2.17)$$

This leaves the unmatched constant term  $-4\varepsilon^2(\log \varepsilon)^2$  on the right-hand side of (2.15). Consequently, it follows that the outer correction  $w_1$  in (2.12) is bounded as  $r \rightarrow 0$  and has the point constraint  $w_1(0) = -4$ . Consequently,  $2\alpha_1 + \beta_1 = 0$  and  $\alpha_1 = 4$  in (2.16). This gives  $\beta_1 = -8$ , and specifies the second-order outer correction term as

$$w_1 = 4 (r^2 - 1) - 8r^2 \log r. \quad (2.18)$$

This expression reproduces that obtained in (2.6) from the perturbation of the exact solution.

The key feature in this model problem is that it is impossible to generate an inner solution that will match to an outer solution that has a prescribed value of  $u_0(0) \neq 0$ . The inner solution is a linear combination of

$\{\rho^2, \rho^2 \log \rho, \log \rho, 1\}$ . Upon setting the coefficients of the  $\rho^2$  and  $\rho^2 \log \rho$  term to zero, and even allowing for a logarithmic gauge function pre-multiplying the  $\log \rho$  term, we would have an over-constrained problem in satisfying the two conditions on  $\rho = 1$  and a prescribed matching condition at infinity. Thus, we must instead specify the point constraint  $u_0(0) = 0$ , so that the outer solution has a singularity of order  $\mathcal{O}(r^2 \log r)$  as  $r \rightarrow 0$ . This model problem is closely related to the biharmonic nonlinear eigenvalue problem analyzed in §4.

Next, we consider **Case II** where  $f = \sin \theta$  in (2.1). The solution to this model problem contains an infinite-order logarithmic expansion, which we show how to sum. The exact solution to (2.1) with  $f = \sin \theta$  is a linear combination of  $\{r^3, r \log r, r, r^{-1}\} \sin \theta$ . Thus, the exact solution to (2.1), which satisfies the two conditions on  $r = 1$ , is

$$u = \left( Ar^3 + Br \log r + \left( -2A + \frac{1}{2} - \frac{B}{2} \right) r + \left( \frac{1}{2} + A + \frac{B}{2} \right) \frac{1}{r} \right) \sin \theta, \quad (2.19)$$

for any constants  $A$  and  $B$ . Then, by imposing that  $u = u_r = 0$  on  $r = \varepsilon$ , we get two equations for  $A$  and  $B$

$$A\varepsilon^3 + B\varepsilon \log \varepsilon + \left( -2A + \frac{1}{2} - \frac{B}{2} \right) \varepsilon + \left( \frac{1}{2} + A + \frac{B}{2} \right) \varepsilon^{-1} = 0, \quad (2.20 a)$$

$$3A\varepsilon^2 + B + B \log \varepsilon + \left( -2A + \frac{1}{2} - \frac{B}{2} \right) - \left( \frac{1}{2} + A + \frac{B}{2} \right) \varepsilon^{-2} = 0. \quad (2.20 b)$$

By comparing the  $\mathcal{O}(\varepsilon^{-1})$  and  $\mathcal{O}(\varepsilon^{-2})$  terms in (2.20), it is convenient to define  $\kappa$  by

$$\frac{1}{2} + A + \frac{B}{2} = \kappa \varepsilon^2, \quad (2.21)$$

where  $\kappa$  is an  $\mathcal{O}(1)$  constant to be found. Substituting (2.21) into (2.20), and neglecting the higher order  $A\varepsilon^3$  and  $3A\varepsilon^2$  terms in (2.20), we obtain the approximate system

$$B \log \varepsilon + \left( -2A + \frac{1}{2} - \frac{B}{2} \right) \approx -\kappa, \quad B + B \log \varepsilon + \left( -2A + \frac{1}{2} - \frac{B}{2} \right) \approx \kappa. \quad (2.22)$$

By adding the two equations above to eliminate  $\kappa$ , we obtain that

$$B + 2B \log \varepsilon + (-4A + 1 - B) = 0. \quad (2.23)$$

From (2.23), together with  $A \sim -(1+B)/2$  from (2.21), we conclude that

$$B \sim \frac{3\nu}{2-\nu}, \quad A = 1 - \frac{3}{2-\nu}, \quad \text{where } \nu \equiv \frac{-1}{\log [\varepsilon e^{1/2}]}. \quad (2.24)$$

Finally, substituting (2.24) into (2.19), we obtain that the outer solution in  $r \gg \mathcal{O}(\varepsilon)$  has the asymptotics

$$u \sim \left( (1 - \tilde{A})r^3 + \nu \tilde{A} r \log r + \tilde{A} r \right) \sin \theta, \quad (2.25 a)$$

where  $\tilde{A}$  is defined by

$$\tilde{A} \equiv \frac{3}{2-\nu}, \quad \nu \equiv \frac{-1}{\log [\varepsilon e^{1/2}]}. \quad (2.25 b)$$

We remark that (2.25) is an infinite-order logarithmic series approximation to the exact solution. However, it does not contain transcendentally small terms of algebraic order in  $\varepsilon$  as  $\varepsilon \rightarrow 0$ .

Next, we show how to recover (2.25) by formulating an appropriate singularity behavior near  $r = 0$ , which has the effect of specifying both the singular and the regular part of a singularity structure.

In the inner region, with inner variable  $\rho \equiv \varepsilon^{-1}r$ , we look for an inner solution of the form  $v_0(\rho) \sin \theta$  where  $v_0$  has growth  $\mathcal{O}(\rho \log \rho)$  as  $\rho \rightarrow \infty$  and satisfies  $v_0(1) = v_{0\rho}(1) = 0$ . Upon multiplying this solution by  $\varepsilon \nu C(\nu)$ , where  $C(\nu)$



is a constant with  $C = \mathcal{O}(1)$  as  $\nu \rightarrow 0$ , we obtain that the inner solution has the form

$$v(\rho, \theta) = u(\varepsilon\rho, \theta) \sim \varepsilon\nu C(\nu) \left( \rho \log \rho - \frac{\rho}{2} + \frac{1}{2\rho} \right) \sin \theta. \quad (2.26)$$

Here  $\nu \equiv -1/\log[\varepsilon e^{1/2}]$  and  $C(\nu)$  is a function of  $\nu$  to be found. The extra factor of  $\varepsilon$  in (2.26) is needed since the solution in the outer region is not algebraically large as  $\varepsilon \rightarrow 0$ . Now letting  $\rho \rightarrow \infty$ , and writing (2.26) in terms of the outer variable  $r = \varepsilon\rho$ , we obtain that the far-field form of (2.26) is

$$v \sim (C\nu r \log r + Cr) \sin \theta. \quad (2.27)$$

Therefore, the outer solution  $u_H$  to (2.1), which sums all the logarithmic terms in powers of  $\nu$ , must satisfy

$$\Delta^2 u_H = 0, \quad 0 < r < 1; \quad u_H = \sin \theta, \quad \partial_r u_H = 0, \quad \text{on } r = 1, \quad (2.28 a)$$

$$u_H = (C\nu r \log r + Cr) \sin \theta + o(r), \quad \text{as } r \rightarrow 0. \quad (2.28 b)$$

The singularity structure in (2.28 b) specifies both the strength of the singular term  $C\nu r \log r \sin \theta$  in addition to the specific form  $Cr \sin \theta$  for the regular part. As such, (2.28 b) provides an equation for the determination of  $C$ .

The solution to (2.28 a) is

$$u_H = \left( \alpha r^3 + \beta r \log r + \left( -2\alpha + \frac{1}{2} - \frac{\beta}{2} \right) r + \left( \frac{1}{2} + \alpha + \frac{\beta}{2} \right) \frac{1}{r} \right) \sin \theta, \quad (2.29)$$

while the singularity condition (2.28 b) yields the three equations

$$\beta = C\nu, \quad -2\alpha + \frac{1}{2} - \frac{\beta}{2} = C, \quad \frac{1}{2} + \alpha + \frac{\beta}{2} = 0, \quad (2.30)$$

for  $\alpha$ ,  $\beta$ , and  $C$ . We solve this system to obtain

$$\beta = C\nu, \quad C = \frac{3}{2 - \nu}, \quad \alpha = 1 - C. \quad (2.31)$$

Upon substituting (2.31) into (2.29), and identifying  $\tilde{A} = C$ , we obtain that the resulting expression agrees exactly with the result (2.25) derived from the asymptotic expansion of the exact solution.

This simple model problem, whose solution contains an infinite-order logarithmic expansion, is closely related to the linear biharmonic eigenvalue problems of §5 and to the low Reynolds number fluid flow problem of [31].

## 2.1 A Model Biharmonic Problem with Lower Order Terms

Next, we consider a mixed biharmonic problem in the annulus  $\varepsilon < r < 1$  in  $\mathbb{R}^2$  formulated as

$$\delta \Delta^2 u - \Delta u = 0, \quad \varepsilon < r < 1, \quad (2.32 a)$$

$$u = 1, \quad u_r = 0, \quad \text{on } r = 1; \quad u = u_r = 0, \quad \text{on } r = \varepsilon. \quad (2.32 b)$$

We will consider (2.32) for various scalings of  $\delta(\varepsilon) = \delta_0^2 \varepsilon^q \ll 1$  for  $q > 0$  where  $\delta_0 = \mathcal{O}(1)$ . The parameter  $q > 0$  is used to control the relative importance of the biharmonic and Laplacian terms in (2.32 a) in the inner region, and as a result can change the character of the inner solution. This problem is closely related to the biharmonic nonlinear eigenvalue problem of §3.

We first consider the case  $\delta = \delta_0^2 \varepsilon^2$ . The asymptotic solution consists of two boundary layers; one in the vicinity of  $r = 1$ , and the other near  $r = \varepsilon$ . A simple boundary layer analysis shows that the boundary layer near  $r = 1$  contributes a correction term of order  $\mathcal{O}(\sqrt{\delta}) = \mathcal{O}(\varepsilon)$ , and hence can be neglected in comparison with logarithmic

terms of the order  $\mathcal{O}(\nu)$ , where  $\nu \equiv -1/\log \varepsilon$ , generated from the inner region near the hole. As such, we impose that the outer solution for  $u$ , labeled by  $u_0$ , satisfies

$$\Delta u_0 = 0, \quad 0 < r < 1; \quad u_0(1) = 1; \quad u_0 \sim A\nu \log r, \quad \text{as } r \rightarrow 0, \quad (2.33)$$

so that  $u_0 = 1 + A\nu \log r$ . In terms of the inner variable  $\rho = r/\varepsilon$ , the local behavior of this solution is

$$u_0 \sim 1 - A + A\nu \log \rho. \quad (2.34)$$

Therefore, by imposing the singularity condition in (2.33) as  $r \rightarrow 0$  we have to leading order that  $u_0$  has an approximate ‘‘point constraint’’ with  $u_0 \sim 1 - A + \mathcal{O}(\nu)$ .

In the inner region near the hole, we introduce the local variables  $v$  and  $\rho$  defined by  $v(\rho) = u(\varepsilon\rho)$  and  $\rho = r/\varepsilon$ . Since  $\delta = \delta_0\varepsilon^2$ , we obtain from (2.32) that  $v$  satisfies

$$\Delta^2 v - \eta^2 \Delta v = 0, \quad \rho > 1; \quad v(1) = v'(1) = 0, \quad \eta \equiv 1/\delta_0. \quad (2.35)$$

The general solution of (2.35) is a linear combination of  $\{K_0(\eta\rho), I_0(\eta\rho), \log \rho, 1\}$ , where  $I_0(z)$  and  $K_0(z)$  are the modified Bessel functions of order zero. By eliminating the exponentially growing  $I_0$  term, we obtain that

$$v = d_0 + d_1 \log \rho + d_2 K_0(\eta\rho), \quad (2.36)$$

for some constants  $d_0$ ,  $d_1$ , and  $d_2$ . Since  $K_0(z)$  decays exponentially as  $z \rightarrow \infty$ , the matching condition that (2.36) as  $\rho \rightarrow \infty$  agrees with (2.34) yields that  $d_0 = 1 - A$  and  $d_1 = A\nu$ . Two further equations are obtained by setting  $v(1) = v'(1) = 0$ . In this way, we obtain in terms of  $\eta = 1/\delta_0$  and  $\nu = -1/\log \varepsilon$  that

$$A = \left[ 1 + \frac{\nu K_0(\eta)}{\eta K_0'(\eta)} \right]^{-1}, \quad d_2 = \frac{(A-1)}{K_0(\eta)}, \quad d_0 = 1 - A, \quad d_1 = A\nu. \quad (2.37)$$

This result is not uniformly valid as  $\eta \rightarrow 0$ , corresponding to  $\delta_0 \rightarrow \infty$ . In this limit, we use  $K_0(z) \sim -\log z + \log 2 - \gamma_e$  as  $z \rightarrow 0$ , where  $\gamma_e$  is Euler’s constant, to obtain that  $A \sim [1 + (\log \eta - b)/\log \varepsilon]^{-1}$ , with  $b \equiv \log 2 - \gamma_e$ . Therefore, (2.37) is not uniformly valid when  $\eta = \mathcal{O}(\varepsilon^q)$  with  $q > 0$ , corresponding to  $\delta_0 = \mathcal{O}(\varepsilon^{-q})$ .

Therefore, we must consider the case where  $\delta_0 = \tilde{\delta}_0 \varepsilon^{-q}$  with  $\tilde{\delta}_0 = \mathcal{O}(1)$  and  $0 < q < 1$ . Then, the solution to

$$\tilde{\delta}_0 \varepsilon^{2-2q} \Delta^2 u - \Delta u = 0, \quad \varepsilon < r < 1, \quad (2.38 a)$$

$$u = 1, \quad u_r = 0, \quad \text{on } r = 1; \quad u = u_r = 0, \quad \text{on } r = \varepsilon, \quad (2.38 b)$$

has a multiple deck structure near the hole. In the inner-most region,  $r = \mathcal{O}(\varepsilon)$ , the biharmonic term dominates, while in the mid-inner layer with  $r = \mathcal{O}(\varepsilon^{1-q})$ , both terms in (2.38 a) balance.

In the mid-inner layer, we define the local variables  $w$  and  $y$  by  $y = r/\varepsilon^{1-q}$  and  $w(y) = u(\varepsilon^{1-q}y)$ , so that

$$\Delta_y^2 w - \tilde{\eta}^2 \Delta_y w = 0, \quad \tilde{\eta} = 1/\tilde{\delta}_0. \quad (2.39)$$

The solution to this problem that has no exponential growth as  $y \rightarrow \infty$  is

$$w = c_0 + c_1 \log y + c_2 K_0(\tilde{\eta}y). \quad (2.40)$$

Next, we must impose the point constraint that  $w \rightarrow 0$  as  $y \rightarrow 0$ , corresponding to the limiting behavior at the edge of the inner-most region near the hole. Since  $K_0(z) \sim -\log z + \log 2 - \gamma_e$  as  $z \rightarrow 0$ , the condition that  $w \rightarrow 0$  as  $y \rightarrow 0$  in (2.40) yields that  $c_1 = c_2$  and  $c_0 = c_2(\log \tilde{\eta} - \log 2 + \gamma_e)$ . Therefore, in terms of one constant  $c_2$ , the mid-inner solution is

$$w = c_2 \log \left( \frac{\tilde{\eta}}{2} \right) + \gamma_e c_2 + c_2 (\log y + K_0(\tilde{\eta}y)). \quad (2.41)$$

The outer solution for (2.38) is given by  $u_0 = 1 + A\nu_q \log r$  where  $\nu_q \equiv -1/\log(\varepsilon^{1-q})$ , so that by calculating the local behavior of this outer solution in terms of  $y = r/\varepsilon^{1-q}$ , we obtain that the required far-field behavior of (2.41) is that  $w \sim 1 - A + A\nu_q \log y$ . This matching condition determines  $A$  and  $c_2$  by

$$A = \left[ 1 + \nu_q \gamma_e + \nu_q \log \left( \frac{\tilde{\eta}}{2} \right) \right]^{-1}, \quad c_2 = A\nu_q, \quad \nu_q \equiv \varepsilon^{1-q}. \quad (2.42)$$

Finally, by expanding (2.41) as  $y \rightarrow 0$ , we obtain that  $w = \mathcal{O}(y^2 \log y)$  as  $y \rightarrow 0$ . Therefore, to leading order in the inner-most region, where we have the balance  $\Delta_\rho^2 v = 0$  with  $\rho = r/\varepsilon$ , we can take  $v = 0$  to leading order. A more precise calculation of the solution in the inner-most layer is required for the biharmonic nonlinear eigenvalue problem of §3.

### 3 Concentration in a Singularly Perturbed Nonlinear Biharmonic Eigenvalue Problem

In the limit  $\delta \rightarrow 0$  we now construct a solution with one concentration point to the singularly perturbed biharmonic nonlinear eigenvalue problem in an arbitrary 2-D domain, formulated as

$$-\delta \Delta^2 u + \Delta u = \frac{\lambda}{(1+u)^2}, \quad x \in \Omega; \quad u = \partial_n u = 0, \quad x \in \partial\Omega. \quad (3.1)$$

In the limit  $\delta \rightarrow 0$ , we characterize such a localized solution by  $\lambda \rightarrow 0$ ,  $u(x_0) \rightarrow -1^+$ , and  $\nabla u(x_0) = 0$ , where the concentration point  $x_0$  is to be found. The concentration point  $x_0$  corresponds to the minimum value of  $u$  in  $\Omega$ , and our solution below will satisfy  $u(x_0) + 1 = \delta \rightarrow 0^+$  as  $\delta \rightarrow 0$ . The asymptotic analysis required to analyze this problem is similar to that for the model problem in §2.1.

We expand  $\lambda$  and the outer solution  $u_0$  for  $u$  in terms of some unknown gauge function  $\nu \ll 1$  as

$$u = \nu u_0 + \nu^2 u_1 + \nu^3 u_2 + \dots, \quad \lambda = \nu \lambda_0 + \nu^2 \lambda_1 + \nu^3 \lambda_2 + \dots. \quad (3.2)$$

As for the model problem in §2.1, we assume that  $\nu^k \gg \delta^{1/2}$  for any  $k > 0$  so that we can neglect the boundary layer term near  $\partial\Omega$  in comparison with the effect of the inner solution near the concentration point  $x_0$ , which generates logarithmic correction terms for the outer solution. We substitute (3.2) into (3.1), and allow  $u_j$  to have a logarithmic singularity at the unknown  $x_0$  so that the  $u_j$  for  $j = 0, 1, 2$ , satisfy

$$\Delta u_0 = \lambda_0, \quad x \in \Omega \setminus \{x_0\}; \quad u_0 \sim a_0 \log |x - x_0|, \quad \text{as } x \rightarrow x_0, \quad (3.3 a)$$

$$\Delta u_1 = \lambda_1 - 2\lambda_0 u_0, \quad x \in \Omega \setminus \{x_0\}; \quad u_1 \sim a_1 \log |x - x_0|, \quad \text{as } x \rightarrow x_0, \quad (3.3 b)$$

$$\Delta u_2 = \lambda_2 - 2\lambda_1 u_0 - 2\lambda_0 u_1 + 3\lambda_0 u_0^2, \quad x \in \Omega \setminus \{x_0\}; \quad u_2 \sim a_2 \log |x - x_0|, \quad \text{as } x \rightarrow x_0. \quad (3.3 c)$$

Assuming, as we have done, that  $\delta^{1/2} \ll \nu^k$  for any  $k > 0$ , a boundary layer analysis near  $\partial\Omega$  shows that the appropriate asymptotic boundary condition for  $u_j$  on  $\partial\Omega$  is that  $u_j = 0$  for  $x \in \partial\Omega$  and  $j = 0, 1, 2$ .

We decompose the solution to (3.3 a) for  $u_0$  as

$$u_0(x) = \lambda_0 u_{0p}(x) + 2\pi a_0 G(x; x_0), \quad (3.4)$$

where  $u_{0p}(x)$  is a smooth solution satisfying

$$\Delta u_{0p} = 1, \quad x \in \Omega; \quad u_{0p} = 0, \quad x \in \partial\Omega, \quad (3.5)$$

and  $G(x; x_0)$  is the Laplacian Green's function satisfying

$$\Delta G = \delta(x - x_0), \quad x \in \Omega; \quad G = 0, \quad x \in \partial\Omega. \quad (3.6 a)$$

We can decompose  $G(x; x_0)$  as

$$G(x; x_0) = \frac{1}{2\pi} \log |x - x_0| + R(x; x_0), \quad (3.6 b)$$

where  $R(x; x_0)$  is the smooth regular part of  $G(x; x_0)$ . Similarly, the solution  $u_1$  to (3.3 b) is decomposed as

$$u_1(x) = \lambda_1 u_{0p}(x) - 2\lambda_0^2 u_{1p}(x) - 4\pi\lambda_0 a_0 u_{1g}(x) + 2\pi a_1 G(x; x_0), \quad (3.7)$$

where  $u_{1p}(x)$  and  $u_{1g}(x)$  satisfy

$$\Delta u_{1p} = u_{0p}, \quad x \in \Omega; \quad u_{1p} = 0, \quad x \in \partial\Omega, \quad (3.8 a)$$

$$\Delta u_{1g} = G(x; x_0), \quad x \in \Omega; \quad u_{1g} = 0, \quad x \in \partial\Omega. \quad (3.8 b)$$

For the mid-inner region we introduce the new variable  $s \equiv \gamma^{-1}(x - x_0)$ , with  $|s| = \rho$ , where  $\gamma \ll 1$  is to be found. As in the analysis of Laplacian eigenvalue problems with holes (cf. [32]), we then choose  $\nu$  in terms of  $\gamma$  as

$$\nu = -1/\log \gamma. \quad (3.9)$$

Next, we expand the three-term approximation (3.2) for the outer solution as  $x \rightarrow x_0$  using (3.4), (3.7), (3.9), and  $u_2 \sim a_2 \log |x - x_0|$  as  $x \rightarrow x_0$ .

First, to satisfy the concentration condition  $u_0 \sim -1$  as  $x \rightarrow x_0$ , we must choose  $a_0$  in (3.3 a) as

$$a_0 = 1. \quad (3.10)$$

Next, to eliminate the gradient term as  $x \rightarrow x_0$ , so that the inner solution becomes radially symmetric about  $x_0$ , we must choose the leading-order term in the concentration point  $x_0$  to be the root of

$$\lambda_0 \nabla_x u_{0p}(x)|_{x=x_0} + 2\pi \nabla_x R(x; x_0)|_{x=x_0} = 0. \quad (3.11)$$

Then, from (3.2), (3.4), (3.7), and (3.9), we obtain the following local behavior of the outer solution when written in terms of the mid-inner radial variable  $\rho$ :

$$u \sim -1 + \nu(\xi_1 - a_1 + \log \rho) + \nu^2(\xi_2 - a_2 + a_1 \log \rho) + \mathcal{O}(\nu^3). \quad (3.12)$$

Here  $\nu \equiv -1/\log \gamma$ , while  $\xi_1$  and  $\xi_2$  are defined by

$$\xi_1 = \lambda_0 u_{0p}(x_0) + 2\pi R_{00}, \quad \xi_2 = \lambda_1 u_{0p}(x_0) - 2\lambda_0^2 u_{1p}(x_0) - 4\pi\lambda_0 u_{1g}(x_0) + 2\pi a_1 R_{00}, \quad (3.13)$$

where  $R_{00} \equiv R(x_0; x_0)$ .

In the mid-inner region we seek a radially symmetric solution in terms of the new variables  $\rho$  and  $v$  defined by

$$u = -1 + \nu v, \quad s = \gamma^{-1}(x - x_0), \quad \rho \equiv |s|, \quad \nu = -1/\log \gamma. \quad (3.14)$$

Then, from (3.1), we obtain that  $v$  satisfies

$$-\frac{\delta}{\gamma^2} \Delta_\rho^2 v + \Delta_\rho v = \gamma^2 (\log \gamma)^2 \frac{[\lambda_0 + \nu\lambda_1 + \dots]}{v^2}, \quad 0 < \rho < \infty, \quad (3.15)$$

where  $\Delta_\rho$  is the radially symmetric part of the Laplacian in terms of  $\rho$ . This suggests that we choose

$$\gamma = \sqrt{\delta}. \quad (3.16)$$

Then, since  $\gamma^2 (\log \gamma)^2 \ll 1$ , we look for a two-term expansion for the solution to (3.15) in the form

$$v \sim v_0 + \nu v_1 + \dots. \quad (3.17)$$

Upon substituting (3.17) into (3.15), and noting the matching condition for  $\rho \rightarrow \infty$ , as obtained from (3.12) and (3.14), we obtain that  $v_0$  and  $v_1$  satisfy

$$-\Delta_\rho^2 v_0 + \Delta_\rho v_0 = 0, \quad 0 < \rho < \infty; \quad v_0 \sim \xi_1 - a_1 + \log \rho, \quad \text{as } \rho \rightarrow \infty. \quad (3.18 a)$$

$$-\Delta_\rho^2 v_1 + \Delta_\rho v_1 = 0, \quad 0 < \rho < \infty; \quad v_1 \sim \xi_2 - a_2 + a_1 \log \rho, \quad \text{as } \rho \rightarrow \infty. \quad (3.18 b)$$

Since the general solution to (3.18) is a linear combination of  $\{K_0(\rho), I_0(\rho), \log \rho, 1\}$ , we must impose that the coefficient of  $I_0(\rho)$  vanishes in order to satisfy the far-field condition in (3.18 a) and (3.18 b). In addition, similar to the model problem of §2.1, we look for a solution to (3.18) for which  $v_0$  and  $v_1$  are singularity-free as  $\rho \rightarrow 0$ . In this way, we obtain that  $v_0$  and  $v_1$  are given explicitly by

$$v_0 = \xi_1 - a_1 + \log \rho + K_0(\rho); \quad v_1 = -a_2 + \xi_2 + a_1 \log \rho + a_1 K_0(\rho). \quad (3.19)$$

Next, in order to construct a solution with concentration at  $x = x_0$ , we will choose  $a_1$  and  $a_2$  so that  $v_0 \rightarrow 0$  and  $v_1 \rightarrow 0$  as  $\rho \rightarrow 0$ . By using the well-known asymptotics for  $K_0(z)$  as  $z \rightarrow 0$  given by

$$K_0(z) = -\log z + \log 2 - \gamma_e - \frac{z^2}{4} \log z + \kappa_0 z^2 + \mathcal{O}(z^4 \log z), \quad \text{as } z \rightarrow 0; \quad \kappa_0 \equiv \frac{1}{4} (1 - \gamma_e + \log 2), \quad (3.20)$$

where  $\gamma_e$  is Euler's constant, the conditions that  $v_j \rightarrow 0$  as  $\rho \rightarrow 0$  for  $j = 0, 1$  determine  $a_1$  and  $a_2$  in (3.19) as

$$a_1 = \xi_1 + \log 2 - \gamma_e, \quad a_2 = \xi_2 + a_1 (\log 2 - \gamma_e), \quad (3.21)$$

where  $\xi_j$  for  $j = 1, 2$  are defined in (3.13). With  $a_1$  and  $a_2$  now known, the problems (3.3 b) and (3.3 c) for the outer correction terms  $u_1$  and  $u_2$ , respectively, can be solved uniquely. Moreover, the first two terms in the mid-inner expansion (3.17), given in (3.19), become

$$v_0 = \gamma_e - \log 2 + \log \rho + K_0(\rho); \quad v_1 = a_1 (\gamma_e - \log 2) + a_1 [\log \rho + K_0(\rho)]. \quad (3.22)$$

Then, from (3.20) and (3.22), we conclude that  $v_0 = \mathcal{O}(\rho^2 \log \rho)$  as  $\rho \rightarrow 0$ .

For the special case of the unit disk, we readily calculate that  $x_0 = 0$ ,  $G(x; 0) = 1/(2\pi) \log r$  and  $R_{00} = 0$  where  $r = |x|$ . Moreover, the explicit solutions to (3.5) and (3.8) are

$$u_{0p} = \frac{1}{4}(r^2 - 1), \quad u_{1p} = \frac{r^4}{64} - \frac{r^2}{16} + \frac{3}{64}, \quad u_{1g} = \frac{1}{8\pi} (r^2 \log r + 1 - r^2). \quad (3.23)$$

From (3.13), this determines  $\xi_1$  and  $\xi_2$  as

$$\xi_1 = -\frac{\lambda_0}{4}, \quad \xi_2 = -\frac{\lambda_1}{4} - \frac{3\lambda_0^2}{32} - \frac{\lambda_0}{2}. \quad (3.24)$$

Finally, from (3.21), we obtain that

$$a_1 = -\frac{\lambda_0}{4} + \log 2 - \gamma_e, \quad a_2 = a_1 (\log 2 - \gamma_e) - \frac{\lambda_1}{4} - \frac{3\lambda_0^2}{32} - \frac{\lambda_0}{2}. \quad (3.25)$$

Next, we construct a solution in the inner-most layer that balances the biharmonic and nonlinear terms in (3.1). In terms of the mid-inner variables  $\rho$  and  $v$ , in the inner-most layer we define  $w$  and a new radial variable  $y$  by

$$y = \rho/\gamma, \quad v = (-\gamma^2 \log \gamma) w. \quad (3.26)$$

The scaling for  $v$  in (3.26) is motivated by the limiting behavior  $v_0 = \mathcal{O}(\rho^2 \log \rho)$  as  $\rho \rightarrow 0$  as obtained from (3.22) and (3.20). In terms of the inner-most variable  $y$ , the local behavior of the two-term mid-inner expansion, as obtained from (3.17), (3.22), and (3.20), is

$$v \sim (-\gamma^2 \log \gamma) \left[ \frac{y^2}{4} + \nu \left( -\frac{y^2}{4} \log y + \left( \kappa_0 + \frac{a_1}{4} \right) y^2 \right) + \nu^2 \left( -\frac{a_1 y^2}{4} \log y + \mathcal{O}(y^2) \right) + \dots \right]. \quad (3.27)$$

With  $v = (-\gamma^2 \log \gamma) w$ , (3.27) gives the far-field behavior for a three-term expansion for the inner-most solution  $w$ . In terms of the new variables (3.26), (3.15) becomes

$$-\Delta_y^2 w + \gamma^2 \Delta_y w = \frac{\nu}{w^2} [\lambda_0 + \nu \lambda_1 + \dots], \quad 0 \leq y < \infty. \quad (3.28)$$

Therefore, we must expand the inner-most solution  $w$  as

$$w = w_0 + \nu w_1 + \nu^2 w_2 + \dots. \quad (3.29)$$

In terms of the original variable  $u$ , the expansion has the form

$$u = -1 + \nu v = -1 + \nu \gamma^2 (-\log \gamma) w = -1 + \gamma^2 (w_0 + \nu w_1 + \nu^2 w_2 + \dots). \quad (3.30)$$

Upon substituting (3.29) into (3.28), and by using  $v = (-\gamma^2 \log \gamma) w$  in the matching condition (3.27), we obtain that the  $w_j$  for  $j = 0, 1, 2$  satisfy

$$-\Delta_y^2 w_0 = 0, \quad 0 \leq y < \infty; \quad w_0 \sim \frac{y^2}{4}, \quad \text{as } y \rightarrow \infty, \quad (3.31 a)$$

$$-\Delta_y^2 w_1 = \frac{\lambda_0}{w_0^2}, \quad 0 \leq y < \infty; \quad w_1 \sim -\frac{y^2}{4} \log y + \left(\kappa_0 + \frac{a_1}{4}\right) y^2, \quad \text{as } y \rightarrow \infty, \quad (3.31 b)$$

$$-\Delta_y^2 w_2 = \frac{\lambda_1}{w_0^2} - \frac{2\lambda_0 w_1}{w_0^3}, \quad 0 \leq y < \infty; \quad w_2 = -\frac{a_1 y^2}{4} \log y + \mathcal{O}(y^2), \quad \text{as } y \rightarrow \infty. \quad (3.31 c)$$

Finally, to complete the formulation of the problems for  $w_j$  for  $j \geq 0$ , we will impose that

$$w_0(0) = 1, \quad w_j(0) = 0, \quad \text{for } j \geq 1; \quad w_j'(0) = w_j''(0) = 0, \quad \text{for } j \geq 0. \quad (3.31 d)$$

From (3.30) and (3.16), the condition  $w_0(0) = 1$  with  $w_j(0) = 0$  for  $j \geq 1$  is equivalent to imposing that  $u(x_0) = -1 + \gamma^2 = -1 + \delta$ . The conditions on the derivatives in (3.31 d) are the usual radial symmetry conditions.

The solution to (3.31 a) and (3.31 d) for  $w_0$  is

$$w_0 = 1 + \frac{y^2}{4}, \quad (3.32)$$

which generates an unmatched constant term. This constant term is accounted for below by inserting appropriate switchback terms into the mid-inner expansion. Next, we integrate (3.31 b) over a large circle  $|y| = L$ , with  $L \gg 1$ , and we take the limit  $L \rightarrow \infty$  to obtain that

$$\lim_{L \rightarrow \infty} \left[ y \frac{\partial}{\partial y} (\Delta_y w_1) \Big|_{y=L} \right] = -\lambda_0 \int_0^\infty \frac{y}{(1 + y^2/4)^2} dy. \quad (3.33)$$

Upon using the far-field behavior for  $w_1$  in (3.31 b), and by evaluating the integral in (3.33), we get that

$$\lambda_0 = 1/2. \quad (3.34)$$

The condition that  $w_1 + y^2/4 \log y \sim (\kappa_0 + a_1/4) |y|^2$  as  $|y| \rightarrow \infty$ , together with  $w_1(0) = w_1'(0) = w_1''(0) = 0$ , then determines  $w_1$  uniquely. In particular, upon integrating the equation for  $w_1$ , we readily derive that

$$w_1'(y) = \zeta y - \frac{1}{y} \left( 1 + \frac{y^2}{4} \right) \log \left( 1 + \frac{y^2}{4} \right), \quad \zeta \equiv -\frac{1}{4} + 2 \left( \kappa_0 + \frac{a_1}{4} \right) - \frac{\log 2}{2}. \quad (3.35)$$

To determine  $\lambda_1$ , we integrate (3.31 c) over a large circle  $|y| = L$ , with  $L \gg 1$ , and take the limit  $L \rightarrow \infty$  to obtain

$$\lim_{L \rightarrow \infty} \left[ y \frac{\partial}{\partial y} (\Delta_y w_2) \Big|_{y=L} \right] = -\lambda_1 \int_0^\infty \frac{y}{w_0^2} dy + 2\lambda_1 \int_0^\infty \frac{y w_1}{w_0^3} dy. \quad (3.36)$$

We use the far-field behavior for  $w_2$  in (3.31 c) to calculate  $\Delta_y w_2 \sim -a_1 \log y$  as  $y \rightarrow \infty$ . In addition, upon using

$\int_0^\infty (y/w_0^2) dy = 2$  and, and by integrating the second integral on the right-hand side of (3.36) by parts using  $w_1(0) = 0$ , we obtain that

$$a_1 = 2\lambda_1 - 2\lambda_0 \left[ 2\zeta - \int_0^\infty \frac{\log(1+y^2/4)}{y(1+y^2/4)} dy \right] = 2\lambda_1 - 4\lambda_0\zeta + \lambda_0 \int_0^\infty \frac{\log(1+u)}{u(1+u)} du. \quad (3.37)$$

Since the integral in the second equality in (3.37) is  $\pi^2/6$ , we can solve for (3.37) for  $\lambda_1$  upon using (3.35) for  $\zeta$ , and then (3.20) for  $\kappa_0$ . In this way, we determine  $\lambda_1$  in terms of  $a_1$  as

$$\lambda_1 = \lambda_0 \left( 2a_1 + \frac{1}{2} - \gamma_e - \frac{\pi^2}{12} \right), \quad a_1 = \frac{1}{2}u_{0p}(x_0) + 2\pi R_{00} + \log 2 - \gamma_e. \quad (3.38)$$

The expression for  $a_1$  in (3.38), which depends on global properties of the domain inherited through  $u_{0p}(x_0)$  and the regular part  $R_{00}$  of the Laplacian Green's function, was obtained by combining (3.21) and (3.13). With  $\lambda_0$  and  $\lambda_1$  as given in (3.34) and (3.38), we have generated a two-term expansion for the nonlinear eigenvalue parameter in (3.2) corresponding to a localized solution of (3.1) with  $u(x_0) = -1 + \delta$  as  $\delta \rightarrow 0^+$ . The result is summarized below in Principal Result 3.1.

To complete the analysis, we must account for the unmatched constant term in the leading-order inner-most solution  $w_0 = 1 + y^2/4$ . To do so, we must modify our expansion in the mid-inner region by inserting appropriate switchback terms. Such switchback terms have a long history in the asymptotic analysis of certain low Reynolds number fluid flow problems (cf. [18], [19]). In the mid-inner region, we refine our expansion for  $v$  by writing

$$v = (v_0 + \nu v_1 + \dots) + \gamma^2 (\log \gamma)^2 V. \quad (3.39)$$

Although we have only calculated  $v_0$  and  $v_1$  explicitly above, there is an infinite logarithmic series of such terms, represented by the round brackets in (3.39), while the correction term  $V$  is transcendentally small in comparison with this series. However, since  $v_0$  and  $v_1$  both tend to zero as  $\rho \rightarrow 0$  with order  $\mathcal{O}(\rho^2 \log \rho)$ , the transcendentally small term  $V$ , which does not vanish as  $\rho \rightarrow 0$ , will have a non-negligible contribution to  $v$  as  $\rho \rightarrow 0$ . Thus, this transcendentally small term will affect the far-field asymptotic behavior of the solution in the inner-most layer.

Upon substituting (3.39) and (3.15), we obtain that  $V$  satisfies

$$\mathcal{L}V \equiv -\Delta_\rho^2 V + \Delta_\rho V = \frac{[\lambda_0 + \nu \lambda_1 + \dots]}{(v_0 + \nu v_1 + \dots)^2} \sim \frac{\lambda_0}{v_0^2} + \nu \left( \frac{\lambda_1}{v_0^2} - \frac{2\lambda_0 v_1}{v_0^3} \right) + \mathcal{O}(\nu^2). \quad (3.40)$$

We then expand  $V$  as

$$V = \log(-\log \gamma) V_{1/2} + V_1 + \frac{\log(-\log \gamma)}{\log \gamma} V_{3/2} + \left( \frac{-1}{\log \gamma} \right) V_2 + \dots. \quad (3.41)$$

Upon substituting (3.41) into (3.40), we obtain that the switchback terms  $V_{1/2}$  and  $V_{3/2}$  satisfy the homogeneous problems

$$\mathcal{L}V_{1/2} = 0, \quad 0 < \rho < \infty; \quad \mathcal{L}V_{3/2} = 0, \quad 0 < \rho < \infty, \quad (3.42)$$

while  $V_1$  and  $V_2$  satisfy

$$\mathcal{L}V_1 = \frac{\lambda_0}{v_0^2}, \quad 0 < \rho < \infty; \quad \mathcal{L}V_2 = \frac{\lambda_1}{v_0^2} - \frac{2\lambda_0 v_1}{v_0^3}, \quad 0 < \rho < \infty. \quad (3.43)$$

As shown below, since  $v_0 \rightarrow 0$  as  $\rho \rightarrow 0$ , we obtain that  $V_1$  and  $V_2$  diverge as  $\rho \rightarrow 0$ . The switchback terms  $V_{1/2}$  and  $V_{3/2}$  are needed to eliminate these divergences.

The solution to (3.42) that has no exponential growth as  $\rho \rightarrow \infty$ , and that is bounded as  $\rho \rightarrow 0$ , must have the

form

$$V_{1/2} = c_{1/2} + d_{1/2} (\log \rho + K_0(\rho) - \log 2 + \gamma_\epsilon) ; \quad V_{3/2} = c_{3/2} + d_{3/2} (\log \rho + K_0(\rho) - \log 2 + \gamma_\epsilon) , \quad (3.44)$$

where the constants  $c_{1/2}$ ,  $c_{3/2}$ ,  $d_{1/2}$  and  $d_{3/2}$  are to be determined. Note that  $V_{1/2}(0) = c_{1/2}$  and  $V_{3/2}(0) = c_{3/2}$ . Next, we determine the behavior of  $V_1$  and  $V_2$  as  $\rho \rightarrow 0$ . Since  $v_0 \sim -(\rho^2/4) \log \rho + \kappa_0 \rho^2$  as  $\rho \rightarrow 0$  from (3.20) and (3.22), we obtain that the particular solution  $V_{1p}$  to (3.43) must satisfy

$$\mathcal{L}V_{1p} \sim \lambda_0 \left[ -\frac{\rho^2}{4} \log \rho + \kappa_0 \rho^2 \right]^{-2} \sim \frac{16\lambda_0}{\rho^4 (\log \rho)^2} + \frac{128\lambda_0 \kappa_0}{\rho^4 (\log \rho)^3} + \dots , \quad \text{as } \rho \rightarrow 0 . \quad (3.45)$$

By integrating (3.45), we obtain that  $V_{1p} \sim 4\lambda_0 \log(-\log \rho) + 16\lambda_0 \kappa_0 / \log \rho$  as  $\rho \rightarrow 0$ . Upon adding the solution to the homogeneous problem for  $V_1$ , we conclude that the solution to (3.43) for  $V_1$  has the limiting asymptotics

$$V_1 \sim 4\lambda_0 \log(-\log \rho) + e_1 + e_2 \log \rho + \frac{16\lambda_0 \kappa_0}{\log \rho} + \dots , \quad \text{as } \rho \rightarrow 0 , \quad (3.46 a)$$

in terms of constants  $e_1$  and  $e_2$  to be determined. In addition, since  $v_1 \sim a_1 [-(\rho^2/4) \log \rho + \kappa_0 \rho^2]$  as  $\rho \rightarrow 0$ , a similar calculation shows that the solution  $V_2$  to (3.43) has the limiting asymptotics

$$V_2 \sim 4[\lambda_1 - 2a_1 \lambda_0] \log(-\log \rho) + f_1 + f_2 \log \rho + \frac{16\lambda_0 \kappa_0}{\log \rho} (\lambda_1 - 2a_1 \lambda_0) + \dots , \quad \text{as } \rho \rightarrow 0 , \quad (3.46 b)$$

in terms of unknown constants  $f_1$  and  $f_2$ .

Next, we substitute (3.44), (3.46 a), and (3.46 b), into (3.41), and we write the resulting expression in terms of the inner-most variable  $y$  defined by  $y = \rho/\gamma$ . To eliminate the divergent leading-order terms in  $V_1$  and  $V_2$  in (3.46 a) and (3.46 b) as  $\rho \rightarrow 0$ , we must choose  $c_{1/2}$  and  $c_{3/2}$  in (3.44) as

$$c_{1/2} = -4\lambda_0 , \quad c_{3/2} = 4(\lambda_1 - 2a_1 \lambda_0) . \quad (3.47)$$

With this choice, we obtain for  $\rho \rightarrow 0$ , with  $\rho = \gamma y$ , that

$$V \sim e_2 \log \gamma + (e_1 - f_2 + e_2 \log y) + \left( \frac{-1}{\log \gamma} \right) [f_1 + f_2 \log y - 4\lambda_0 \log y - 16\lambda_0 \kappa_0] + \mathcal{O} \left( \frac{-1}{\log \gamma} \right)^2 . \quad (3.48)$$

Then, we substitute (3.48), together with the local behavior of  $v_0$  and  $v_1$  as  $\rho \rightarrow 0$ , into (3.39), to obtain that

$$v \sim \gamma^2 (\log \gamma)^3 e_2 + \gamma^2 (\log \gamma)^2 [e_1 - f_2 + e_2 \log y] + \gamma^2 (-\log \gamma) \left[ \frac{y^2}{4} + f_1 - 16\lambda_0 \kappa_0 + (f_2 - 4\lambda_0) \log y \right] . \quad (3.49)$$

Finally, upon recalling that  $v = \gamma^2 (-\log \gamma) w$  and  $w = w_0 + \mathcal{O}(\nu)$  with  $w_0 = y^2/4 + 1$ , we observe from (3.49) that we must choose the constants  $e_1$ ,  $e_2$ ,  $f_1$ , and  $f_2$ , as

$$e_2 = 0 , \quad e_1 = f_2 = 4\lambda_0 , \quad f_1 = 16\lambda_0 \kappa_0 + 1 . \quad (3.50)$$

With the constants determined in this way, there exist unique solutions  $V_1$  and  $V_2$  to (3.43), with limiting behavior (3.46) as  $\rho \rightarrow 0$ , and which do not grow exponentially as  $\rho \rightarrow +\infty$ .

In summary, a two-term asymptotic expansion for the nonlinear eigenvalue parameter has been obtained by analyzing (3.1) via a triple-deck asymptotic matching procedure, which must incorporate transcendentally small switchback terms in the mid-inner expansion. We summarize our main result for (3.1) as follows:

**Principal Result 3.1:** *In the limit  $\delta \rightarrow 0$ , (3.1) has a solution with  $u(x_0) + 1 = \delta \rightarrow 0^+$  and  $\nabla u(x_0) = 0$ , where the concentration point  $x_0$  satisfies (3.11). Labeling  $\gamma \equiv \sqrt{\delta}$ , the two-term expansion for  $\lambda$  is*

$$\lambda \sim \left( \frac{-1}{\log \gamma} \right) \left[ \lambda_0 + \left( \frac{-1}{\log \gamma} \right) \lambda_1 + \dots \right] , \quad (3.51 a)$$



where

$$\lambda_0 = \frac{1}{2}, \quad \lambda_1 = \lambda_0 \left( u_{0p}(x_0) + 4\pi R_{00} + 2 \log 2 - 3\gamma_e - \frac{\pi^2}{12} + \frac{1}{2} \right), \quad (3.51 \text{ b})$$

where  $R_{00} \equiv R(x_0, x_0)$  is the regular part of the Laplacian Green's function in (3.6),  $u_{0p}$  satisfies (3.5), and  $\gamma_e$  is Euler's constant. A three-term outer expansion for  $u$ , valid for  $|x - x_0| \gg \mathcal{O}(\gamma)$ , is

$$u \sim \left( \frac{-1}{\log \gamma} \right) u_0 + \left( \frac{-1}{\log \gamma} \right)^2 u_1 + \left( \frac{-1}{\log \gamma} \right)^3 u_2 + \dots. \quad (3.52)$$

Here  $u_j$  for  $j = 0, 1, 2$  satisfy (3.3) subject to  $u_j \sim a_j \log |x - x_0|$  as  $x \rightarrow x_0$ , with  $u_0$  and  $u_1$  given explicitly in (3.4) and (3.7), respectively. The constants  $a_0$ ,  $a_1$ , and  $a_2$ , are given in (3.10) and (3.21). The solution in the inner-most layer with inner variable  $y = r/\gamma^2$  and  $r = |x - x_0|$  has the expansion

$$u = -1 + \gamma^2 \left( w_0 + \left( \frac{-1}{\log \gamma} \right) w_1 + \left( \frac{-1}{\log \gamma} \right)^2 w_2 + \dots \right). \quad (3.53)$$

Here  $w_0 = 1 + y^2/4$ , while  $w_1$  and  $w_2$  satisfy (3.31 b) and (3.31 c), respectively. Finally, in the mid-inner region with inner variable  $\rho = r/\gamma$  and  $r = |x - x_0|$  then

$$u = -1 + \left( \frac{-1}{\log \gamma} \right) v, \quad (3.54)$$

where  $v$  has the expansion

$$v = \left( v_0 + \left( \frac{-1}{\log \gamma} \right) v_1 + \dots \right) + \gamma^2 (\log \gamma)^2 \left[ \log(-\log \gamma) V_{1/2} + V_1 + \frac{\log(-\log \gamma)}{\log \gamma} V_{3/2} + \left( \frac{-1}{\log \gamma} \right) V_2 + \dots \right], \quad (3.55)$$

where  $v_0$  and  $v_1$  are given explicitly in (3.22). The switchback terms  $V_{1/2}$  and  $V_{3/2}$  are defined in (3.44) and (3.47), while  $V_1$  and  $V_2$  are the unique solutions to (3.43) with no exponential growth as  $\rho \rightarrow 0$ , and that are subject to the limiting behavior (3.46) as  $\rho \rightarrow 0$  with coefficients as given in (3.50).

We remark that the constants  $d_{1/2}$  and  $d_{3/2}$  in the switchback terms  $V_{1/2}$  and  $V_{3/2}$  in (3.44) are not determined at this order of the expansion. They can only be determined by including transcendentally small terms in the asymptotic expansion in the outer region.

For the special case of the unit disk, we use (3.23) for  $u_{0p}$  in (3.51) to obtain that

$$\lambda \sim \frac{\nu}{2}, \quad (\text{1-term}); \quad \lambda \sim \frac{\nu}{2} \left( 1 + \nu \left( \frac{1}{4} + 2 \log 2 - 3\gamma_e - \frac{\pi^2}{12} \right) \right), \quad (\text{two-term}), \quad (3.56 \text{ a})$$

where  $\nu \equiv (-1/\log[\sqrt{\delta}])$ . An asymptotically equivalent two-term expansion is given by the renormalized expansion

$$\lambda \sim \frac{\tilde{\nu}}{2} \left( 1 + \tilde{\nu} \left( \frac{1}{4} + \log 2 - 2\gamma_e - \frac{\pi^2}{12} \right) \right), \quad (\text{renormalized}); \quad \tilde{\nu} \equiv \frac{1}{(-\log[\sqrt{\delta}] + \gamma_e - \log 2)}. \quad (3.56 \text{ b})$$

As a remark, the leading-order asymptotics in (3.56 a) for the unit disk can also be obtained from the asymptotic result of [22]. For the unit disk, in [22] a radial symmetric solution  $u(r)$ , with concentration at the origin  $r = 0$ , was constructed for the biharmonic nonlinear eigenvalue problem

$$\delta \Delta^2 u - \Delta u = -\frac{\lambda}{(1+u)^2}, \quad 0 < r < 1; \quad u(1) = u_r(1) = 0, \quad (3.57)$$

in the limit  $u(0) + 1 = \varepsilon \rightarrow 0^+$  and for each fixed  $\delta > 0$ , with  $\delta$  independent of  $\varepsilon$ . For a fixed  $\delta > 0$ , and for  $\varepsilon \rightarrow 0$ , it was shown in [22] that

$$\lambda \sim \delta \varepsilon [-\log \beta] \lambda_0 + \delta \varepsilon \lambda_1 + \dots, \quad (3.58 \text{ a})$$

where the boundary layer width  $\beta$  near  $r = 0$  is defined implicitly in terms of  $\varepsilon$  by

$$\varepsilon = -\beta^2 \log \beta. \quad (3.58 b)$$

In (3.58 a), the coefficients  $\lambda_0$  and  $\lambda_1$  are given by

$$\lambda_0 = 8\alpha^2, \quad \lambda_1 = -\frac{\lambda_0}{2} \left[ \frac{\pi^2}{6} - \log(-\alpha) + \left( 1 + \frac{2\varphi}{\alpha} \right) \right], \quad (3.58 c)$$

where  $\alpha$  and  $\varphi$  are defined in terms of  $\delta$ , modified Bessel functions, and the Euler constant, by

$$\alpha = -\left( \frac{\eta^3}{4} \right) I_0'(\eta) \mathcal{G}(\eta), \quad \varphi = -\frac{\eta^2}{4} [\eta I_0'(\eta) (\log(\eta/2) + \gamma_e - 1) + (1 + \eta K_0'(\eta))] \mathcal{G}(\eta), \quad \eta \equiv 1/\sqrt{\delta}. \quad (3.58 d)$$

Here  $\mathcal{G}(\eta)$  is defined by

$$\mathcal{G}(\eta) \equiv [\eta I_0'(\eta) (K_0(\eta) + \log(\eta/2) + \gamma_e) + (1 + \eta K_0'(\eta)) (1 - I_0(\eta))]^{-1}. \quad (3.58 e)$$

A plot of the coefficients  $\alpha$  and  $\varphi$  versus  $\delta$  is shown in Fig. 3.

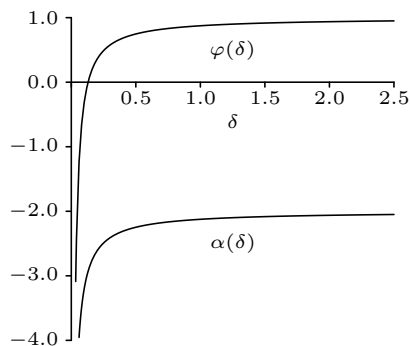


FIGURE 3. Plot of the coefficients  $\alpha(\delta)$  and  $\varphi(\delta)$ , defined in (3.58 d) on the range  $0 < \delta < 2.5$ .

Although (3.58) pertains to the limit  $\varepsilon \rightarrow 0$  with  $\delta > 0$  fixed, we do recover the leading-order result in (3.56 a) if we set  $\varepsilon = \delta$  in (3.58 a) and (3.58 b), and then let  $\delta \rightarrow 0$ . To show this, we first let  $\delta \rightarrow 0$ , corresponding to  $\eta \rightarrow \infty$  in (3.58 d). By using the large argument asymptotics of  $I_0(\eta)$  and  $K_0(\eta)$ , we obtain from (3.58 d) and (3.58 e) that

$$\alpha \sim -\frac{\delta^{-1}}{4 \left[ -\log(\sqrt{\delta}) + \gamma_e - \log 2 \right]}, \quad \frac{\varphi}{\alpha} \sim -\log(\sqrt{\delta}) - \log 2 + \gamma_e - 1, \quad \text{as } \delta \rightarrow 0. \quad (3.59)$$

Next, we solve the implicit relation (3.58 b) asymptotically with  $\varepsilon = \delta$  to obtain

$$\log \beta = \log(\sqrt{\delta}) - \frac{1}{2} \log \left[ -\log(\sqrt{\delta}) \right] + o(1), \quad \text{as } \delta \rightarrow 0. \quad (3.60)$$

Upon substituting  $\varepsilon = \delta$ , (3.59), and (3.60), into (3.58 a) and (3.58 c), we obtain that

$$\lambda \sim \frac{1}{2 \left[ -\log(\sqrt{\delta}) + \gamma_e - \log 2 \right]^2} \left[ -\log(\sqrt{\delta}) + \mathcal{O}(1) \right] \sim \frac{1}{2 \left[ -\log(\sqrt{\delta}) \right]}, \quad \text{as } \delta \rightarrow 0,$$

which agrees with the leading-order term in (3.56 a), and suggests the equivalent renormalized form used in (3.56 b).

In Fig. 4 we compare the asymptotic result (3.56) for  $\sqrt{\delta}$  versus  $\lambda$  with the full numerical results for (3.1). The ODE shooting method of [22] was used to obtain the full numerical results from (3.1). As seen from Fig. 4(a) the two-term asymptotic result provides only a moderately good determination of the full numerical result unless  $\sqrt{\delta}$  is rather small, but is significantly better than the leading-order asymptotic approximation. In contrast, as seen in

Fig. 4(b), the two-term asymptotic expansion for the outer solution agrees very well with the full numerical result for (3.1) when  $\sqrt{\delta} = 0.01$ .

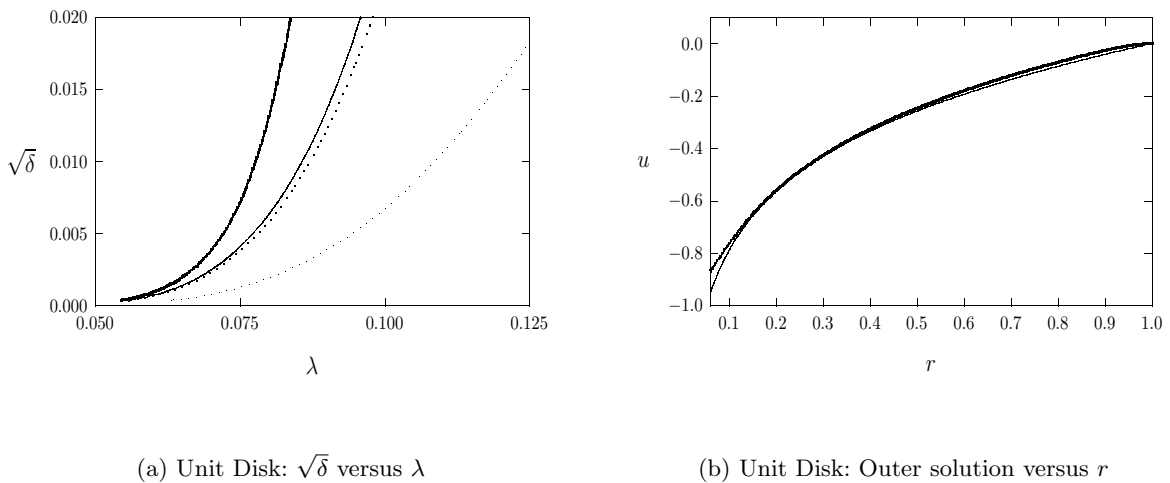


FIGURE 4. Comparison of asymptotics and numerics for (3.1) in the unit disk. Left figure: the numerical result for  $\sqrt{\delta}$  versus  $\lambda$  computed from (3.1) (heavy solid curve) is compared with the one-term (faint dotted curve), two-term (dotted curve), and renormalized two-term (solid curve), asymptotic results for  $\lambda$  as obtained from (3.56). Right figure: comparison of the two-term outer expansion (3.52) (solid curve) with the full numerical solution to (3.1) (heavy solid curve) for  $\sqrt{\delta} = 0.01$ .

#### 4 Concentration in a Nonlinear Biharmonic Eigenvalue Problem

In this section we analyze single-point concentration behavior in the limit  $\varepsilon \rightarrow 0$  for the solution to the pure biharmonic nonlinear eigenvalue problem in an arbitrary 2-D domain  $\Omega$ , formulated as

$$\Delta^2 u = -\frac{\lambda}{(1+u)^2}, \quad x \in \Omega; \quad u = \partial_n u = 0, \quad x \in \partial\Omega; \quad \|u\|_\infty = 1 - \varepsilon. \quad (4.1)$$

We will construct a solution to (4.1) that concentrates at a single point  $x_0 \in \Omega$  in the sense that  $u(x_0) + 1 = \varepsilon \rightarrow 0^+$ .

For the case of the unit ball, where the concentration point is at the origin, i.e.  $x_0 = 0$ , (4.1) was analyzed in §4 of [22] by using the method of matched asymptotic expansions. In §4 of [22] it was shown that certain switchback terms are required to augment the outer expansion, and that there is a boundary layer of width  $\mathcal{O}(\gamma)$  near the concentration point  $x_0 = 0$ , where  $\gamma$  is determined implicitly in terms of  $\varepsilon$  by

$$\gamma^2 \sigma^{-1} = \varepsilon, \quad \sigma \equiv \frac{-1}{\log \gamma}. \quad (4.2)$$

Here, we will extend the analysis of [22] to the case of an arbitrary 2-D domain by relying on detailed properties of the biharmonic Green's function defined by (1.4).

Motivated by the expansion in equation (4.18) of [22], in the outer region we expand the solution to (4.1) as

$$u = u_0 + \frac{\varepsilon}{\sigma} \sum_{j=1}^{\infty} \sigma^{j-1} [u_j + (-\log \sigma) u_{(2j-1)/2}] + \mathcal{O}(\varepsilon \mu), \quad \lambda = \frac{\varepsilon}{\sigma} \sum_{i=0}^{\infty} \sigma^i \lambda_i + \mathcal{O}(\varepsilon \mu), \quad (4.3)$$

where  $\mu \ll \sigma^k$  for any integer  $k > 0$  and  $\sigma$  is defined in (4.2). The leading-order problem for  $u_0$  is

$$\Delta^2 u_0 = 0, \quad x \in \Omega; \quad u_0 = \partial_n u_0 = 0, \quad x \in \partial\Omega; \quad (4.4 a)$$

$$u_0(x_0) = -1, \quad \nabla_x u_0(x)|_{x=x_0} = 0. \quad (4.4 b)$$

Notice that  $u_0$  is to satisfy a point constraint at  $x_0$ . In terms of the biharmonic Green's Function satisfying (1.4), the solution to (4.4) is

$$u_0(x; x_0) = -\frac{G(x; x_0)}{R(x_0; x_0)}. \quad (4.5)$$

The condition that  $\nabla_x u_0(x)|_{x=x_0} = 0$  requires  $\nabla_x R(x; x_0)|_{x=x_0} = 0$ , whereas the condition that  $u(x) \geq -1$  requires that  $R(x_0; x_0) > 0$ . These two conditions are necessary conditions for a solution of (4.1) to concentrate at  $x_0$ .

**Definition** (Single Concentration Point): *If the maximal solution branch of (4.1) concentrates at some  $x_0 \in \Omega$ , then*

$$R(x_0; x_0) > 0, \quad \nabla_x R(x; x_0)|_{x=x_0} = 0, \quad (4.6)$$

where  $R(x; x_0)$  is the regular part of the biharmonic Green's function defined in (1.4).

By expanding (4.5) as  $x \rightarrow x_0$ , we can readily show that

$$u_0 \sim -1 + \alpha r^2 \log r + r^2[\beta + a_c \cos 2\theta + a_s \sin 2\theta] + \mathcal{O}(r^3), \quad \text{as } r = |x - x_0| \rightarrow 0. \quad (4.7 a)$$

Here  $x - x_0 = r(\cos \theta, \sin \theta)$  and the coefficients  $\alpha$ ,  $\beta$ ,  $a_c$ , and  $a_s$ , are defined by

$$\begin{aligned} \alpha &\equiv \frac{-1}{8\pi R(x_0; x_0)}, & \beta &\equiv \frac{-1}{4R(x_0; x_0)} \left[ \frac{\partial^2 R}{\partial x_1^2} + \frac{\partial^2 R}{\partial x_2^2} \right]_{x=x_0}, \\ a_s &\equiv \frac{-1}{2R(x_0; x_0)} \left[ \frac{\partial^2 R}{\partial x_1 \partial x_2} \right]_{x=x_0}, & a_c &\equiv \frac{-1}{4R(x_0; x_0)} \left[ \frac{\partial^2 R}{\partial x_1^2} - \frac{\partial^2 R}{\partial x_2^2} \right]_{x=x_0}. \end{aligned} \quad (4.7 b)$$

This complete the specification of the leading order solution. The key qualitative feature of this solution is its  $r^2 \log r$  singularity as  $r \rightarrow 0$  which permits the point constraint  $u_0(x_0) = -1$  to be satisfied. In addition, the assumption that  $R(x_0; x_0) > 0$  implies, from the  $r^2 \log r$  term, that  $\alpha < 0$ , which yields  $u_0(x_0) + 1 > 0$  as  $r \rightarrow 0$ .

Next, by substituting (4.3) into (4.1), we obtain that the outer correction terms  $u_j$  for  $j \geq 1$  satisfy

$$\Delta^2 u_j = \frac{-\lambda_{j-1}}{(1 + u_0)^2}, \quad x \in \Omega; \quad u_j = \partial_n u_j = 0, \quad x \in \partial\Omega. \quad (4.8)$$

To determine the local behavior of  $u_j$  as  $x \rightarrow x_0$ , we substitute (4.7 a) into (4.8) to obtain for  $r \rightarrow 0$  that

$$\Delta^2 u_j \sim \frac{-\lambda_{j-1}}{\alpha^2 r^4 \log^2 r} \left[ 1 + \frac{\bar{\beta}}{\alpha \log r} \right]^{-2}, \quad \bar{\beta} \equiv \beta + a_s \sin 2\theta + a_c \cos 2\theta. \quad (4.9)$$

To establish the asymptotic behavior of the solution to (4.9) as  $r \rightarrow 0$ , it is convenient to introduce the variable  $\eta \equiv -\log r$  and to seek a solution for  $h(\eta, \theta) \equiv u(e^{-\eta}, \theta)$  as  $\eta \rightarrow \infty$ . This transformation reduces (4.9) to

$$h_{\eta\eta\eta\eta} + 4h_{\eta\eta\eta} + 4h_{\eta\eta} + 4h_{\theta\theta} + 4h_{\theta\theta\eta} + 2h_{\theta\theta\eta\eta} + h_{\theta\theta\theta\theta} = \frac{-\lambda_{j-1}}{\alpha^2 \eta^2} \left[ 1 + \frac{2\bar{\beta}}{\alpha\eta} + \frac{3\bar{\beta}^2}{\alpha^2 \eta^2} + \frac{4\bar{\beta}^3}{\alpha^3 \eta^3} + \dots \right]. \quad (4.10)$$

A solution to (4.10) is developed that is accurate to  $\mathcal{O}(\eta^{-3})$  as  $\eta \rightarrow \infty$ . By noting that

$$\begin{aligned} \bar{\beta}^2 &= \beta^2 + \frac{(a_c^2 + a_s^2)}{2} + 2\beta(a_c \cos 2\theta + a_s \sin 2\theta) + a_c a_s \sin 4\theta + \frac{(a_c^2 - a_s^2)}{2} \cos 4\theta, \\ \bar{\beta}^3 &= \left[ \beta^3 + \frac{3\beta}{2}(a_c^2 + a_s^2) \right] + \sum_{n=1}^3 (\bar{a}_n \cos n\theta + \bar{b}_n \sin n\theta), \end{aligned} \quad (4.11)$$

for some  $\bar{a}_n$  and  $\bar{b}_n$ , we obtain from (4.10) that for  $\eta \rightarrow \infty$ ,

$$h \sim \frac{\lambda_{j-1}}{4\alpha^2} \left[ \log \eta + \frac{\Gamma_1}{\eta} + \frac{\Gamma_2}{\eta^2} + \frac{\Gamma_3}{\eta^3} - \frac{1}{4\alpha\eta^2} [a_c \cos 2\theta + a_s \sin 2\theta] + \frac{1}{2\alpha\eta^3} \left[ \frac{\beta}{\alpha} + \frac{1}{4} \right] (a_c \cos 2\theta + a_s \sin 2\theta) + \mathcal{O}(\eta^{-4}) \right], \quad (4.12)$$

where the constants  $\Gamma_1, \Gamma_2$ , and  $\Gamma_3$ , are defined by

$$\begin{aligned} \Gamma_1 &= - \left( 1 + \frac{\beta}{\alpha} \right), & \Gamma_2 &= - \left[ \frac{3}{4} + \frac{\beta}{\alpha} + \frac{\beta^2}{2\alpha^2} + \frac{(a_c^2 + a_s^2)}{4\alpha^2} \right], \\ \Gamma_3 &= - \left[ 1 + \frac{3\beta}{2\alpha} + \frac{\beta^2}{\alpha^2} + \frac{\beta^3}{3\alpha^3} + \left( 1 + \frac{\beta}{\alpha} \right) \frac{(a_c^2 + a_s^2)}{2\alpha^2} \right]. \end{aligned} \quad (4.13)$$

Lengthy expressions for the constants  $\bar{a}_n$  and  $\bar{b}_n$  for  $n = 1, 2, 3$  can be obtained, but these terms do not play a role in capturing behavior to  $\mathcal{O}(\eta^{-3})$ , and so these formulae are omitted. By returning to the variable  $r = e^{-\eta}$ , equation (4.12) provides the following singular behavior as  $r \rightarrow 0$  for the solution  $u_j$  to (4.8):

$$\begin{aligned} u_j &\sim \frac{\lambda_{j-1}}{4\alpha^2} \left[ \log(-\log r) - \frac{\Gamma_1}{\log r} + \frac{\Gamma_2}{\log^2 r} - \frac{\Gamma_3}{\log^3 r} - \left( \frac{a_c}{4\alpha} \cos 2\theta + \frac{a_s}{4\alpha} \sin 2\theta \right) \frac{1}{\log^2 r} \right. \\ &\quad \left. - \frac{1}{2\alpha \log^3 r} \left( \frac{\beta}{\alpha} + \frac{1}{4} \right) (a_c \cos 2\theta + a_s \sin 2\theta) + \mathcal{O}(\log^{-4} r) \right] \\ &\quad + b_j \log r + c_j + d_j \cos 2\theta + e_j \sin 2\theta + \dots, \quad \text{as } r \rightarrow 0. \end{aligned} \quad (4.14)$$

In (4.14), the terms  $b_j \log r, c_j, d_j \sin 2\theta, e_j \cos 2\theta$  relate to an arbitrary solution of the homogeneous problem for  $u_j$ .

Next, by substituting the outer expansion (4.3) into (4.1), we obtain that the logarithmic switchback terms  $u_{(2j-1)/2}$  for  $j \geq 1$  satisfy

$$\Delta^2 u_{(2j-1)/2} = 0, \quad x \in \Omega; \quad u_{(2j-1)/2} = \partial_n u_{(2j-1)/2} = 0, \quad x \in \partial\Omega, \quad (4.15 a)$$

$$u_{(2j-1)/2}(x_0) = f_{(2j-1)/2}, \quad \nabla_x u_{(2j-1)/2}(x)|_{x=x_0} = 0, \quad (4.15 b)$$

for some constants  $f_{(2j-1)/2}$  for  $j \geq 1$  to be found. Therefore, in terms of  $u_0$ , we can solve for  $u_{(2j-1)/2}$  to get

$$u_{(2j-1)/2} = -f_{(2j-1)/2} u_0, \quad x \in \Omega; \quad u_{(2j-1)/2} \sim f_{(2j-1)/2} + \mathcal{O}(r^2 \log r), \quad \text{as } r \rightarrow 0. \quad (4.15 c)$$

The constants  $f_{(2j-1)/2}$  for  $j \geq 1$  will be chosen below to remove certain logarithmic divergences in the near-field behavior of the outer expansion.

In the inner region near  $x_0$ , we introduce the local coordinates  $v$  and  $y$  by

$$u = -1 + \varepsilon v, \quad x - x_0 = \gamma y, \quad y = \rho(\cos \theta, \sin \theta), \quad (4.16)$$

where  $\gamma$  is defined implicitly in terms of  $\varepsilon$  by (4.2). By substituting (4.7 a), (4.14), and (4.15 c), into (4.3), we obtain

that the local behavior of the outer expansion (4.3) for  $u$ , when written in terms of the inner variables  $\rho$  and  $\theta$ , is

$$\begin{aligned}
u \sim & -1 + \varepsilon \left[ -\alpha\rho^2 + \sigma\rho^2(\beta + a_c \cos 2\theta + a_s \sin 2\theta) \right. \\
& + \frac{1}{4\alpha^2} \left[ \frac{\lambda_0}{\sigma} + \lambda_1 + \lambda_2\sigma + \dots \right] \left[ \log(1 - \sigma \log \rho) + \frac{\sigma\Gamma_1}{1 - \sigma \log \rho} + \frac{\sigma^2\Gamma_2}{(1 - \sigma \log \rho)^2} \right. \\
& - \frac{\sigma^3\Gamma_3}{(1 - \sigma \log \rho)^3} - \frac{1}{4\alpha} \frac{\sigma^2}{(1 - \sigma \log \rho)^2} (a_c \cos 2\theta + a_s \sin 2\theta) \\
& \left. + \frac{1}{2\alpha} \left( \frac{\beta}{\alpha} + \frac{1}{4} \right) \frac{\sigma^3}{(1 - \sigma \log \rho)^3} (a_c \cos 2\theta + a_s \sin 2\theta) \right] \\
& + \sigma^{-2}b_1 + \sum_{j=1}^3 \sigma^{j-1} (b_j \log \rho + c_j - b_{j+1} + d_j \cos 2\theta + e_j \sin 2\theta) - \log \sigma \sum_{j=1}^3 \sigma^{j-1} \left( \frac{\lambda_j}{4\alpha^2} + f_{(2j-1)/2} \right) \left. \right].
\end{aligned}$$

Expanding this local behavior for  $\sigma \ll 1$  and retaining terms up to  $\mathcal{O}(\sigma^2)$ , we obtain from  $u = -1 + \varepsilon v$  that  $v(\rho, \theta)$  satisfies

$$\begin{aligned}
v \sim & \sigma^{-2}b_1 + \sigma^{-1}(c_1 - b_2 + b_1 \log \rho + d_1 \cos 2\theta + e_1 \sin 2\theta) + \left( b_2 - \frac{\lambda_0}{4\alpha^2} \right) \log \rho \\
& - \alpha\rho^2 + c_2 - b_3 + \frac{\lambda_0\Gamma_1}{4\alpha^2} + d_2 \cos 2\theta + e_2 \sin 2\theta - \log \sigma \sum_{j=1}^3 \sigma^{j-1} \left[ \frac{\lambda_j}{4\alpha^2} + f_{(2j-1)/2} \right] \\
& + \sigma \left[ \alpha\rho^2 \log \rho + \rho^2(\beta + a_c \cos 2\theta + a_s \sin 2\theta) - \frac{\lambda_0}{8\alpha^2} \log^2 \rho + \left( b_3 + \frac{\lambda_0\Gamma_1}{4\alpha^2} - \frac{\lambda_1}{4\alpha^2} \right) \log \rho \right. \\
& \left. + \left( d_3 - \frac{\lambda_0 a_c}{16\alpha^3} \right) \cos 2\theta + \left( e_3 - \frac{\lambda_0 a_s}{16\alpha^3} \right) \sin 2\theta + c_3 - b_4 + \frac{\lambda_0\Gamma_2}{4\alpha^2} + \frac{\lambda_1\Gamma_1}{4\alpha^2} \right] \tag{4.17} \\
& + \sigma^2 \left[ -\frac{\lambda_0}{12\alpha^2} \log^3 \rho + \left( \frac{\lambda_0\Gamma_1}{4\alpha^2} - \frac{\lambda_1}{8\alpha^2} \right) \log^2 \rho + \left( b_4 + \frac{\lambda_0\Gamma_2}{2\alpha^2} + \frac{\lambda_1\Gamma_1}{4\alpha^2} - \frac{\lambda_2}{4\alpha^2} \right) \log \rho \right. \\
& - \frac{\lambda_0}{8\alpha^2} (a_c \cos 2\theta + a_s \sin 2\theta) \log \rho + \left( d_4 - \frac{\lambda_1 a_c}{16\alpha^3} + \frac{\lambda_0 a_c}{8\alpha^3} \left( \frac{\beta}{\alpha} + \frac{1}{4} \right) \right) \cos 2\theta \\
& \left. + \left( e_4 - \frac{\lambda_1 a_s}{16\alpha^3} + \frac{\lambda_0 a_s}{8\alpha^3} \left( \frac{\beta}{\alpha} + \frac{1}{4} \right) \right) \sin 2\theta \right] + \mathcal{O}(\sigma^3).
\end{aligned}$$

The condition  $v(0, \theta) = 1$  suggests the largest term in expansion (4.17) should be  $\mathcal{O}(1)$ , which yields the following values on certain constants:

$$b_1 = e_1 = e_2 = d_1 = d_2 = 0; \quad c_1 = b_2; \quad f_{(2j-1)/2} = -\frac{\lambda_j}{4\alpha^2}, \quad j = 1, 2, 3, \dots \tag{4.18}$$

Next, in terms of the inner variables (4.2) and (4.16), (4.1) transforms to the following problem for  $v(\rho, \theta)$ :

$$\Delta^2 v = -\frac{\sigma^2 \lambda}{\varepsilon v^2}, \quad \rho > 0; \quad v = 1, \quad v_\rho = v_{\rho\rho} = 0, \quad \text{at } \rho = 0. \tag{4.19 a}$$

From the matching condition (4.17), the far-field behavior of  $v$  as  $\rho \rightarrow \infty$  must be

$$\begin{aligned}
 v \sim & -\alpha\rho^2 + \left(b_2 - \frac{\lambda_0}{4\alpha^2}\right) \log \rho + c_2 - b_3 + \frac{\lambda_0\Gamma_1}{4\alpha^2} \\
 & + \sigma \left[ \alpha\rho^2 \log \rho + \rho^2(\beta + a_c \cos 2\theta + a_s \sin 2\theta) - \frac{\lambda_0}{8\alpha^2} \log^2 \rho + \left(b_3 + \frac{\lambda_0\Gamma_1}{4\alpha^2} - \frac{\lambda_1}{4\alpha^2}\right) \log \rho \right. \\
 & + \left. \left(d_3 - \frac{\lambda_0 a_c}{16\alpha^3}\right) \cos 2\theta + \left(e_3 - \frac{\lambda_0 a_s}{16\alpha^3}\right) \sin 2\theta + c_3 - b_4 + \frac{\lambda_0\Gamma_2}{4\alpha^2} + \frac{\lambda_1\Gamma_1}{4\alpha^2} \right] \\
 & + \sigma^2 \left[ -\frac{\lambda_0}{12\alpha^2} \log^3 \rho + \left(\frac{\lambda_0\Gamma_1}{4\alpha^2} - \frac{\lambda_1}{8\alpha^2}\right) \log^2 \rho + \left(b_4 + \frac{\lambda_0\Gamma_2}{2\alpha^2} + \frac{\lambda_1\Gamma_1}{4\alpha^2} - \frac{\lambda_2}{4\alpha^2}\right) \log \rho \right. \\
 & - \frac{\lambda_0}{8\alpha^2} (a_c \cos 2\theta + a_s \sin 2\theta) \log \rho + \left. \left(d_4 - \frac{\lambda_1 a_c}{16\alpha^3} + \frac{\lambda_0 a_c}{8\alpha^3} \left(\frac{\beta}{\alpha} + \frac{1}{4}\right)\right) \cos 2\theta \right. \\
 & + \left. \left(e_4 - \frac{\lambda_1 a_s}{16\alpha^3} + \frac{\lambda_0 a_s}{8\alpha^3} \left(\frac{\beta}{\alpha} + \frac{1}{4}\right)\right) \sin 2\theta + c_4 - b_5 - \frac{\lambda_0\Gamma_3}{4\alpha^2} + \frac{\lambda_1\Gamma_2}{4\alpha^2} + \frac{\lambda_2\Gamma_1}{4\alpha^2} \right] + \mathcal{O}(\sigma^3).
 \end{aligned} \tag{4.19 b}$$

The form of the far-field condition (4.19 b) suggests that the solution to (4.19 a) should be expanded as

$$v = v_0 + \sigma v_1 + \sigma^2 v_2 + \mathcal{O}(\sigma^3). \tag{4.20}$$

Upon substituting (4.20) for  $v$  and (4.3) for  $\lambda$  into (4.19), we obtain that the leading-order solution  $v_0$  satisfies

$$\Delta^2 v_0 = 0, \quad \rho > 0; \quad v_0 = 1, \quad v_{0\rho} = v_{0\rho\rho} = 0, \quad \text{at } \rho = 0, \tag{4.21 a}$$

with far-field behavior

$$v_0 \sim -\alpha\rho^2 + \left(b_2 - \frac{\lambda_0}{4\alpha^2}\right) \log \rho + c_2 - b_3 + \frac{\lambda_0\Gamma_1}{4\alpha^2} \quad \text{as } \rho \rightarrow \infty. \tag{4.21 b}$$

This problem admits the unique solution  $v_0(\rho) = 1 - \alpha\rho^2$ , which in turn specifies that

$$b_2 = \frac{\lambda_0}{4\alpha^2}, \quad c_2 = 1 + b_3 - \frac{\lambda_0\Gamma_1}{4\alpha^2}. \tag{4.22}$$

By equating terms at  $\mathcal{O}(\sigma)$ , we obtain that  $v_1(\rho, \theta)$  in (4.20) satisfies

$$\Delta^2 v_1 = -\frac{\lambda_0}{v_0^2}, \quad \rho > 0; \quad v_1(0, \theta) = v_{1\rho}(0, \theta) = v_{1\rho\rho}(0, \theta) = 0, \tag{4.23 a}$$

with far-field behavior

$$\begin{aligned}
 v_1 \sim & \alpha\rho^2 \log \rho + \rho^2(\beta + a_c \cos 2\theta + a_s \sin 2\theta) - \frac{\lambda_0}{8\alpha^2} \log^2 \rho + \left(b_3 + \frac{\lambda_0\Gamma_1}{4\alpha^2} - \frac{\lambda_1}{4\alpha^2}\right) \log \rho \\
 & + \left(d_3 - \frac{\lambda_0 a_c}{16\alpha^3}\right) \cos 2\theta + \left(e_3 - \frac{\lambda_0 a_s}{16\alpha^3}\right) \sin 2\theta + c_3 - b_4 + \frac{\lambda_0\Gamma_2}{4\alpha^2} + \frac{\lambda_1\Gamma_1}{4\alpha^2}, \quad \text{as } \rho \rightarrow \infty.
 \end{aligned} \tag{4.23 b}$$

It is convenient to decompose  $v_1$  as  $v_1(\rho, \theta) = \mathcal{V}(\rho, \theta) + \bar{v}(\rho)$ , where  $\mathcal{V}$  satisfies

$$\Delta^2 \mathcal{V} = 0, \quad \rho > 0; \quad \mathcal{V}(0, \theta) = \mathcal{V}_\rho(0, \theta) = \mathcal{V}_{\rho\rho}(0, \theta) = 0, \tag{4.24 a}$$

with far-field behavior

$$\mathcal{V} \sim \rho^2(a_c \cos 2\theta + a_s \sin 2\theta) + \left(d_3 - \frac{\lambda_0 a_c}{16\alpha^3}\right) \cos 2\theta + \left(e_3 - \frac{\lambda_0 a_s}{16\alpha^3}\right) \sin 2\theta, \quad \text{as } \rho \rightarrow \infty. \tag{4.24 b}$$

The solution to (4.24) is  $\mathcal{V} = \rho^2(a_c \cos 2\theta + a_s \sin 2\theta)$ , which in turn specifies that

$$d_3 = \frac{\lambda_0 a_c}{16\alpha^3}, \quad e_3 = \frac{\lambda_0 a_s}{16\alpha^3}. \tag{4.25}$$

In the decomposition for  $v_1$ , the problem for the radially symmetric function  $\bar{v}(\rho)$  is

$$\Delta^2 \bar{v} = -\frac{\lambda_0}{v_0^2}, \quad \rho > 0; \quad \bar{v}(0) = \bar{v}_\rho(0) = \bar{v}_{\rho\rho}(0) = 0, \quad (4.26 a)$$

subject to the far-field behavior

$$\bar{v} \sim \alpha\rho^2 \log \rho + \beta\rho^2 - \frac{\lambda_0}{8\alpha^2} \log^2 \rho + \left( b_3 + \frac{\lambda_0\Gamma_1}{4\alpha^2} - \frac{\lambda_1}{4\alpha^2} \right) \log \rho + c_3 - b_4 + \frac{\lambda_0\Gamma_2}{4\alpha^2} + \frac{\lambda_1\Gamma_1}{4\alpha^2}, \quad \text{as } \rho \rightarrow \infty. \quad (4.26 b)$$

By recalling that  $v_0 = 1 - \alpha\rho^2$ , we integrate (4.26 a) over a large circle  $\rho = L$ , with  $L \gg 1$ , and then take the limit  $L \rightarrow \infty$  to obtain

$$\lim_{L \rightarrow \infty} \left[ \rho \frac{d}{d\rho} (\Delta \bar{v}) |_{\rho=L} \right] = -\lambda_0 \int_0^\infty \frac{\rho}{(1 - \alpha\rho^2)^2} d\rho. \quad (4.27)$$

Upon using the far-field behavior for  $\bar{v}$  in (4.26 b), and by evaluating the integral in (4.27), we get that

$$\lambda_0 = 8\alpha^2. \quad (4.28)$$

We then integrate (4.26) directly to obtain

$$\Delta \bar{v} = 2\alpha \log(1 - \alpha\rho^2) + 4(\alpha + \beta) - 2\alpha \log(-\alpha). \quad (4.29)$$

A further integration yields

$$\bar{v}_\rho = \alpha\rho \log(\rho^2 - 1/\alpha) - \frac{\log(1 - \alpha\rho^2)}{\rho} + \rho(\alpha + 2\beta), \quad \rho > 0; \quad \bar{v}(0) = 0, \quad (4.30)$$

and one final additional integration gives

$$\bar{v} = \frac{\alpha}{2} \left( \rho^2 - \frac{1}{\alpha} \right) \log(\rho^2 - 1/\alpha) + \beta\rho^2 - \frac{1}{2} \log(-\alpha) - \int_0^\rho \frac{\log(1 - \alpha x^2)}{x} dx. \quad (4.31)$$

The integral in (4.31) is then rewritten as

$$\begin{aligned} \int_0^\rho \frac{\log(1 - \alpha x^2)}{x} dx &= \frac{1}{2} \int_0^1 \frac{\log(1+y)}{y} dy + \frac{1}{2} \int_1^{-\alpha\rho^2} \left( \frac{\log(1+y)}{y} - \frac{\log y}{y} \right) dy + \int_1^{-\alpha\rho^2} \frac{\log y}{y} dy \\ &= \frac{\pi^2}{24} + \frac{1}{4} [\log(-\alpha\rho^2)]^2 + \frac{1}{2} \int_1^{-\alpha\rho^2} \frac{\log(1+1/y)}{y} dy, \end{aligned} \quad (4.32)$$

so that (4.31) becomes

$$\begin{aligned} \bar{v}(\rho) &= \frac{\alpha}{2} \left( \rho^2 - \frac{1}{\alpha} \right) \log(\rho^2 - 1/\alpha) + \beta\rho^2 - (\log \rho)^2 - \log(-\alpha) \log \rho \\ &\quad - \left[ \frac{\pi^2}{24} + \frac{1}{4} [\log(-\alpha)]^2 + \frac{1}{2} \int_1^{-\alpha\rho^2} \frac{\log(1+1/x)}{x} dx \right]. \end{aligned} \quad (4.33)$$

In (4.33), the integral term on the right-hand side of (4.33) is finite as  $\rho \rightarrow \infty$ . In fact, (4.33) has the far-field behavior

$$\bar{v} \sim \alpha\rho^2 \log \rho + \beta\rho^2 - \log^2 \rho - (1 + \log(-\alpha)) \log \rho - \frac{1}{2} \left[ \frac{\pi^2}{6} + \frac{1}{2} \log^2(-\alpha) + \log(-\alpha) + 1 \right], \quad (4.34)$$

as  $\rho \rightarrow \infty$ , where the identity  $\int_1^\infty x^{-1} \log(1+1/x) dx = \pi^2/12$  has been used. A comparison of (4.34) with the required far-field behavior (4.26 b) indicates that

$$b_3 = \frac{\lambda_1}{4\alpha^2} - \frac{\lambda_0\Gamma_1}{4\alpha^2} - 1 - \log(-\alpha), \quad c_3 = b_4 - \frac{\lambda_0\Gamma_2}{4\alpha^2} - \frac{\lambda_1\Gamma_1}{4\alpha^2} - \frac{1}{2} \left[ \frac{\pi^2}{6} + \frac{1}{2} \log^2(-\alpha) + \log(-\alpha) + 1 \right]. \quad (4.35)$$

This concludes the analysis of terms at  $\mathcal{O}(\sigma)$ .



At order  $\mathcal{O}(\sigma^2)$ , the inner problem for  $v_2$  is

$$\Delta^2 v_2 = -\frac{\lambda_1}{v_0^2} + \frac{2\lambda_0}{v_0^3} v_1, \quad \rho > 0; \quad v_2 = v_{2\rho} = v_{2\rho\rho} = 0, \quad \text{at } \rho = 0, \quad (4.36 a)$$

where  $v_2$  satisfies the far-field condition

$$\begin{aligned} v_2 \sim & -\frac{\lambda_0}{12\alpha^2} \log^3 \rho + \left( \frac{\lambda_0 \Gamma_1}{4\alpha^2} - \frac{\lambda_1}{8\alpha^2} \right) \log^2 \rho + \left( b_4 + \frac{\lambda_0 \Gamma_2}{2\alpha^2} + \frac{\lambda_1 \Gamma_1}{4\alpha^2} - \frac{\lambda_2}{4\alpha^2} \right) \log \rho \\ & - \frac{\lambda_0}{8\alpha^2} (a_c \cos 2\theta + a_s \sin 2\theta) \log \rho + \left( d_4 - \frac{\lambda_1 a_c}{16\alpha^3} + \frac{\lambda_0 a_c}{8\alpha^3} \left( \frac{\beta}{\alpha} + \frac{1}{4} \right) \right) \cos 2\theta \\ & + \left( e_4 - \frac{\lambda_1 a_s}{16\alpha^3} + \frac{\lambda_0 a_s}{8\alpha^3} \left( \frac{\beta}{\alpha} + \frac{1}{4} \right) \right) \sin 2\theta + c_4 - b_5 - \frac{\lambda_0 \Gamma_3}{4\alpha^2} + \frac{\lambda_1 \Gamma_2}{4\alpha^2} + \frac{\lambda_2 \Gamma_1}{4\alpha^2} + \dots, \quad \text{as } \rho \rightarrow \infty. \end{aligned} \quad (4.36 b)$$

To determine  $\lambda_1$  we integrate (4.36 a) over  $0 < \rho < L$ , and then let  $L \rightarrow \infty$ . Since the far-field behavior of  $v_2$  gives no contribution to the flux of  $\Delta v_2$ , we get

$$\lambda_1 \int_0^{2\pi} \int_0^\infty \frac{1}{v_0^2} \rho d\rho d\theta = \lambda_0 \int_0^{2\pi} \int_0^\infty \frac{2v_1}{v_0^3} \rho d\rho d\theta.$$

The integration over the angular component gives no contribution to the integral, and so with  $v_0 = 1 - \alpha\rho^2$  we get

$$\lambda_1 = -4\alpha\lambda_0 \int_0^\infty \frac{\bar{v}}{v_0^3} \rho d\rho, \quad (4.37)$$

where  $\bar{v}(\rho)$  is the radially symmetric component of  $v_1(\rho, \theta)$ , as defined in (4.31). Upon setting  $v_0 = 1 - \alpha\rho^2$ , and then integrating (4.37) by parts, we obtain that

$$\begin{aligned} \lambda_1 &= -\lambda_0 \int_0^\infty \bar{v} \left[ \frac{1}{(1 - \alpha\rho^2)^2} \right]_\rho d\rho = \lambda_0 \int_0^\infty \bar{v}_\rho \left[ \frac{1}{(1 - \alpha\rho^2)^2} \right] d\rho \\ &= \lambda_0 \int_0^\infty \left[ \alpha\rho \log(\rho^2 - 1/\alpha) - \frac{\log(1 - \alpha\rho^2)}{\rho} + \rho(\alpha + 2\beta) \right] \left( \frac{1}{1 - \alpha\rho^2} \right)^2 d\rho \\ &= \lambda_0 [\alpha + 2\beta - \alpha \log(-\alpha)] \int_0^\infty \frac{\rho d\rho}{(1 - \alpha\rho^2)^2} - \lambda_0 \int_0^\infty \frac{\log(1 - \alpha\rho^2)}{\rho(1 - \alpha\rho^2)} d\rho \\ &= -\frac{\lambda_0}{2} \left[ 1 + \frac{2\beta}{\alpha} + \log(-\alpha) \right] - \frac{\lambda_0}{2} \int_0^\infty \frac{\log(1+x)}{x(1+x)} dx = -\frac{\lambda_0}{2} \left[ \frac{\pi^2}{6} - \log(-\alpha) + \left( 1 + \frac{2\beta}{\alpha} \right) \right]. \end{aligned}$$

In the preceding calculation, the identity  $\int_0^\infty \log(1+x)/(x+x^2) dx = \pi^2/6$  has been used. This completes the two-term asymptotic construction of the limiting asymptotic behavior of the maximal solution to (4.1) in an arbitrary 2-D domain. We summarize our result as follows:

**Principal Result 4.1:** *In the limit  $\varepsilon \equiv u(x_0) + 1 \rightarrow 0^+$ , the limiting behavior of the maximal solution branch of (4.1) has the asymptotic behavior*

$$u = u_0 - \frac{\varepsilon \log \sigma}{\sigma} u_{1/2} + \frac{\varepsilon}{\sigma} u_1 - \varepsilon \log \sigma u_{3/2} + \varepsilon u_2 + \mathcal{O}(\varepsilon \sigma \log \sigma), \quad \lambda = \frac{\varepsilon}{\sigma} \lambda_0 + \varepsilon \lambda_1 + \mathcal{O}(\varepsilon \sigma), \quad (4.38 a)$$

where  $\sigma = -1/\log \gamma$  and the boundary layer width  $\gamma$  near  $x_0$  is determined implicitly in terms of  $\varepsilon$  by  $-\gamma^2 \log \gamma = \varepsilon$ . The concentration point  $x_0 \in \Omega$  satisfies

$$\nabla_x R(x; x_0)|_{x=x_0} = 0, \quad R(x_0; x_0) > 0, \quad (4.38 b)$$

where  $R(x; x_0)$  is the Regular part of the biharmonic Green's function, as defined in (1.4). In terms of this Green's

function,

$$u_0 = -\frac{G(x; x_0)}{R(x_0; x_0)}, \quad u_{1/2} = \frac{\lambda_0}{4\alpha^2} u_0, \quad u_{1/2} = \frac{\lambda_1}{4\alpha^2} u_0, \quad (4.38 c)$$

where

$$u_0 \sim -1 + \alpha r^2 \log r + r^2(\beta + a_c \cos 2\theta + a_s \sin 2\theta) + \dots, \quad (4.38 d)$$

as  $x - x_0 = r(\cos \theta, \sin \theta) \rightarrow 0$  and  $(\alpha, \beta, a_c, a_s)$  are given in (4.7 b) in terms of properties of  $R(x; x_0)$ . Additionally,  $u_1$  and  $u_2$  satisfy

$$\Delta u_1 = -\frac{\lambda_0}{(1 + u_0)^2}, \quad x \in \Omega; \quad u_1 = \partial_n u_1 = 0, \quad x \in \partial\Omega \quad (4.38 e)$$

$$u_1 \sim \frac{\lambda_0}{4\alpha^2} \log(-\log r) + \frac{\lambda_0}{4\alpha^2} + \mathcal{O}(\log^{-1} r), \quad r \rightarrow 0,$$

$$\Delta u_2 = -\frac{\lambda_1}{(1 + u_0)^2}, \quad x \in \Omega; \quad u_2 = \partial_n u_2 = 0, \quad x \in \partial\Omega, \quad (4.38 f)$$

$$u_2 \sim \frac{\lambda_1}{4\alpha^2} \log(-\log r) + \frac{\lambda_0}{4\alpha^2} \log r + \frac{\lambda_0}{2\alpha^2} \left(1 + \frac{\beta}{\alpha}\right) + \frac{\lambda_1}{4\alpha^2} - \log(-\alpha) + \mathcal{O}(\log^{-1} r).$$

Finally,  $\lambda_0$  and  $\lambda_1$  are given by

$$\lambda_0 = 8\alpha^2, \quad \lambda_1 = -\frac{\lambda_0}{2} \left[ \frac{\pi^2}{6} - \log(-\alpha) + \left(1 + \frac{2\beta}{\alpha}\right) \right]. \quad (4.38 g)$$

By assumption, we have  $\alpha < 0$  and so all formulae in this result are well-defined.

From (4.38 g), (4.38 a), and (4.7 b), we observe that the two-term asymptotic result depends only on the regular part  $R(x_0; x_0)$  of the biharmonic Green's function together with the trace of the Hessian of  $R(x; x_0)$  at  $x = x_0$ , which we denote by  $\text{Trace}(\mathcal{R}_{00})$ . For an arbitrary 2-D domain, in §4.1 we outline a boundary integral numerical method to compute these quantities from the biharmonic Green's function problem defined by (1.4). We now illustrate Principal Result 4.1 for a few specific domain shapes.

Our first example is the unit disk, which was considered previously in [22]. Then,  $x_0 = 0$ , and  $G(r, 0)$  is given in (2.7), which yields  $R_{00} = 1/16\pi$ . Then, from (4.7 b), we obtain that  $\alpha = -2$  and  $\beta = 1$ , so that from (4.38 g) we get

$$\lambda_0 = 32, \quad \lambda_1 = 16 (\log 2 - \pi^2/6). \quad (4.39)$$

In Fig. 5(a) we show a very favorable comparison between the asymptotic result for  $\lambda$  versus  $\varepsilon$ , obtained from (4.39) and (4.38 a), and the full numerical result computed numerically from (4.1).

Our second example is for a square domain of sidelength two given by  $[-1, 1]^2$ . For this domain, where by symmetry the concentration point  $x_0$  is at the origin, the numerical method outlined in §4.1 provides

$$R(x_0; x_0) \approx 0.0226\dots, \quad \text{Trace}(\mathcal{R}_{00}) \equiv (R_{x_1 x_1} + R_{x_2 x_2})|_{x=x_0} \approx -0.0892\dots \quad (4.40)$$

From (4.7 b), (4.38 a), (4.38 g), and (4.40), we obtain our two-term asymptotic result for  $\lambda$  versus  $\varepsilon$ . In Fig. 5(b) we show a very favorable comparison between this asymptotic result and the corresponding full numerical result computed from (4.1) for the square. To obtain our full numerical results we used the approach of [21] consisting of a combination of a finite difference discretization of (4.1) with  $100^2$  mespoints together with a pseudo-arclength continuation method to compute the maximal solution branch for  $\lambda$ .

Our final example is for a one-parameter family of dumbbell-shaped domains. Let  $z \in \mathcal{B}$ , where  $\mathcal{B}$  is the unit disk,

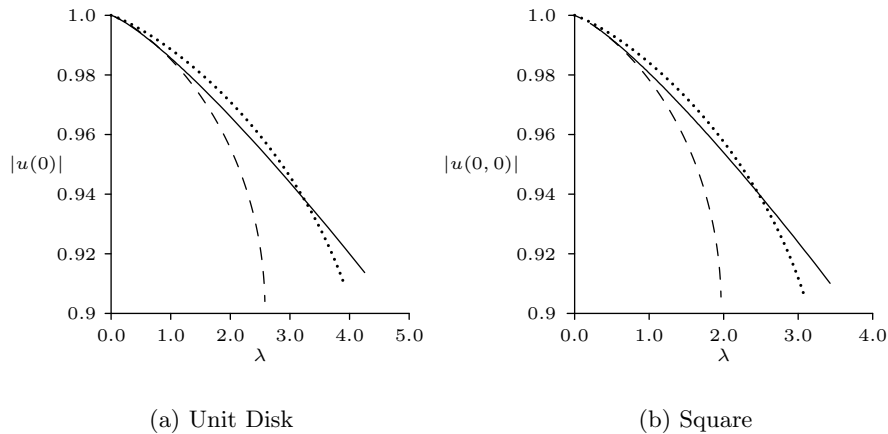


FIGURE 5. Numerical solutions for  $|u(0)|$  versus  $\lambda$  (solid curves) computed for the unit disk  $|x| \leq 1$  (left figure) and for the square  $\Omega \equiv [-1, 1]^2$  (right figure) are compared with the one-term (closely spaced dots) and the two-term (dashed lines) asymptotic results for  $\lambda$  obtained from Principal Result 4.1.

$b$	$x_0$	$R(x_0, x_0)$	$\text{Trace}(\mathcal{R}_{00})$
2.00000	0.00000	$1.05312 \times 10^{-2}$	$-2.44476 \times 10^{-2}$
1.83995	0.00000	$9.08917 \times 10^{-3}$	$-2.44656 \times 10^{-2}$
1.50000	-0.39000	$6.48716 \times 10^{-3}$	$1.12095 \times 10^{-2}$
	0.00000	$5.15298 \times 10^{-3}$	$4.00099 \times 10^{-2}$
1.05000	0.39000	$6.48716 \times 10^{-3}$	$1.12095 \times 10^{-2}$
	-0.49450	$4.94718 \times 10^{-3}$	$3.11557 \times 10^{-2}$
	0.000000	$9.59768 \times 10^{-5}$	$0.379489 \times 10^{-2}$
	0.494500	$4.94718 \times 10^{-3}$	$3.11557 \times 10^{-2}$

Table 1. Let  $\mathcal{B}$  be the unit disk, and consider the one-parameter family of mappings  $\Omega = f(\mathcal{B}; b)$ , where  $f(z; b)$  is defined in (4.41). Numerical results for the regular part  $R(x_0; x_0)$  of the biharmonic Green's function and the Hessian  $\text{Trace}(\mathcal{R}_{00})$  are given for four values of  $b$  at each available concentration point  $x_0 = (x_0, 0)$ , for which  $\nabla_x R(x; x_0)|_{x=x_0} = 0$  and  $R(x_0; x_0) > 0$ .

and define the complex mapping  $w = f(z; b)$  by

$$w = f(z; b) = \frac{(1 - b^2)z}{z^2 - b^2}, \quad (4.41)$$

where  $b$  is real and  $b > 1$ . The resulting domain  $\Omega = f(\mathcal{B}; b)$  is shown in Fig. 6 for several values of  $b$ . Notice that  $\Omega \rightarrow \mathcal{B}$  as  $b \rightarrow \infty$ . Moreover, as  $b \rightarrow 1^+$ ,  $\Omega$  approaches the union of two circles centered at  $(\pm 1/2, 0)$ , with radius  $1/2$ , that are connected by a thin neck region. This class of dumbbell-shaped domains is symmetric with respect to both coordinate axes, and hence for any  $b > 1$  there is always a concentration point  $x_0$  at the origin, i.e.  $x_0 = 0$ . With this example we show that there can be multiple concentration points lying along the horizontal axis  $x_0 = (x_0, 0)$  when the domain is sufficiently non-convex. In Table 1 we give numerical values for  $R(x_0; x_0)$  and  $\text{Trace}(\mathcal{R}_{00})$  as computed from the numerical method of §4.1. Our numerical results show that there are two additional concentration points, one in each lobe of the dumbbell, when  $b < b_c \approx 1.83995$ . Thus,  $b_c$  corresponds to a pitchfork bifurcation point for the set of concentration points. In Fig. 6 we plot the numerically computed  $R(x_0; x_0)$  versus  $x_0 = (x_0, 0)$ , together with the dumbbell-shaped domain, for four representative values of the domain-shape parameter  $b$ . The numerical values in Table 1 can be used in Principal Result 4.1 to obtain a two-term expansion for the nonlinear eigenvalue

parameter  $\lambda$  when the solution to (4.1) is chosen to concentrate at any one of the available choices for  $x_0$ . Given the considerable difficulty of providing a high resolution numerical solution for the biharmonic nonlinear eigenvalue problem in an arbitrarily-shaped domain, it is an open problem to numerically validate the predicted asymptotic behavior of the maximal solution branch, and the possibility of multiple concentration points.

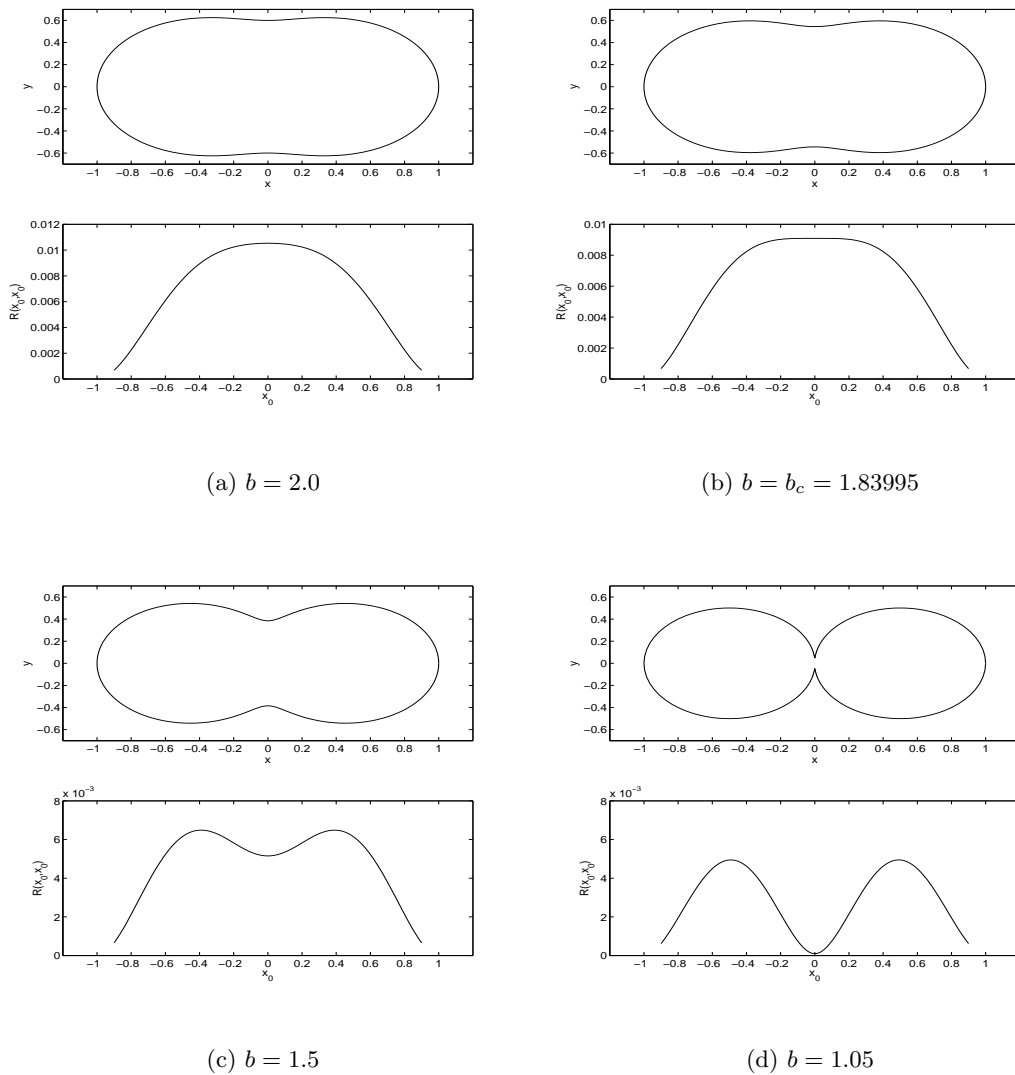


FIGURE 6. Let  $\mathcal{B}$  be the unit disk and take  $z \in \mathcal{B}$ . For the one-parameter family of mappings  $\Omega = f(\mathcal{B}; b)$ , where  $f(z; b)$  is defined in (4.41), we plot the numerically computed regular part  $R(x_0; x_0)$  of the biharmonic Green's function, defined in (1.4), versus  $x_0 = (x_0, 0)$  for four different values of  $b$  (bottom in each subfigure). A plot of the dumbbell-shaped domain at the given value of  $b$  is also shown (top in each subfigure). Notice that when  $1 < b < b_c$ , there are three possible concentration points  $x_0$  for (4.1) on the horizontal axis where  $\nabla_x R(x; x_0)|_{x=x_0} = 0$  and  $R(x_0; x_0) > 0$ .

#### 4.1 Numerical Computation of Biharmonic Green's Function

In order to numerically compute the biharmonic Green's function defined by (1.4), we use the integral equation methods presented in [12] that were developed to solve biharmonic boundary value problems associated with two-

$N$	$x_0$	Error $R(x_0, x_0)$	Error $\nabla_x R(x; x_0) _{x=x_0}$	Error Trace( $\mathcal{R}_{00}$ )
64	(-0.3, 0.2)	$4.3368 \times 10^{-18}$	$1.9102 \times 10^{-17}$	$1.3878 \times 10^{-17}$
64	(0.9, -0.1)	$8.4811 \times 10^5$	$2.0243 \times 10^9$	$2.6956 \times 10^{10}$
128		$7.3877 \times 10^{-9}$	$2.7754 \times 10^{-7}$	$5.7836 \times 10^{-8}$
256		$5.7051 \times 10^{-13}$	$1.6329 \times 10^{-12}$	$2.2552 \times 10^{-11}$
512		$3.9465 \times 10^{-17}$	$1.3341 \times 10^{-17}$	$7.2164 \times 10^{-16}$
512	(-0.95, -0.3)	$1.6657 \times 10^7$	$1.9099 \times 10^8$	$4.4241 \times 10^{10}$
1024		$5.0545 \times 10^{-4}$	$2.3108 \times 10^{-5}$	$1.7146 \times 10^{-2}$
2048		$5.6127 \times 10^{-6}$	$1.0205 \times 10^{-6}$	$1.1839 \times 10^{-4}$
4096		$6.7720 \times 10^{-9}$	$8.8722 \times 10^{-10}$	$4.0415 \times 10^{-8}$
8192		$1.0167 \times 10^{-15}$	$3.2269 \times 10^{-16}$	$4.0745 \times 10^{-14}$

Table 2. Errors in the computed solution to the regular part  $R(x_0; x_0)$  of the biharmonic Green's function in the unit disk for  $x_0 \neq (0, 0)$ . The analytical result for  $R(x_0; x_0)$  is given in (4.42). Above,  $N$  indicates the number of points used in the discretization of the boundary. Due to the singular nature of the integral operators in the integral equation, quadrature errors are large when  $x_0$  is close to the boundary; however, these errors decay exponentially as  $N$  increases.

dimensional Stokes flow and isotropic elasticity in the plane. The analytic formulation for the integral equations is based on the complex variable theory for the biharmonic and the classical Sherman-Lauricella equation (cf. [23], [24]). The numerical methods use a spectrally accurate, fast-multipole accelerated, iterative solution procedure. We will not discuss these methods in any detail here, as they are discussed at length in [12] and [31].

In order to verify the correctness of the numerical methods for computing the biharmonic Green's function of (1.4), we note that there is an exact formula for  $G(x; x_0)$  in the unit disk in  $\mathbb{R}^2$ , valid for any  $x_0$  in the disk. This solution, due to Boggio [1] (see also [30]), is

$$G(x; x_0) = \frac{1}{8\pi} |x - x_0|^2 \int_1^{\theta(x, x_0)} \frac{(v^2 - 1)}{v} dv, \quad \text{where} \quad \theta(x, x_0) \equiv \sqrt{1 + \frac{(1 - |x_0|^2)(1 - |x|^2)}{|x - x_0|^2}}.$$

From this expression and (1.4), we can identify the regular part  $R(x; x_0)$  of  $G$  as

$$R(x; x_0) = \frac{1}{16\pi} (1 - |x_0|^2)(1 - |x|^2) - \frac{1}{16\pi} |x - x_0|^2 \log [ |x - x_0|^2 + (1 - |x|^2)(1 - |x_0|^2) ].$$

From this formula for  $R(x; x_0)$ , we readily calculated that

$$R(x_0; x_0) = \frac{1}{16\pi} (1 - |x_0|^2)^2, \quad \nabla_x R(x; x_0)|_{x=x_0} = \frac{1}{8\pi} (|x_0|^2 - 1) x_0, \quad (4.42 a)$$

$$\text{Trace}(\mathcal{R}_{00}) = \frac{1}{4\pi} (|x_0|^2 - 1) - \frac{1}{2\pi} \log(1 - |x_0|^2). \quad (4.42 b)$$

These formulae are used to check the errors in our numerical solution. The results are shown in Table 2.

## 5 A Biharmonic Eigenvalue Problem for a Perforated Plate

In this section we consider a singularly perturbed linear biharmonic eigenvalue problem in a two-dimensional domain  $\Omega$  that is perforated by a small arbitrarily-shaped hole  $\Omega_\varepsilon$  of "radius"  $\varepsilon$  such that  $\Omega_\varepsilon \rightarrow x_0 \in \Omega$  as  $\varepsilon \rightarrow 0$ . The

perturbed eigenvalue problem is formulated as

$$\Delta^2 u - \lambda u = 0, \quad x \in \Omega \setminus \Omega_\varepsilon; \quad \int_{\Omega \setminus \Omega_\varepsilon} u^2 dx = 1, \quad (5.1 a)$$

$$u = \partial_n u = 0, \quad x \in \partial\Omega; \quad u = \partial_n u = 0, \quad x \in \partial\Omega_\varepsilon. \quad (5.1 b)$$

We will determine an asymptotic expansion for  $\lambda(\varepsilon)$  as  $\varepsilon \rightarrow 0$ , with limiting behavior  $\lambda(\varepsilon) \rightarrow \lambda_0$  as  $\varepsilon \rightarrow 0$ . This leading term  $\lambda_0$ , and its corresponding eigenfunction  $u_0$ , are an eigenpair of the following limiting problem with a point constraint, referred to as the punctured plate problem:

$$\Delta^2 u_0 - \lambda_0 u_0 = 0, \quad x \in \Omega \setminus \{x_0\}; \quad \int_{\Omega} u_0^2 dx = 1, \quad (5.2 a)$$

$$u_0 = \partial_n u_0 = 0, \quad x \in \partial\Omega; \quad u_0(x_0) = 0. \quad (5.2 b)$$

The key feature in this problem, as shared by the model problem in Case I of §2, is that we must introduce the point constraint  $u_0(x_0) = 0$ . Therefore, in the limit of small hole radius, the eigenvalue for the perforated eigenvalue problem (5.1) does not tend to an eigenvalue of the biharmonic eigenvalue problem in the domain without a hole. The limiting punctured plate eigenvalue problem (5.2) has a countably infinite set of eigenvalues with corresponding orthogonal eigenfunctions (cf. [2]), each with singular behavior  $\mathcal{O}(|x - x_0|^2 \log |x - x_0|)$  as  $x \rightarrow x_0$ .

To solve the limiting problem (5.2) it is convenient to introduce the Green's function  $G(x; x_0, \lambda_0)$  satisfying

$$\Delta^2 G - \lambda_0 G = 0, \quad x \in \Omega \setminus \{x_0\}; \quad G = \partial_n G = 0, \quad x \in \partial\Omega. \quad (5.3 a)$$

Then,  $G(x; x_0, \lambda_0)$  can be decomposed in terms of its singular part and its  $C^2$  smooth ‘‘regular’’ part  $R(x; x_0, \lambda_0)$  as

$$G(x; x_0, \lambda_0) = \frac{1}{8\pi} |x - x_0|^2 \log |x - x_0| + R(x; x_0, \lambda_0). \quad (5.3 b)$$

In terms of  $G$ , the solution to (5.2), up to a normalization factor, is simply  $u_0 = G(x; x_0, \lambda_0)$ , where  $\lambda_0$  is a root of

$$R(x_0; x_0, \lambda_0) = 0. \quad (5.4)$$

In developing an asymptotic expansion for  $\lambda(\varepsilon)$  below, we will consider two specific cases. Case I (see §5.1):  $\lambda_0$  is a root of (5.4) of multiplicity one with  $\nabla_x R(x; x_0, \lambda_0)|_{x=x_0} \neq 0$ . Case II (see §5.2):  $\lambda_0$  is a root of (5.4) of multiplicity one with  $\nabla_x R(x; x_0, \lambda_0)|_{x=x_0} = 0$ .

### 5.1 Case I: A Simple Eigenvalue With Non-Degeneracy Condition

In this subsection we consider the generic case where  $\lambda_0$  is a root of (5.4) of multiplicity one with  $\nabla_x R(x; x_0, \lambda_0)|_{x=x_0} \neq 0$ . The asymptotic methodology needed to treat this problem is similar to that of Case II of §2.

We expand the eigenvalue  $\lambda(\varepsilon)$  of (5.1), together with the outer solution for this problem, as

$$\lambda(\varepsilon) = \lambda_0 + \sum_{k=1}^{\infty} \nu^k \lambda_k + \cdots, \quad u = u_0 + \sum_{k=1}^{\infty} \nu^k u_k + \cdots, \quad \nu \equiv \frac{-1}{\log \varepsilon}, \quad (5.5)$$

where  $u_0 = G(x; x_0, \lambda_0)$ . Upon substituting these expansions into (5.1), we obtain that  $u_1$  and  $u_k$  for  $k > 1$  satisfy

$$\Delta^2 u_1 - \lambda_0 u_1 = \lambda_1 u_0, \quad x \in \Omega \setminus \{x_0\}; \quad u_1 = \partial_n u_1 = 0, \quad x \in \partial\Omega; \quad \int_{\Omega} u_0 u_1 dx = 0, \quad (5.6 a)$$

$$\Delta^2 u_k - \lambda_0 u_k = \lambda_k u_0 + \sum_{i=1}^{k-1} \lambda_i u_{k-i}, \quad x \in \Omega \setminus \{x_0\}; \quad u_k = \partial_n u_k = 0, \quad x \in \partial\Omega, \quad (5.6 b)$$

with some normalization condition on  $u_k$  for  $k > 1$ . The singularity behaviors for  $u_k$  for  $k \geq 1$  as  $x \rightarrow x_0$ , which are required for determining  $\lambda_k$  for  $k \geq 1$ , are derived below after matching  $u_k$  as  $x \rightarrow x_0$  to the far-field behavior of certain inner solutions near the hole.

In the inner region, we let  $y = \varepsilon^{-1}(x - x_0)$  and we introduce the canonical vector-valued inner solution  $\psi_c$  defined as the unique solution of

$$\Delta_y^2 \psi_c = 0, \quad y \in \mathbb{R}^2 \setminus \Omega_0; \quad \psi_c = \partial_n \psi_c = 0, \quad y \in \partial\Omega_0; \quad \psi_c \sim y \log |y|, \quad \text{as } |y| \rightarrow \infty. \quad (5.7 a)$$

Here  $\Omega_0 \equiv \varepsilon^{-1}\Omega_\varepsilon$ . In terms of this solution, there exists a unique  $2 \times 2$  matrix  $\mathcal{M}$ , which depends on the shape of the hole, such that

$$\psi_c \sim y \log |y| + \mathcal{M}y + o(1), \quad \text{as } |y| \rightarrow \infty. \quad (5.7 b)$$

For an arbitrarily-shaped subdomain  $\Omega_0$ , the matrix  $\mathcal{M}$  in (5.7 b) can be computed numerically from the integral equation method described in §5.1 of [31]. There are a few cases when  $\mathcal{M}$  is known analytically. When  $\Omega_0$  is the unit disk, then the solution to (5.7) is

$$\psi_c = y \log |y| - \frac{y}{2} + \frac{y}{2|y|^2}, \quad (5.8)$$

so that  $\mathcal{M} = -I/2$ , where  $I$  is the identity matrix. In addition, when  $\Omega_0$  is an ellipse with semi-major axis  $a$  and semi-minor axis  $b$ , where  $a > b$ , and where the semi-major axis is inclined at an angle  $\alpha$  to the horizontal coordinate  $y_1 > 0$ , it can be shown that the matrix entries of  $\mathcal{M}$  are (see Appendix B of [31])

$$m_{11} = \frac{(b-a)\cos^2\alpha - b}{a+b} - \log\left(\frac{a+b}{2}\right), \quad m_{22} = \frac{(a-b)\cos^2\alpha - a}{a+b} - \log\left(\frac{a+b}{2}\right), \quad (5.9 a)$$

$$m_{12} = m_{21} = -\frac{(a-b)\sin\alpha\cos\alpha}{a+b}. \quad (5.9 b)$$

In the inner region, we expand  $u = \varepsilon\nu \sum_{k=0}^{\infty} \nu^k \psi_k$ , where  $\Delta_y^2 \psi_k = 0$ . We take  $\psi_k = a_k \cdot \psi_c$ , where  $a_k$  is an unknown vector,  $\cdot$  denotes dot product, and where the vector-valued function  $\psi_c$  satisfies (5.7). Thus, the inner expansion is

$$u = \varepsilon\nu \sum_{k=0}^{\infty} \nu^k a_k \cdot \psi_c. \quad (5.10)$$

Then, by using the far-field behavior (5.7 b) of  $\psi_c$  in (5.10), we write the resulting expression in terms of the outer variable  $x - x_0 = \varepsilon y$  to get

$$u \sim a_0 \cdot (x - x_0) + \sum_{k=1}^{\infty} \nu^k [a_{k-1} \cdot (x - x_0) \log |x - x_0| + a_k \cdot (x - x_0) + a_{k-1} \cdot \mathcal{M}(x - x_0)]. \quad (5.11)$$

This gives the required singular behavior as  $x \rightarrow x_0$  for each term in the outer expansion (5.5).

By comparing the leading-order terms in (5.5) and (5.11) for  $u$ , we obtain that  $u_0 \sim a_0 \cdot (x - x_0)$  as  $x \rightarrow x_0$ . Since  $u_0 = G(x; x_0, \lambda_0)$ , we conclude from (5.3 b) that

$$a_0 = \nabla_x R(x; x_0, \lambda_0)|_{x=x_0}. \quad (5.12)$$

Then, by equating the  $\mathcal{O}(\nu^k)$  terms in  $u$  in (5.5) and (5.11), we conclude that each  $u_k$  for  $k \geq 1$  satisfies (5.6) subject to the singular behavior

$$u_k \sim a_{k-1} \cdot (x - x_0) \log |x - x_0| + [a_{k-1} \cdot \mathcal{M}(x - x_0) + a_k \cdot (x - x_0)], \quad \text{as } x \rightarrow x_0, \quad (5.13)$$

where  $a_0$  is given in (5.12).

The problems (5.6) for  $k \geq 1$ , with singularity behavior (5.13), allows for the recursive determination of the unknown vectors  $a_k$  for  $k \geq 1$ , with  $a_0$  as given in (5.12). In particular, with a known value for  $a_{k-1}$ , the singular behavior  $u_k \sim a_{k-1} \cdot (x - x_0) \log |x - x_0|$  as  $x \rightarrow x_0$  will determine  $\lambda_k$  from a solvability condition applied to (5.6). Then, the coefficient  $a_k$  in (5.13) is found from the regular part of the solution for  $u_k$ . Finally,  $u_k$  can be made unique by imposing a normalization condition.

The first step in this procedure is the calculation of  $\lambda_k$ . This is done with the following Lemma:

**Lemma 5.1:** *Let  $u_0, \lambda_0$  be an eigenpair of (5.2) with multiplicity one, and assume that  $\nabla_x R(x; x_0, \lambda_0)|_{x=x_0} \neq 0$ . Then, a necessary condition for the problem*

$$\Delta^2 u_k - \lambda_0 u_k = \lambda_k u_0 + f(x), \quad x \in \Omega \setminus \{x_0\}; \quad u = \partial_n u = 0, \quad x \in \partial\Omega, \quad (5.14 a)$$

$$u_k \sim a_{k-1} \cdot (x - x_0) \log |x - x_0|, \quad \text{as } x \rightarrow x_0, \quad (5.14 b)$$

to have a solution is that  $\lambda_k$  satisfies

$$\lambda_k (u_0, u_0) = -(f, u_0) + 4\pi a_{k-1} \cdot \nabla_x R_0. \quad (5.15)$$

Here  $\nabla_x R_0 \equiv \nabla_x R(x; x_0, \lambda_0)$ , and we have defined the inner product  $(g, h) \equiv \int_{\Omega} gh \, dx$ .

The proof of this result follows by applying Green's identity to  $u_0$  and  $u_k$  over the punctured domain  $\Omega \setminus B_\delta$ , where  $B_\delta$  is a circular disk of radius  $\delta \ll 1$  centered at  $x_0$ . This identity readily yields that

$$\lambda_k \int_{\Omega \setminus B_\delta} u_0^2 \, dx + \int_{\Omega \setminus B_\delta} f u_0 \, dx = \int_{\partial B_\delta} [u_0 \partial_n (\Delta u_1) - \Delta u_1 \partial_n u_0 - u_1 \partial_n (\Delta u_0) + \Delta u_0 \partial_n u_1] \, ds. \quad (5.16)$$

Here  $\partial_n$  denotes the normal derivative directed inwards to  $B_\delta$ , so that  $\partial_n = -\partial_r$  where  $r = |x - x_0|$ . Next, we let  $\delta \rightarrow 0$ , and use (5.3 b) for  $u_0 = G(x; x_0, \lambda_0)$  together with (5.14 b) to calculate for  $r \rightarrow 0$  that

$$u_k \sim (a_{k-1} \cdot e) r \log r, \quad \partial_r u_k \sim (a_{k-1} \cdot e) [\log r + 1], \quad \Delta u_k \sim \frac{2}{r} (a_{k-1} \cdot e), \quad \partial_r (\Delta u_k) \sim -\frac{2}{r^2} (a_{k-1} \cdot e),$$

$$u_0 \sim (a_0 \cdot e) r + \frac{r^2}{8\pi} \log r, \quad \partial_r u_0 \sim (a_0 \cdot e) + \frac{r}{4\pi} \log r + \frac{r}{8\pi}, \quad \Delta u_0 \sim \frac{1}{2\pi} \log r + \frac{1}{2\pi}, \quad \partial_r (\Delta u_0) \sim \frac{1}{2\pi r},$$

where  $a_0 = \nabla_x R(x; x_0, \lambda_0)|_{x=x_0}$ . Here we have defined  $e$  by  $e \equiv (\cos \theta, \sin \theta)^T$ . Upon substituting these limiting relations into (5.16), and then taking the limit  $\delta \rightarrow 0$ , we obtain that

$$\lambda_k (u_0, u_0) + (f, u_0) = \int_0^{2\pi} 4 (a_{k-1} \cdot e) (a_0 \cdot e) \, d\theta = 4\pi a_{k-1} \cdot a_0 = 4\pi a_{k-1} \cdot \nabla_x R_0, \quad (5.18)$$

which completes the proof of Lemma 5.1. ■

By using Lemma 5.1, we can calculate the coefficients  $\lambda_k$  in the asymptotic expansion of  $\lambda(\varepsilon)$  from (5.6) and (5.13) to obtain the following main result:

**Principal Result 5.2:** *Let  $u_0, \lambda_0$  be an eigenpair of (5.2) with multiplicity one, and assume that  $\nabla_x R(x; x_0, \lambda_0)|_{x=x_0} \neq 0$ . Then, the eigenvalue  $\lambda(\varepsilon)$  for the perturbed problem (5.1) has the expansion*

$$\lambda(\varepsilon) \sim \lambda_0 + \nu \lambda_1 + \sum_{k=2}^{\infty} \nu^k \lambda_k, \quad \nu \equiv \frac{-1}{\log \varepsilon}, \quad (5.19 a)$$



where  $\lambda_1$  and  $\lambda_k$  for  $k \geq 2$  are given by

$$\lambda_1 = 4\pi \frac{|\nabla_x R_0|^2}{(u_0, u_0)}, \quad \lambda_k = \frac{1}{(u_0, u_0)} \left[ 4\pi a_{k-1} \cdot \nabla_x R_0 - \sum_{i=1}^{k-1} \lambda_i (u_{k-i}, u_0) \right], \quad (5.19 b)$$

and  $\nabla_x R_0 \equiv \nabla_x R(x; x_0, \lambda_0)|_{x=x_0}$ . In (5.19 b) the vectors  $a_k$  for  $k \geq 1$ , with  $a_0 = \nabla_x R_0$ , are determined recursively from the problems (5.6) and (5.13) for  $u_k$  for  $k \geq 1$ .

For the case of a circular hole of radius  $\varepsilon$ , then  $\psi_c$  satisfies (5.8) and  $\mathcal{M} = -I/2$ . For this special case we can conveniently replace  $\nu$  and  $a_k$  in (5.19 a) and (5.19 b) with  $\tilde{\nu} \equiv -1/\log(\varepsilon e^{1/2})$  and  $b_k$ , respectively, where each  $u_k$  for  $k \geq 1$ , with  $b_0 \equiv \nabla_x R_0$ , satisfies (5.6) subject to the singularity behavior

$$u_k \sim b_{k-1} \cdot (x - x_0) \log|x - x_0| + b_k \cdot (x - x_0), \quad \text{as } x \rightarrow x_0.$$

Finally, we remark that instead of evaluating the individual vector coefficients  $a_k$  for  $k \geq 1$  needed in Principal Result 5.2, it is possible to formulate a hybrid problem similar to that in [31] that effectively sums the infinite logarithmic expansion in (5.19 a). To do so, we write the inner solution in terms of an unknown vector  $A = A(\nu)$  as

$$u = \varepsilon \nu A \cdot \psi_c(y), \quad (5.20)$$

where  $\psi_c(y)$  is the unique solution to (5.7). By using (5.7 b), the far-field behavior of this solution, as written in terms of the outer variable  $x = x_0 + \varepsilon y$ , is

$$u \sim A \cdot (x - x_0) + \nu A \cdot [(x - x_0) \log|x - x_0| + \mathcal{M}(x - x_0)], \quad \nu = \frac{-1}{\log \varepsilon}. \quad (5.21)$$

This expression gives the required singularity behavior for the outer solution accurate to within all logarithmic terms. In this way, the hybrid method for summing the infinite logarithmic expansion for  $\lambda(\varepsilon)$  is to solve the following hybrid problem for  $u^*$ ,  $\lambda^*$ , and the vector  $A = A(\nu)$ :

$$\Delta^2 u^* - \lambda^* u^* = 0, \quad x \in \Omega \setminus \{x_0\}; \quad u^* = \partial_n u^* = 0, \quad x \in \partial\Omega; \quad \int_{\Omega} (u^*)^2 dx = 1, \quad (5.22 a)$$

$$u \sim A \cdot (x - x_0) + \nu A \cdot [(x - x_0) \log|x - x_0| + \mathcal{M}(x - x_0)], \quad \nu = \frac{-1}{\log \varepsilon}. \quad (5.22 b)$$

Then, to within a negligible transcendentally small algebraic error term in  $\varepsilon$ , we have  $\lambda(\varepsilon) \sim \lambda^*$ , as  $\varepsilon \rightarrow 0$ .

We now illustrate the theory by way of a specific example that can be solved analytically. Let  $\Omega$  be the unit disk that contains an arbitrarily-shaped hole of ‘‘radius’’  $\varepsilon$  centered at the origin. For  $\varepsilon \rightarrow 0$ , we look for an eigenfunction of the limiting problem (5.2) that has either a  $\cos \theta$  or  $\sin \theta$  dependence. A simple calculation shows that this type of solution to the limiting punctured plate eigenvalue problem (5.2) is given by

$$u_0 = c_0 \left( J_1(\eta_0 r) - \frac{J_1(\eta_0) I_1(\eta_0 r)}{I_1(\eta_0)} \right) \cos \theta + d_0 \left( J_1(\eta_0 r) - \frac{J_1(\eta_0) I_1(\eta_0 r)}{I_1(\eta_0)} \right) \sin \theta, \quad (5.23 a)$$

where  $\eta_0 \equiv \lambda_0^{1/4}$  is taken to be the first positive root of the transcendental equation

$$J_1(\eta) I_1'(\eta) - J_1'(\eta) I_1(\eta) = 0. \quad (5.23 b)$$

Here  $c_0$  and  $d_0$  are arbitrary constants, while  $I_1$  and  $J_1$  denote Bessel functions in the standard notation. Therefore, the limiting eigenvalue problem has two independent eigenfunctions corresponding to the eigenvalue  $\lambda_0 = \eta_0^4$ .

For a non-circular hole, this degeneracy in the leading-order eigenpair is broken only at order  $\mathcal{O}(\nu^2)$  in the expansion of the eigenvalue. To determine precisely how the eigenvalue is split by the asymmetry induced by the small arbitrarily-shaped hole, we will determine an infinite order expansion to the eigenvalue by using the hybrid formulation (5.22).

This approach is more tractable analytically than evaluating all of the individual coefficients in the expansion of the eigenvalue as in Principal Result 5.2.

From the hybrid formulation (5.22),  $u^*$ ,  $\lambda^*$  and  $A = (A_1, A_2)^T$  satisfy (5.22 a) subject to the singular behavior (5.22 b) as  $r \rightarrow 0$ , which we write in expanded form as

$$u^* \sim [A_1 \nu r \log r + A_1 r + \nu A_1 m_{11} r + \nu A_2 m_{21} r] \cos \theta + [A_2 \nu r \log r + A_2 r + \nu A_1 m_{12} r + \nu A_2 m_{22} r] \sin \theta. \quad (5.24)$$

Here  $m_{jk}$ , for  $j, k = 1, 2$ , are the entries of the matrix  $\mathcal{M}$  defined by (5.7 b). Since the required solution to (5.22 a) is a linear combination of  $\{J_1(\eta r), Y_1(\eta r), I_1(\eta r), K_1(\eta r)\}(\cos \theta, \sin \theta)$ , where  $\eta \equiv (\lambda^*)^{1/4}$ , it can be written in terms of six unknown coefficients as

$$u^* = \left[ c_0 J_1(\eta r) + c_2 I_1(\eta r) + c_1 \left( Y_1(\eta r) + \frac{2}{\pi} K_1(\eta r) \right) \right] \cos \theta + \left[ d_0 J_1(\eta r) + d_2 I_1(\eta r) + d_1 \left( Y_1(\eta r) + \frac{2}{\pi} K_1(\eta r) \right) \right] \sin \theta. \quad (5.25)$$

Notice that this particular linear combination of  $Y_1$  and  $K_1$  eliminates the  $1/r$  singularity in  $u^*$  as  $r \rightarrow 0$ .

From the well-known local behaviors of  $J_1$ ,  $I_1$ ,  $Y_1$ , and  $K_1$ , we calculate for  $r \rightarrow 0$  that

$$Y_1(\eta r) + \frac{2}{\pi} K_1(\eta r) \sim \frac{2}{\pi} \eta r \log r + \frac{2\eta r}{\pi} \left[ \log \left( \frac{\eta}{2} \right) + \gamma_e - \frac{1}{2} \right], \quad J_1(\eta r) \sim \frac{\eta r}{2}, \quad I_1(\eta r) \sim \frac{\eta r}{2}, \quad (5.26)$$

where  $\gamma_e$  is Euler's constant. Then, we use (5.26) in (5.25) to obtain the local behavior of  $u^*$  as  $r \rightarrow 0$ . By comparing this local behavior of  $u^*$  with the required behavior in (5.24) we obtain upon examining the  $\mathcal{O}(r \log r)$  term that

$$c_1 = \frac{A_1 \nu \pi}{2\eta}, \quad d_1 = \frac{A_2 \nu \pi}{2\eta}. \quad (5.27 a)$$

Similarly, by comparing the  $\mathcal{O}(r)$  terms in the local behavior of  $u^*$ , we obtain

$$\frac{(c_0 + c_2)}{2} \eta + A_1 b_{11} + A_2 b_{12} = 0, \quad \frac{(d_0 + d_2)}{2} \eta + A_1 b_{21} + A_2 b_{22} = 0, \quad (5.27 b)$$

where the coefficients  $b_{jk}$  for  $j, k = 1, 2$  are defined by

$$b_{jj} = \nu \left( \log \left( \frac{\eta}{2} \right) + \gamma_e - \frac{1}{2} \right) - 1 - \nu m_{jj}, \quad j = 1, 2; \quad b_{12} = -\nu m_{12}, \quad b_{21} = -\nu m_{21}. \quad (5.27 c)$$

Finally, to ensure that  $u^*$  in (5.25) satisfies  $u^* = \partial_r u^* = 0$  on  $r = 1$ , we must impose that

$$\begin{pmatrix} c_0 \\ d_0 \end{pmatrix} J_1(\eta) + \begin{pmatrix} c_2 \\ d_2 \end{pmatrix} I_1(\eta) = -\frac{\nu \pi}{2\eta} \begin{pmatrix} A_1 \\ A_2 \end{pmatrix} \left( Y_1(\eta) + \frac{2}{\pi} K_1(\eta) \right) = 0, \quad (5.27 d)$$

$$\begin{pmatrix} c_0 \\ d_0 \end{pmatrix} J_1'(\eta) + \begin{pmatrix} c_2 \\ d_2 \end{pmatrix} I_1'(\eta) = -\frac{\nu \pi}{2\eta} \begin{pmatrix} A_1 \\ A_2 \end{pmatrix} \left( Y_1'(\eta) + \frac{2}{\pi} K_1'(\eta) \right) = 0. \quad (5.27 e)$$

The system (5.27) is a linear homogeneous system for the unknowns  $c_0, d_0, c_2, d_2, A_1, A_2$ , with eigenvalue parameter  $\eta = (\lambda^*)^{1/4}$ . By using (5.27 d) and (5.27 e) to eliminate  $A_1$  and  $A_2$ , a simple calculation shows that this system can be written as the equivalent  $4 \times 4$  homogeneous system

$$\mathcal{A} \zeta = 0, \quad \mathcal{A} \equiv \begin{pmatrix} b_{11} J_1(\eta) - \frac{\nu}{2\gamma_1} & b_{11} I_1(\eta) - \frac{\nu}{2\gamma_1} & b_{12} J_1(\eta) & b_{12} I_1(\eta) \\ J_1'(\eta) - \gamma_0 J_1(\eta) & I_1'(\eta) - \gamma_0 I_1(\eta) & 0 & 0 \\ b_{21} J_1(\eta) & b_{21} I_1(\eta) & b_{22} J_1(\eta) - \frac{\nu}{2\gamma_1} & b_{22} I_1(\eta) - \frac{\nu}{2\gamma_1} \\ 0 & 0 & J_1'(\eta) - \gamma_0 J_1(\eta) & I_1'(\eta) - \gamma_0 I_1(\eta) \end{pmatrix}, \quad (5.28 a)$$

where  $\zeta \equiv (c_0, c_2, d_0, d_2)^T$  and  $\nu = -1/\log \varepsilon$ . In (5.28 a),  $\gamma_0$  and  $\gamma_1$  are defined by

$$\gamma_0 \equiv \left( \frac{Y_1'(\eta) + \frac{2}{\pi} K_1'(\eta)}{Y_1(\eta) + \frac{2}{\pi} K_1(\eta)} \right), \quad \gamma_1 \equiv \frac{2}{\pi} \left[ Y_1(\eta) + \frac{2}{\pi} K_1(\eta) \right]^{-1}. \quad (5.28 b)$$

In (5.28 a) the coefficients  $b_{jk}$ , for  $j, k = 1, 2$ , are defined in (5.27 c).

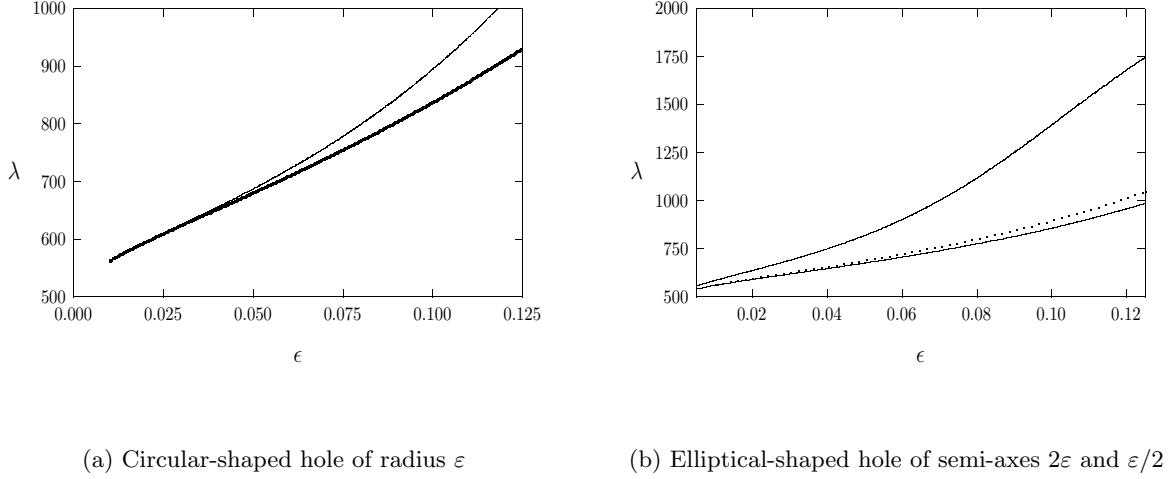


FIGURE 7. Left figure: For the annulus  $\varepsilon < |x| < 1$ , the asymptotic approximation  $\lambda^*$  (solid curve), as obtained from (5.29), is compared with the exact solution  $\lambda(\varepsilon)$  (heavy solid curve), as obtained by requiring that (5.30) satisfy  $u = u_r = 0$  on  $r = \varepsilon$  and  $r = 1$ . Right figure: for the elliptical-shaped hole  $x_1^2/4 + 4x_2^2 = \varepsilon^2$  of area  $\pi\varepsilon^2$ , the asymptotic approximations  $\lambda_{\pm} = \eta_{\pm}^4$  (solid curves) are plotted versus  $\varepsilon$ , where  $\eta_{\pm}$  are the first two roots of  $\det(\mathcal{A}) = 0$  with  $\mathcal{A}$  is defined in (5.28). The dotted curve is the asymptotic approximation  $\lambda^*$ , as computed from (5.29), corresponding to the eigenvalue of multiplicity two for the case of a circular hole of the same area  $\pi\varepsilon^2$ .

For the special case of a circular hole of radius  $\varepsilon$ , so that  $m_{12} = m_{21} = 0$  and  $m_{11} = m_{22} = -1/2$ , then  $b_{12} = b_{21}$  and  $b_{11} = b_{22} = b_c \equiv \nu(\log(\eta/2) + \gamma_e - 1/2) - 1 + \nu/2$ . For this special case, where the eigenfunction degeneracy is not broken, the matrix  $\mathcal{A}$  can be written in block diagonal form and there are two independent vectors  $\zeta_1 = (c_0, c_2, 0, 0)^T$  and  $\zeta_2 = (0, 0, d_0, d_2)^T$  for the common eigenvalue  $\lambda^* = \eta^4$ , where  $\eta$  is the first positive root of

$$J_1(\eta)I_1'(\eta) - J_1'(\eta)I_1(\eta) = \frac{\nu}{2b_c\gamma_1} [I_1'(\eta) - J_1'(\eta) - \gamma_0(I_1(\eta) - J_1(\eta))]. \quad (5.29)$$

For a circular hole of radius  $\varepsilon$ , in Fig. 7(a) we compare the asymptotic approximation  $\lambda^*$  versus  $\varepsilon$ , as obtained from (5.29), with the exact result for  $\lambda(\varepsilon)$  as obtained by requiring that the solution

$$u = [c_0 J_1(\eta r) + c_2 I_1(\eta r) + c_3 K_1(\eta r) + c_4 Y_1(\eta r)] \cos \theta \quad (5.30)$$

to (5.1) satisfy the four conditions  $u = u_r = 0$  on  $r = \varepsilon$  and  $r = 1$ . As seen from this figure, the asymptotic and full numerical results agree rather well on the range  $0 < \varepsilon < 0.1$ .

Next, consider an elliptical-shaped hole  $x_1^2/a^2 + x_2^2/b^2 = \varepsilon^2$ , for which the matrix entries of  $\mathcal{M}$  are given in (5.9) with inclination angle  $\alpha = 0$ . For this example, when  $\varepsilon$  is small there are two nearby roots  $\eta_{\pm}$  to  $\det(\mathcal{A}) = 0$ , where  $\mathcal{A}$  is defined in (5.28), which have the common limiting behavior  $\eta_{\pm} \rightarrow \eta_{00}$  as  $\nu \rightarrow 0$ . Here  $\eta_{00}$  is the first positive root of  $J_1(\eta)I_1'(\eta) - J_1'(\eta)I_1(\eta) = 0$ . In Fig. 7(b) we plot the two curves  $\lambda_{\pm} = \eta_{\pm}^4$  versus  $\varepsilon$  for an elliptical-shaped hole with semi-axes  $a = 2$  and  $b = 1/2$ . This example clearly shows how the asymmetry of the hole breaks the degeneracy of the eigenvalue of multiplicity two for the limiting problem (5.2), and leads to the creation of two closely-spaced simple eigenvalues for the perturbed problem (5.1).

## 5.2 The Degenerate Case

We now consider the degenerate case when the hole is centered at a nodal point  $x_0$  of the limiting punctured plate eigenfunction  $u_0$ , so that  $\nabla u_0(x_0) = 0$ . Then, since

$$u_0(x) = G(x; x_0, \lambda_0) = \frac{1}{8\pi} |x - x_0|^2 \log |x - x_0| + R(x; x_0, \lambda_0), \quad (5.31 a)$$

with  $R(x_0; x_0, \lambda_0) = 0$  and  $\nabla_x R(x; x_0, \lambda_0)|_{x=x_0} = 0$ , we obtain that  $u_0$  has the following local behavior as  $x \rightarrow x_0$ :

$$u_0 \sim \frac{1}{8\pi} |x - x_0|^2 \log |x - x_0| + \frac{1}{2} (x - x_0)^T \mathcal{H} (x - x_0) + \mathcal{O}(|x - x_0|^3). \quad (5.31 b)$$

Here  $T$  denotes transpose, and  $\mathcal{H}$  is the  $2 \times 2$  Hessian matrix of  $R$  at  $x = x_0$  with matrix entries

$$\mathcal{H}_{i,j} = \left( \frac{\partial^2}{\partial x_i \partial x_j} R(x; x_0, \lambda_0) \right) \Big|_{x=x_0}, \quad i, j = 1, 2. \quad (5.31 c)$$

Upon writing the limiting behavior (5.31 b) in terms of the inner variable  $y = \varepsilon^{-1}(x - x_0)$ , we obtain that

$$u_0 \sim (-\varepsilon^2 \log \varepsilon) \left( -\frac{|y|^2}{8\pi} \right) + \varepsilon^2 \left( \frac{1}{8\pi} |y|^2 \log |y| + \frac{1}{2} y^T \mathcal{H} y \right). \quad (5.32)$$

The local behavior (5.32) suggests that we write the inner expansion with  $y = \varepsilon^{-1}(x - x_0)$  as

$$v(y) = u(x_0 + \varepsilon y) = (-\varepsilon^2 \log \varepsilon) \left[ v_0 + \nu v_1 + \sum_{j=2}^{\infty} \nu^j v_j \right], \quad \nu \equiv -1/\log \varepsilon. \quad (5.33)$$

Upon substituting (5.33) into (5.1) we obtain that  $v_k$  for  $k \geq 0$  satisfies

$$\Delta_y^2 v_k = 0, \quad y \notin \Omega_0; \quad v_k = \partial_n v_k = 0, \quad y \in \partial\Omega_0, \quad (5.34 a)$$

with the following far-field asymptotic behavior as  $|y| \rightarrow \infty$ ;

$$v_0 \sim -\frac{1}{8\pi} |y|^2; \quad v_1 \sim \frac{1}{8\pi} |y|^2 \log |y| + \frac{1}{2} y^T \mathcal{H} y; \quad v_k = o(y^2), \quad k \geq 2. \quad (5.34 b)$$

Since the solutions of the homogeneous problem for  $v_k$  for  $k \geq 0$  are linear combinations of  $\{\rho^2 \log \rho, \rho^2, \log \rho, 1\}$ ,  $\{\rho^3, \rho \log \rho, \rho, \rho^{-1}\} \times \{\cos \theta, \sin \theta\}$ , and  $\{\rho^4, \rho^2, 1, \rho^{-2}\} \times \{\cos 2\theta, \sin 2\theta\}$  etc., where  $y = \rho(\cos \theta, \sin \theta)$ , the far-field behavior of the solution  $v_0$  to (5.34) must have the form

$$v_0 \sim -\frac{1}{8\pi} |y|^2 + A_0 \log |y| + f_0 \cdot y + \frac{y^T \mathcal{D}_0 y}{|y|^2} + o(1), \quad \text{as } |y| \rightarrow \infty, \quad (5.35 a)$$

for some constant  $A_0$ , vector  $f_0$ , and matrix  $\mathcal{D}_0$ , all determined by the shape of  $\Omega_0$ . Notice that we have imposed that  $|y|^{-1} (v_0 + |y|^2/(8\pi))$  is bounded as  $|y| \rightarrow \infty$ . In contrast, for  $v_k$  for  $k \geq 1$  we will allow for a growth of the order  $\mathcal{O}(y \log |y|)$  as  $|y| \rightarrow \infty$ . In terms of an arbitrary vector  $b_1$ , the far-field behavior of the solution to (5.34) has the form

$$v_1 \sim \frac{1}{8\pi} |y|^2 \log |y| + \frac{1}{2} y^T \mathcal{H} y + b_1 \cdot y \log |y| + f_1 \cdot y + A_1 \log |y| + \frac{y^T \mathcal{D}_1 y}{|y|^2} + o(1), \quad \text{as } |y| \rightarrow \infty, \quad (5.35 b)$$

for some constant  $A_1$ , vector  $f_1$ , and matrix  $\mathcal{D}_1$  determined in terms of the unknown  $b_1$  and the shape of  $\Omega_0$ . Finally, for  $v_k$  for  $k \geq 2$ , we have the far-field behavior

$$v_k \sim b_k \cdot (y \log y + \mathcal{M} y) + A_k \log |y| + \frac{y^T \mathcal{D}_k y}{|y|^2} + o(1), \quad \text{as } |y| \rightarrow \infty. \quad (5.35 c)$$

Here  $\mathcal{M}$  is the matrix defined in (5.7), while the scalar  $A_k$  and matrix  $\mathcal{D}_k$  are determined in terms of the unknown

vector  $b_k$  and the shape of  $\Omega_0$ . The need for including the, as yet, arbitrary vectors  $b_k$  for  $k \geq 1$  is explained below after matching the inner and outer expansions.

For the special case of a circular hole of radius  $\varepsilon$ , the solutions  $v_k$  for  $k \geq 0$  to (5.34) on  $|y| \geq 1$  can be readily calculated explicitly as

$$v_0 = -\frac{|y|^2}{8\pi} + \frac{1}{4\pi} \log |y| + \frac{1}{8\pi}, \quad (5.36 a)$$

$$v_1 = \frac{|y|^2}{8\pi} \log |y| + \frac{1}{4} (\text{Trace}\mathcal{H}) |y|^2 - \left( \frac{\text{Trace}\mathcal{H}}{2} + \frac{1}{8\pi} \right) \log |y| - \frac{\text{Trace}\mathcal{H}}{4} + b_1 \cdot \left( y \log |y| - \frac{y}{2} + \frac{y}{2|y|^2} \right) \quad (5.36 b)$$

$$+ (|y|^2 - 2 + |y|^{-2}) \left( \frac{1}{4} (R_{x_1x_1} - R_{x_2x_2}) \cos(2\theta) + \frac{1}{2} R_{x_1x_2} \sin(2\theta) \right), \quad (5.36 c)$$

$$v_k = b_k \cdot \left( y \log |y| - \frac{y}{2} + \frac{y}{2|y|^2} \right) \quad k \geq 2. \quad (5.36 d)$$

Here  $\text{Trace}\mathcal{H}$  denotes the trace of the Hessian matrix  $\mathcal{H}$  in (5.31). Upon comparing (5.36) with (5.35), we identify  $A_k$ ,  $f_0$ ,  $f_1$ ,  $\mathcal{M}$ , and  $\mathcal{D}_k$ , for the case of a circular hole of radius  $\varepsilon$  as

$$A_0 = \frac{1}{4\pi}, \quad A_1 = -\frac{1}{2} (\text{Trace}\mathcal{H}) - \frac{1}{8\pi}, \quad A_k = 0, \quad k \geq 2; \quad f_0 = 0, \quad f_1 = -\frac{b_1}{2}, \quad \mathcal{M} = -\frac{I}{2}, \quad (5.37 a)$$

$$\mathcal{D}_0 = \frac{I}{8\pi}, \quad \mathcal{D}_1 = \frac{1}{4} (\text{Trace}\mathcal{H}) I - \mathcal{H}, \quad \mathcal{D}_k = 0, \quad k \geq 2, \quad (5.37 b)$$

where  $I$  is the identity matrix.

Next, we substitute the far-field expansions (5.35) into the inner expansion in (5.33), and we write the resulting expression in terms of the outer variable  $x = x_0 + \varepsilon y$ . In this way, we obtain the following matching condition for the outer solution:

$$\begin{aligned} u \sim & \frac{1}{8\pi} |x - x_0|^2 \log |x - x_0| + \frac{1}{2} (x - x_0)^T \mathcal{H} (x - x_0) + (-\varepsilon \log \varepsilon) [(f_0 + b_1) \cdot (x - x_0)] \\ & + \varepsilon \sum_{k=1}^{\infty} \nu^{k-1} [b_k \cdot (x - x_0) \log |x - x_0| + (b_{k+1} + f_k) \cdot (x - x_0)] + (-\varepsilon \log \varepsilon)^2 A_0 \\ & + (-\varepsilon^2 \log \varepsilon) \left[ A_0 \log |x - x_0| + A_1 + \frac{(x - x_0)^T \mathcal{D}_0 (x - x_0)}{|x - x_0|^2} \right] + \varepsilon^2 \left[ A_1 \log |x - x_0| + A_2 + \frac{(x - x_0)^T \mathcal{D}_1 (x - x_0)}{|x - x_0|^2} \right]. \end{aligned} \quad (5.38 a)$$

Here  $f_1$  is defined from (5.35 b), and we have labeled  $f_k$  for  $k \geq 2$  by  $f_k = \mathcal{M}b_k$ .

The matching condition (5.38) suggest that we expand the eigenvalue  $\lambda$  and the outer solution as

$$u = u_0 + \frac{\varepsilon}{\nu} \sum_{k=1}^{\infty} \nu^{k-1} \tilde{u}_k + \frac{\varepsilon^2}{\nu^2} (u_1 + \nu u_2 + \nu^2 u_3 + \dots), \quad (5.39 a)$$

$$\lambda = \lambda_0 + \frac{\varepsilon}{\nu} \sum_{k=1}^{\infty} \nu^{k-1} \tilde{\lambda}_k + \frac{\varepsilon^2}{\nu^2} (\lambda_1 + \nu \lambda_2 + \nu^2 \lambda_3 + \dots). \quad (5.39 b)$$

Upon substituting (5.39) into (5.1), and by using the matching condition (5.38), we obtain that  $\tilde{u}_k$  for  $k \geq 1$  satisfies

$$\Delta^2 \tilde{u}_k - \lambda_0 \tilde{u}_k = \tilde{\lambda}_k u_0, \quad x \in \Omega; \quad \tilde{u}_k = \partial_n \tilde{u}_k = 0, \quad x \in \partial\Omega, \quad (5.40 a)$$

subject to the following local behavior as  $x \rightarrow x_0$ :

$$\tilde{u}_1 \sim (f_0 + b_1) \cdot (x - x_0); \quad \tilde{u}_k \sim b_{k-1} \cdot (x - x_0) \log |x - x_0| + (f_{k-1} + b_k) \cdot (x - x_0), \quad k \geq 1. \quad (5.40 b)$$

Since  $u_0(x_0; x_0, \lambda_0) = \nabla_x u_0(x; x_0, \lambda_0)|_{x=x_0} = 0$ , a simple calculation similar to the proof of Lemma 5.1 yields that  $\tilde{\lambda}_k = 0$  for  $k \geq 1$ . Therefore, the solution to (5.40) for  $k = 1$  is simply  $\tilde{u}_1 = N_1 u_0$  for any normalization constant  $N_1$ . Then, since  $\nabla_x u_0(x; x_0, \lambda_0)|_{x=x_0} = 0$ , we must choose  $b_1$  as  $b_1 = -f_0$  to eliminate the gradient term in the local expansion (5.40 b) for  $\tilde{u}_1$ . Moreover, we can take  $N_1 = 0$  so that  $\tilde{u}_1 \equiv 0$ . To solve (5.40) for  $\tilde{u}_k$  for  $k \geq 2$ , and in the process identify the vectors  $b_k$  for  $k \geq 2$ , we first look for a solution  $\tilde{u}_k$  to (5.40 a) for  $k \geq 2$  in the form

$$\tilde{u}_k = b_{k-1} \cdot U, \quad (5.41)$$

where the vector-valued function  $U$  is the unique solution to

$$\Delta^2 U - \lambda_0 U = 0, \quad x \in \Omega; \quad U = \partial_n U = 0, \quad x \in \partial\Omega; \quad \int_{\Omega} u_0 U \, dx = 0, \quad (5.42 a)$$

$$U \sim (x - x_0) \log |x - x_0|, \quad \text{as } x \rightarrow x_0. \quad (5.42 b)$$

In terms of this solution, we identify a unique matrix  $\mathcal{C}$  such that

$$U - (x - x_0) \log |x - x_0| \rightarrow C(x - x_0) + o(|x - x_0|^2), \quad \text{as } x \rightarrow x_0. \quad (5.42 c)$$

Upon comparing (5.42 c) and (5.41) with the nonsingular part of the local behavior for  $u_k$  in (5.40 b), and recalling that  $f_k = \mathcal{M}b_k$ , we conclude that the  $b_k$  for  $k \geq 2$  are determined recursively from

$$b_1 = -f_0; \quad b_2 = \mathcal{C}^t b_1 - f_1; \quad b_k = (\mathcal{C}^T - \mathcal{M}) b_{k-1}, \quad k \geq 3. \quad (5.43)$$

With the vector coefficients  $b_k$  for  $k \geq 1$  determined in this way, we can calculate the middle term in the outer expansion (5.39 a) as

$$\frac{\varepsilon}{\nu} \sum_{k=1}^{\infty} \nu^{k-1} \tilde{u}_k = \frac{\varepsilon}{\nu} U \cdot \left[ -\nu f_0 - \nu^2 (\mathcal{C}^T f_0 + f_1) + \sum_{k=3}^{\infty} \nu^k b_k \right], \quad (5.44)$$

where  $b_k = (\mathcal{C}^T - \mathcal{M}) b_{k-1}$  for  $k \geq 3$ . Suppose that the matrix  $(\mathcal{C}^T - \mathcal{M})$  is diagonalizable with eigenvalues  $\sigma_1$  and  $\sigma_2$ . Then, the infinite series in (5.44) is not only asymptotic, but is convergent when  $\varepsilon$  is sufficiently small such that  $\nu \sigma_m < 1$ , where  $\sigma_m = \max(|\sigma_1|, |\sigma_2|)$ . A similar convergence result holds for the non-generic case where  $\sigma_1 = \sigma_2$  and the matrix is degenerate.

We remark that if we did not include the vector coefficient  $b_1$  in (5.35 b), then the problem for  $\tilde{u}_1$ , given by  $\Delta^2 \tilde{u}_1 - \lambda_0 \tilde{u}_1 = 0$  with  $\tilde{u}_1 \sim f_0 \cdot (x - x_0)$  as  $x \rightarrow x_0$  with  $f_0$  as specified by the far-field behavior (5.35 a) for  $v_0$ , would have no solution. More specifically, since the vector  $f_0$ , as determined (5.34 a) and (5.35 a), does not in general satisfy  $f_0 = 0$ , the solution  $\tilde{u}_1 = N_0 u_0$  with  $\nabla_x u_0(x; x_0, \lambda_0)|_{x=x_0} = 0$ , cannot be made to satisfy the condition  $\tilde{u}_1 \sim f_0 \cdot (x - x_0)$  as  $x \rightarrow x_0$ .

Next, we continue the expansion to higher order to determine the first nonzero terms in the expansion  $\lambda - \lambda_0$  in (5.39 b). To do so, we substitute (5.39) into (5.1), and use  $\tilde{\lambda}_k = 0$ , to obtain that  $u_k$  for  $k = 1, 2, 3$  satisfies

$$\Delta^2 u_k - \lambda_0 u_k = \lambda_k u_0, \quad x \in \Omega; \quad u_k = \partial_n u_k = 0, \quad x \in \partial\Omega. \quad (5.45 a)$$

We can make  $u_k$  unique by imposing that  $\int_{\Omega} u_0 u_k \, dx = 0$ . From the  $\mathcal{O}(\varepsilon^2 \nu^j)$  terms in the matching condition (5.38) we obtain that  $u_k$  must satisfy the following local behavior as  $x \rightarrow x_0$ :

$$u_1 \sim A_0; \quad u_k \sim A_{k-2} \log |x - x_0| + A_{k-1} + \frac{(x - x_0)^T \mathcal{D}_{k-2} (x - x_0)}{|x - x_0|^2}, \quad k = 2, 3. \quad (5.45 b)$$

In a similar manner as in the proof of Lemma 5.1, a solvability condition for each of the problems (5.45) determine the eigenvalue corrections  $\lambda_k$  for  $k = 1, 2, 3$ . More specifically, by applying Green's identity to  $u_0$  and  $u_k$  over the

punctured domain  $\Omega \setminus B_\delta$ , where  $B_\delta$  is a circular disk of radius  $\delta \ll 1$  centered at  $x_0$  with  $r = |x - x_0|$ , we obtain for  $k = 1, 2, 3$  that

$$\lambda_k \int_{\Omega \setminus B_\delta} u_0^2 dx = \int_{\partial B_\delta} [-u_0 \partial_r (\Delta u_k) + \Delta u_k \partial_r u_0 + u_k \partial_r (\Delta u_0) - \Delta u_0 \partial_r u_k] ds. \quad (5.46)$$

From (5.31 b), we calculate for  $r \rightarrow 0$  that

$$u_0 \sim r^2 \log r + \mathcal{O}(r^2), \quad \partial_r u_0 \sim \frac{1}{4\pi} r \log r + \mathcal{O}(r), \quad \Delta u_0 \sim \frac{1}{2\pi} \log r + \frac{1}{2\pi} + \text{Trace} \mathcal{H}, \quad \partial_r (\Delta u_0) \sim \frac{1}{2\pi r}. \quad (5.47)$$

To determine  $\lambda_1$ , we let  $\delta \rightarrow 0$  in (5.46) with  $k = 1$  and use  $u_1 \sim A_0$  as  $r \rightarrow 0$  from (5.45 b). Only the third term on the right-hand side of (5.46) is non-vanishing in the  $\delta \rightarrow 0$  limit, and we get

$$\lambda_1 \int_{\Omega} u_0^2 dx = \lim_{\delta \rightarrow 0} \int_{\partial B_\delta} u_1 \partial_r (\Delta u_0) ds = \lim_{\delta \rightarrow 0} \int_0^{2\pi} A_0 \left( \frac{1}{2\pi\delta} \right) \delta d\theta = A_0. \quad (5.48)$$

To determine  $\lambda_2$  we use (5.45 b) for  $k = 2$  to calculate for  $r \rightarrow 0$  that

$$u_2 \sim A_0 \log r + A_1 + \mathcal{D}_{011} \cos^2 \theta + \mathcal{D}_{022} \sin^2 \theta + \mathcal{D}_{012} \sin(2\theta), \quad \partial_r u_2 \sim \frac{A_0}{r}, \quad (5.49 a)$$

$$\Delta u_2 \sim -\frac{2}{r^2} [(\mathcal{D}_{011} - \mathcal{D}_{022}) \cos(2\theta) + 2\mathcal{D}_{012} \sin(2\theta)], \quad \partial_r (\Delta u_2) \sim \frac{4}{r^3} [(\mathcal{D}_{011} - \mathcal{D}_{022}) \cos(2\theta) + 2\mathcal{D}_{012} \sin(2\theta)], \quad (5.49 b)$$

Here  $\mathcal{D}_{0ij}$  for  $1 \leq i, j \leq 2$ , denote the entries of the matrix  $\mathcal{D}_0$ . Since  $\int_0^{2\pi} \cos(2\theta) d\theta = \int_0^{2\pi} \sin(2\theta) d\theta = 0$ , only the third and the fourth terms on the right-hand side of (5.46) are non-vanishing in the limit  $\delta \rightarrow 0$ . From (5.46), (5.47) and (5.49), we obtain that

$$\begin{aligned} \lambda_2 \int_{\Omega} u_0^2 dx &= \lim_{\delta \rightarrow 0} \int_{\partial B_\delta} (u_2 \partial_r (\Delta u_0) - \Delta u_0 \partial_r u_2) ds \\ &= \lim_{\delta \rightarrow 0} \left[ \frac{1}{2\pi} \int_0^{2\pi} (A_0 \log \delta + A_1 + \mathcal{D}_{011} \cos^2 \theta + \mathcal{D}_{022} \sin^2 \theta) d\theta - \int_0^{2\pi} \left( \frac{A_0}{2\pi} + A_0 \text{Trace} \mathcal{H} + \frac{A_0}{2\pi} \right) d\theta \right] \\ &= A_1 - A_0 - 2\pi A_0 \text{Trace} \mathcal{H} + \frac{1}{2} \text{Trace} \mathcal{D}_0. \end{aligned}$$

An identical calculation determines  $\lambda_3$ . We summarize our result for the expansion of the eigenvalue as follows:

**Principal Result 5.3:** *Let  $u_0 = G(x; x_0, \lambda_0)$ ,  $\lambda_0$  be an eigenpair of (5.2) with multiplicity one, and assume that  $\nabla_x R(x; x_0, \lambda_0)|_{x=x_0} = 0$ . Here  $G(x; x_0, \lambda_0)$  is the Green's function satisfying (5.3) with regular part  $R(x; x_0, \lambda_0)$  given by (5.3 b). Then, the eigenvalue  $\lambda(\varepsilon)$  for the perturbed problem (5.1) has the expansion*

$$\lambda(\varepsilon) \sim \lambda_0 + (-\varepsilon \log \varepsilon)^2 \lambda_1 + \varepsilon^2 (-\log \varepsilon) \lambda_2 + \varepsilon^2 \lambda_3 + \dots, \quad (5.50 a)$$

where  $\lambda_1 \int_{\Omega} u_0^2 dx = A_0$ , and  $\lambda_k$  for  $k = 2, 3$  are given by

$$\lambda_k \int_{\Omega} u_0^2 dx = A_{k-1} - A_{k-2} - 2\pi A_{k-2} \text{Trace} \mathcal{H} + \frac{1}{2} \text{Trace} \mathcal{D}_{k-2}. \quad (5.50 b)$$

In (5.50 b) the coefficients  $A_0, A_1, A_2$ , and matrices  $\mathcal{D}_0$  and  $\mathcal{D}_1$  are determined from the far-field behavior (5.35) of the inner problems near the hole, while  $\mathcal{H}$  is the Hessian of  $u_0$  at  $x_0$  given in (5.31 b). For the special case of a circular hole of radius  $\varepsilon$ , (5.37) yields that

$$\lambda_1 \int_{\Omega} u_0^2 dx = \frac{1}{4\pi}; \quad \lambda_2 \int_{\Omega} u_0^2 dx = -\frac{1}{4\pi} - \text{Trace} \mathcal{H}; \quad \lambda_3 \int_{\Omega} u_0^2 dx = \frac{1}{8\pi} + \pi (\text{Trace} \mathcal{H})^2 + \frac{1}{2} \text{Trace} \mathcal{H}. \quad (5.50 c)$$

We now illustrate the theory for the case of the annular region  $0 < \varepsilon < |x| < 1$ . For this special domain, the

radially symmetric solutions of the limiting punctured plate problem (5.2) have the form

$$u_0 = c_0 \left[ \left( Y_0(\eta r) + \frac{2}{\pi} K_0(\eta r) \right) - \beta (J_0(\eta r) - I_0(\eta r)) \right], \quad \beta \equiv \frac{[Y_0(\eta) + \frac{2}{\pi} K_0(\eta)]}{J_0(\eta) - I_0(\eta)}, \quad (5.51)$$

where  $\eta = \lambda_0^{1/4}$ . This function satisfies  $u_0(1) = 0$  together with the point constraint  $u_0(0) = 0$ . Upon setting  $u_{0r}(1) = 0$  and using the Wronskian relations for  $I_0, K_0$ , and for  $J_0, Y_0$ , we obtain the eigenvalue relation

$$\frac{2}{\pi} [K_0(\eta)J_0'(\eta) - K_0'(\eta)J_0(\eta)] + Y_0'(\eta)I_0(\eta) - Y_0(\eta)I_0'(\eta) = \frac{4}{\pi\eta}. \quad (5.52)$$

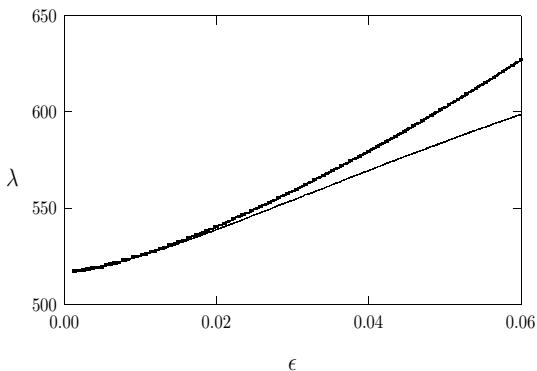
We let  $\eta_0$  denote the smallest root of (5.52), so that  $\lambda_0 = \eta_0^4$  is the smallest eigenvalue in the class of radially symmetric eigenfunctions of the limiting punctured plate problem (5.2).

We choose  $c_0 = -1/(8\eta^2)$  in (5.51) so that  $u_0 \sim (r^2/(8\pi)) \log r$  as  $r \rightarrow 0$  has the same singularity as the biharmonic Green's function in (5.3). Then, by using the well-known small-argument asymptotics of the Bessel functions  $I_0, K_0, J_0$ , and  $I_0$ , in (5.51) we readily calculate the following local behavior of  $u_0$  as  $r \rightarrow 0$ :

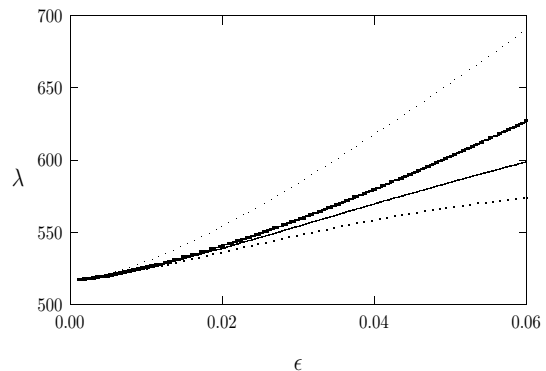
$$u_0 \sim \frac{1}{8\pi} r^2 \log r + d_0 r^2 + o(r^2), \quad \text{as } r \rightarrow 0; \quad d_0 = \frac{1}{8\pi} \left[ \log\left(\frac{\eta}{2}\right) + \gamma_e - 1 - \frac{\pi\beta^2}{2} \right]. \quad (5.53)$$

Here  $\gamma_e$  is Euler's constant, and  $\beta$  is defined in (5.51). Upon comparing the local behaviors (5.53) and (5.31 b) we identify  $\text{Trace}\mathcal{H}$ , required in Principal Result 5.3, as

$$\text{Trace}\mathcal{H} = 4d_0 = \frac{1}{2\pi} \left[ \log\left(\frac{\eta}{2}\right) + \gamma_e - 1 - \frac{\pi\beta^2}{2} \right]. \quad (5.54)$$



(a)  $\lambda$  versus  $\varepsilon$



(b)  $\lambda$  versus  $\varepsilon$

FIGURE 8. For an annulus  $\varepsilon < |x| < 1$  consider the smallest eigenvalue of (5.1) in the class of radially symmetric eigenfunctions. Left figure: plot of the exact relation for  $\lambda(\varepsilon)$  (heavy solid curve) and the three-term expansion for  $\lambda(\varepsilon)$  (solid curve) as obtained from (5.50) with  $\text{Trace}\mathcal{H}$  as given in (5.54). Right figure: comparison of one-term (faint dots), two-term (dots), and three-term (solid curve), asymptotic results for  $\lambda(\varepsilon)$  with the exact result for  $\lambda(\varepsilon)$  (heavy solid curve).

Setting  $\eta = \eta_0$  in (5.54) and (5.51) to calculate  $\beta$ , (5.54) determines  $\text{Trace}\mathcal{H}$  in terms of the smallest positive root of (5.52). In terms of  $\text{Trace}\mathcal{H}$ , a three-term asymptotic expansion for the perturbed eigenvalue  $\lambda(\varepsilon)$  for the annular domain is obtained by substituting (5.50 c) into (5.50 a). In Fig. 8(a) we show a very favorable comparison of this three-term result for  $\lambda(\varepsilon)$  with the exact result obtained by finding the lowest eigenvalue in the class of radially symmetric eigenfunctions for the full problem (5.1) in an annular domain. To obtain the exact result for  $\lambda(\varepsilon)$  we



numerically calculated the smallest root  $\lambda(\varepsilon)$  for the existence of a nontrivial solution of the form

$$u = b_0 J_0(\eta r) + b_1 I_0(\eta r) + b_2 Y_0(\eta r) + b_3 K_0(\eta r), \quad \eta = \lambda_0^{1/4}, \quad (5.55)$$

which satisfies the boundary conditions  $u = u_r = 0$  on  $r = \varepsilon$  and on  $r = 1$ . In Fig. 8(b) we compare the one-term, two-term, and three-term asymptotic results for  $\lambda(\varepsilon)$ , as obtained by truncating (5.50 *a*) at different orders, with the exact result for  $\lambda(\varepsilon)$ . From this figure, the three-term approximation provides a significantly better prediction of the exact result than the lower order asymptotic approximations.

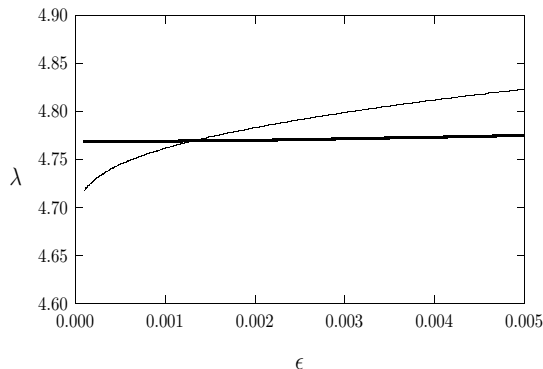


FIGURE 9. Consider the biharmonic eigenvalue problem  $\Delta^2 u = \lambda u$  in the annulus  $\varepsilon < r < 1$  with  $u = u_r = 0$  on  $r = \varepsilon, 1$ . As a function of  $\varepsilon$ , we plot the asymptotic result, obtained from (5.50) and (5.54), for the lowest eigenvalue in the class of radially symmetric eigenfunctions (heavy solid curve) together with the asymptotic result, obtained from (5.29), for the lowest eigenvalue in the class of eigenfunctions with one nodal line (solid curve). The two curves cross at  $\varepsilon \approx 0.0013$ .

Finally, we use our asymptotic results to illustrate the phenomena first observed in [5] relating to the fundamental mode of vibration for the clamped annular plate  $\varepsilon < |x| < 1$ . From a numerical evaluation of certain Bessel functions arising in the exact eigenvalue relation, it was shown in [5] that the lowest eigenvalue does not correspond to a radially symmetric eigenfunction on the range  $\varepsilon < 0.00131\dots$ , but instead arises from an eigenfunction that has one nodal line. Hence, for  $\varepsilon < 0.00131\dots$ , it was shown in [5] that the fundamental mode of vibration is not of one sign in the annulus. In Fig. 9 we plot our asymptotic results, valid for  $\varepsilon \rightarrow 0$ , for the lowest eigenvalue in the class of radially symmetric eigenfunctions, obtained from (5.50) and (5.54), and in the class of eigenfunctions with one nodal line, as obtained from (5.29). From this figure, we observe that the fundamental mode is not radially symmetric when  $\varepsilon < 0.0013$ , confirming the full numerical results of [5].

## 6 Discussion

In an arbitrary bounded 2-D domain, a singular perturbation approach was used to analyze the asymptotic behavior of some biharmonic linear and nonlinear eigenvalue problems for which the solution exhibits a concentration behavior either due to a hole in the domain, or as a result of a nonlinearity that is non-negligible only in some localized region in the domain. These singularly perturbed problem have a global outer scale, and one or more inner or local scales near the localized perturbation. A novel feature that arises in several of our biharmonic problems, which is absent in similar second-order elliptic problems, is that a point constraint must be imposed on the leading-order outer solution in order to asymptotically match inner and outer representations of the solution. In this sense, the effect of a strong localized perturbation on a biharmonic problem can influence the solution in a much more global way than for similar

second-order elliptic problems. In addition to the requirement of imposing a point constraint, our asymptotic analysis also relied heavily on the use of logarithmic switchback terms.

In §4 we constructed a solution to the nonlinear eigenvalue problem  $\Delta^2 u = -\lambda/(1+u)^2$  in  $\Omega$  with clamped boundary conditions on  $\partial\Omega$ , such that the solution exhibits single-point concentration at  $x_0 \in \Omega$  in the sense that  $\lambda \rightarrow 0$  as  $\varepsilon \rightarrow 0^+$ , where  $u(x_0) = -1 + \varepsilon$ . The condition determining the concentration point  $x_0$  was that  $\nabla_x R(x; x_0)|_{x=x_0} = 0$  with  $R(x_0; x_0) > 0$ , where  $R(x; x_0)$  is the regular part of the biharmonic Green's function. The analysis also determined the limiting asymptotic behavior for  $\lambda$  as  $\varepsilon \rightarrow 0$ . The asymptotic results for  $\lambda(\varepsilon)$  were shown to agree very well with full numerical solutions computed for the square and disc geometries. In addition to the challenge of providing a rigorous PDE framework to confirm our asymptotic results, there are a few further problems that warrant further study. Firstly, it would be interesting to study how the set of concentration points depend on the topology of the domain. In §4, we showed numerically for a one-parameter family of dumbbell-shaped domains that the set of concentration points exhibits a pitchfork bifurcation in terms of the parameter characterizing the shape of the domain. Can this and similar results be established rigorously? In addition, is it possible to construct a domain  $\Omega$  for which  $\nabla_x R(x; x_0)|_{x=x_0} = 0$ , but  $R(x_0; x_0) < 0$  at some  $x_0 \in \Omega$ ? From our analysis in §4, concentration would not occur at  $x_0$ . Such a scenario does not appear to be theoretically impossible since there are domains for which the biharmonic Green's function is not of one sign (cf. [30]). Furthermore, it would be interesting to construct a solution that exhibits concentration at multiple points in  $\Omega$ .

Finally, it would be interesting to apply our methodology to some specific problems in elasticity. More specifically, in [6] the buckling behavior of an annular elastic plate subject to a uniform in-plane compressive load on its outer boundary was studied asymptotically in the limit of small radius of the inner hole. The critical buckling load was calculated asymptotically, and it was shown that an asymmetric buckling pattern, leading to wrinkling behavior near the small hole, was typically the dominant instability. It would be interesting to apply our asymptotic methodology to extend this analysis of [6] to the more general case of a thin elastic plate of arbitrary shape that contains a small circular hole centered at an arbitrary point in the domain. How does the location of the hole within the domain determine the dominant angular mode associated with the localized wrinkling pattern near the hole?

### Acknowledgements

M. C. K. and M. J. W. gratefully acknowledge the grant support of NSERC (Canada). While at UBC, A. E. L. was supported by an NSERC graduate fellowship. M. J. W. thanks Prof. J. Wei of the Chinese University of Hong Kong for some helpful discussions.

### References

- [1] T. Boggio, *Sulle funzioni di Green d'ordine m*, Rend. Circ. Mat. Palermo, **20**, (1905), pp. 97–135.
- [2] A. Campbell, S. A. Nazarov, *Asymptotics of Eigenvalues of a Plate with a Small Clamped Zone*, Positivity, **5**, (2001), pp. 275–295.
- [3] A. Campbell, S. A. Nazarov, *An Asymptotic Study of a Plate Problem by a Rearrangement Method. Application to the Mechanical Impedance*, Mathematical Modeling and Numerical Analysis, **325**, (1998), pp. 579–610.
- [4] C. V. Coffman, R. J. Duffin, *On the Fundamental Eigenfunctions of a Clamped Punctured Disk*, Adv. in Appl. Math. **13**, No. 2, (1992), pp. 142–151.
- [5] C. V. Coffman, R. J. Duffin, D. H. Shaffer, *The Fundamental Mode of Vibration of a Clamped Annular Plate is not of One Sign*, Constructive Approaches to Mathematical Models (Proc. Conf. in honor of R. J. Duffin, Pittsburgh, Pa., 1978), pp. 267–277, Academic Press, New York-London-Toronto, Ont. 1979.
- [6] C. Coman, A. Bassom, *On a Class of Buckling Problems in a Singularly Perturbed Domain*, Q. J. Mech. Appl. Math., **62**(1), (2009), pp. 89–103.

- [7] C. Cowan, P. Esposito, N. Ghoussoub, A. Moradifam, *The Critical Dimension for a Fourth Order Elliptic Problem with Singular Nonlinearity*, Arch. Rational Mech. Anal., to appear, (2010), (19 pages).
- [8] C. Cowan, P. Esposito, N. Ghoussoub *Regularity of Extremal Solutions in Fourth Order Nonlinear Eigenvalue Problems on General Domains*, Discrete Contin. Dyn. Sys. Ser. A, **28**(3), (2010), pp. 1033-1050.
- [9] P. Esposito, N. Ghoussoub, Y. Guo, *Mathematical Analysis of Partial Differential Equations Modeling Electrostatic MEMS*, Courant Lecture Notes, in press, (2009), 332 pp.
- [10] A. Ferrero, H.C. Grunau, *The Dirichlet Problem for Supercritical Biharmonic Equations with Power-Law Nonlinearity*, J. Differential Equations, **234**, (2007), pp. 582-606.
- [11] N. Ghoussoub, Y. Guo, *On the Partial Differential Equations of Electrostatic MEMS Devices: Stationary Case*, SIAM J. Math. Anal., **38**, No. 5, (2006/07), pp. 1423-1449.
- [12] L. Greengard, M. C. Kropinski, A. Mayo, *Integral Equation Methods for Stokes Flow and Isotropic Elasticity in the Plane*, J. Comput. Physics, **125**(2), (1996), pp. 403-414.
- [13] Y. Guo, Z. Pan, M. J. Ward, *Touchdown and Pull-In Voltage Behaviour of a MEMS Device with Varying Dielectric Properties*, SIAM J. Appl. Math., **66**, No. 1, (2005), pp. 309-338.
- [14] Z. Guo, J. Wei, *Asymptotic Behavior of Touchdown Solutions and Global Bifurcations for an Elliptic Problem with a Singular Nonlinearity*, Comm. Pure. Appl. Analysis, **7**, No. 4, (2008), pp. 765-787.
- [15] Z. Guo, J. Wei, *Entire Solutions and Global Bifurcations for a Biharmonic Equation with Singular Nonlinearity in  $\mathbb{R}^3$* , Advances Diff. Equations, **13**, (2008), No. 7-8, pp. 743-780.
- [16] D. Joseph, T. Lundgren *Quasilinear Dirichlet Problems Driven by Positive Sources*, Arch. Rational Mech. Anal. **49** (1972/73), pp. 241-269.
- [17] T. Kolokolnikov, M. Titcombe, M. J. Ward, *Optimizing the Fundamental Neumann Eigenvalue for the Laplacian in a Domain with Small Traps*, Europ. J. Appl. Math., **16**(2), (2005), pp. 161-200.
- [18] P. Lagerstrom, *Matched Asymptotic Expansions: Ideas and Techniques*, Applied Mathematical Sciences, **76**, Springer-Verlag, New York, (1988).
- [19] P. Lagerstrom, D. Reinelt, *Note on Logarithmic Switchback Terms in Regular and Singular Perturbation Problems*, SIAM J. Appl. Math., **44**, No. 3, (1984), pp. 451-462.
- [20] F. H. Lin, Y. Yang, *Nonlinear Non-Local Elliptic Equation Modeling Electrostatic Actuation*, Proc. Roy. Soc. A, **463**. (2007), pp. 1323-1337.
- [21] A. Lindsay, M. J. Ward, *Asymptotics of Some Nonlinear Eigenvalue Problems for a MEMS Capacitor: Part I: Fold Point Asymptotics*, Methods Appl. Anal., **15**, No. 3, (2008), pp. 297-325.
- [22] A. E. Lindsay M. J. Ward, *Asymptotics of Some Nonlinear Eigenvalue Problems Modelling a MEMS Capacitor: Part II: Multiple Solutions and Singular Asymptotics*, accepted, Europ. J. Appl. Math., (2010), (33 pages).
- [23] S. G. Mikhailin, *Integral Equations and Their Applications to Certain Problems in Mechanics, Mathematical Physics, and Technology*, Pergamon Press, London, (1957).
- [24] S. G. Muskhelishvili, *Some Basic Problems of the Mathematical Theory of Elasticity*, P. Noordhoff Ltd., Groningen, (1953).
- [25] S. Ozawa, *Singular Variation of Domains and Eigenvalues of the Laplacian*, Duke Math. J., **48**(4), (1981), pp. 767-778.
- [26] J. A. Pelesko, D. H. Bernstein, *Modeling MEMS and NEMS*, Chapman Hall and CRC Press, (2002).
- [27] J. A. Pelesko, *Mathematical Modeling of Electrostatic MEMS with Tailored Dielectric Properties*, SIAM J. Appl. Math., **62**, No. 3, (2002), pp. 888-908.
- [28] O. Rey, J. Wei, *Blowing Up Solutions for an Elliptic Neumann Problem with Sub- or Super-Critical Nonlinearity. I.  $N = 3$* , J. Funct. Anal., **212**(2), (2004), pp. 472-479.
- [29] S. Santra, J. Wei, *Asymptotic Behavior of Solutions of a Biharmonic Dirichlet Problem With Large Exponents*, Journ. d'Analyse Math., to appear, (2010), (26 pages).
- [30] G. Sweers, *When is the First Eigenfunction for the Clamped Plate Equation of Fixed Sign?*, Electronic J. Differ. Equ. Conf., **6**, Southwest Texas State Univ., San Marcos, Texas, (2001), pp. 285-296.
- [31] M. Titcombe, M. J. Ward, M. C. Kropinski, *A Hybrid Asymptotic-Numerical Method for Low Reynolds Number Flow Past an Asymmetric Cylindrical Body*, **105**(2), (2000), pp. 165-200.
- [32] M. J. Ward, W. D. Henshaw, J. Keller, *Summing Logarithmic Expansions for Singularly Perturbed Eigenvalue Problems*, SIAM J. Appl. Math., **53**(3), (1993), pp. 799-828.
- [33] M. J. Ward, J. B. Keller, *Strong Localized Perturbations of Eigenvalue Problems*, SIAM J. Appl. Math., **53**(3), (1993), pp. 770-798.
- [34] P. Wessel, D. Bercovici, *Interpolation with Splines in Tension: A Green's Function Approach*, Mathematical Geology, **30**(1), (1998), pp. 77-93.